Translating Genetic Data into Actionable Clinical Guidelines: *Succinate Dehydrogenase Subunit A* Variants of Unknown Significance in Gastrointestinal Stromal Tumors

By

Amber Elizabeth Bannon

A DISSERTATION

Presented to the Department of Cell, Developmental, & Cancer Biology

Of the Oregon Health & Science University

School of Medicine

In partial fulfillment of the requirements for the degree of

Doctor of Philosophy

In Cell & Developmental Biology

September 2017

School of Medicine

Oregon Health & Science University

Certificate of Approval

This is to certify that the PhD Dissertation of

Amber Bannon

Translating Genetic Data into Actionable Clinical Guidelines: *Succinate Dehydrogenase Subunit A* Variants of Unknown Significance in Gastrointestinal Stromal Tumors

Has been approved

Mentor: Michael C. Heinrich, M.D.

Member/Chair: Amanda McCullough, Ph.D.

Member: David Koeller, M.D.

Member: Maureen Hoatlin, Ph.D.

Member: Christopher Corless, M.D., Ph.D.

TABLE OF CONTENTS

List of Figures

Necessary permissions have been obtained.

List of Tables

Abbreviations

2-HG	2-hydroxyglutarate
5mC	5-methlycytosine
ANO1	anoctamin-1
CNS	central nervous system
CSF	cerebral spinal fluid
ETC	electron transport chain
ETS	E26 transformation-specific
FAD	flavin adenine dinucleotide
Fe-S	iron-sulfur
FFPE	formalin fixed parafin embedded
GIST	gastrointestinal stromal tumor
HIFα	hypoxia-inducible factor alpha
ICC	interstitial cells of Cajal
ISA	iron sulfur assembly
ISU	iron sulfur cluster
LOF	loss of function
MRI	magnetic resonance imaging
N/A	not available

ND	not done
NF1	neurofibromatosis type I
NGS	next generation sequencing
PDGFRA	platelet-derived growth factor receptor alpha
PGL-PC	hereditary paraganglioma-pheochromocytoma syndromes
PHD	prolyl hydroxylase
QFR	fumarate:menaquinol oxidoreductase
ROS	reactive oxygen species
RTK	receptor tyrosine kinase
SDH	succinate dehydrogenase
SDHA	succinate dehydrogenase subunit A
SDHB	succinate dehydrogenase subunit B
SIRT3	sirtuin (silent mating type information regulation two homologs) 3
SQR	succinate:ubiquinone reductase
TCA	tricarboxylic acid
TET	ten-eleven translocation
TOM	translocase of the outer membrane
VUS	variants of unknown significance
WT	wild type

α-KG	alpha-ketoglutarate

Acknowledgements

I am especially indebted to Dr. Michael Heinrich, the greatest boss man in the world. He has been extremely supportive of my personal and career goals, even when they strayed from the traditional academic model. He has shown me what a great scientist (and person) looks like by mentoring me in the lab, exposing me to how our work affects patients in the clinic, and challenging me in our half marathon battles. He created the best possible environment for learning and thriving in this very difficult industry and I cannot imagine surviving this process with any other mentor.

Thank you to the members of my Dissertation Advisory Committee. Each one of them played a valuable role in my success as a scientist. Dr. Amanda McCullough provided me with guidance since day one as my first-year advisor and taught me the many benefits of the yeast model system. Dr. David Koeller, the mitochondrial wizard, had the most challenging questions during our meetings that pushed me to think outside the box. Dr. Maureen Hoatlin always encouraged me to pursue my goals of entering a career in industry. Dr. Chris Corless provided me with seemingly endless resources and expertise in all my projects.

A special thank you for the opportunity to work with Dr. Charles Keller. Thank you for exposing me to the business side of science which sparked a passion that I will continue to pursue.

To the ladies of the lab, I am so grateful to have them as my extended family. I feel incredibly fortunate to be surrounded by great friends through this process. To Ajia Town for her technical expertise and teaching me all the things about DNA. To Arin McKinley for being the best running/de-stressing partner. To Diana Griffith for making me laugh at the most random times. To Jason Kent for taking over the SDH project. To Ashley Young for the chats during a much-needed science break. Also, a huge thank you to Dr. Isaac Forquer for taking me under his wing and the countless hours of showing me how to do the coolest mitochondrial assays.

I am so appreciative of my many friends. Dr. Lillian Klug- thank you for being my fellow student, postdoc, second mentor, editor, the alpha, craft buddy, and friend (as well as so many other things). And Dr. Erin Meermeier who was always there for the best and the worst days. Thank you to my “non-science” friends, especially Tricia Burns, Joslin Cach, Kaitlin Fossati and Karen Frank, for being supportive through the ups and downs of life. And for their very cute babies to play with on the weekends.

This would not have been possible without my family, especially my loving parents. They gave me the best childhood (except the whole not teaching me how to ride a bike thing) which fostered a confidence and curiosity that continued into adulthood. I am so grateful that they instilled in me a strong work ethic. All of my successes are because of them.

Most importantly, thank you to Timothy Mineo. I am very grateful he joined me on this journey through graduate school. He definitely got me on my worst days but managed to always talk me off the cliff. He never allowed me to be too hard on myself and put all the bad days in perspective. As I look back, all of my favorite moments through this crazy adventure are with him. He provided me with endless laughter, lots of beer (& wine), bike rides, and Bend get-a-ways. I would not have made it through without him.

Abstract

This dissertation explores the importance of understanding the genetic mechanisms that lead to cancer. Specifically, in Chapter 2 succinate dehydrogenase subunit A variants of unknown significance are categorized based on how they affect succinate dehydrogenase complex function and therefore whether or not they predispose patients to succinate dehydrogenase-deficient cancer. Chapter 3 works to identify novel mechanisms of succinate dehydrogenase-deficiency in tumors with an unknown molecular classification. Finally, Chapter 4 reviews the genetic landscape of gastrointestinal stromal tumors and how it can be used to optimize clinical treatment. The overarching goal of this project is to establish a relationship between a patient's genetic abnormality and the cancer it will initiate in order to guide clinical practice.

1. CHAPTER ONE: Introduction

1.1. Preface

Chapter One provides an overview of succinate dehydrogenase (SDH), the key player in my dissertation work. In order to understand the biochemical, molecular, and clinical implications of genetic variants in SDH it was important to first understand the basic biology of the SDH complex and its role in human disease. This Chapter reviews decades of studies that were necessary for me to complete my research.

"If I have seen a little further it is by standing on the shoulders of giants."

–Sir Isaac Newton

1.2. Overview of succinate dehydrogenase's role in aerobic respiration

Mitochondria are the energy powerhouses of the cell; they function to efficiently produce a large amount of usable energy, stored in the form of ATP. Energy production starts with the breakdown of various energy storing sources including glucose, fatty acids, and amino acids to produce acetyl-CoA. When oxygen is present, acetyl-CoA enters the tricarboxylic acid (TCA) cycle where it undergoes a series of oxidation reactions. The resulting electrons from the oxidation reactions are sent to the electron transport chain (ETC) via the electron carriers NADH and $FADH_2$. In addition to the electrons, the TCA cycle is necessary for producing substrates involved in many other metabolic processes for the cell. The ETC consists of five protein complexes that use the high energy state of the

electrons to generate a proton gradient in the mitochondria, which drives ATP synthesis. Together the TCA cycle and the ETC comprise aerobic respiration.

Succinate dehydrogenase (SDH) also known as Complex II in the ETC is a heterotetrameric complex (SDHA/B/C/D, collectively referred to as SDH, individually referred to as SDHx) located on the inner membrane of the mitochondria (**Figure 1).** SDH links the TCA cycle and the ETC, making it critical for aerobic respiration. In the TCA cycle, SDHA oxidizes succinate to fumarate. The resulting electrons are transferred through SDHB, SDHC, and SDHD to catalyze the reduction of ubiquinone to ubiquinol. Ubiquinol carries these electrons to Complex III, contributing to the ETC and ATP synthesis.

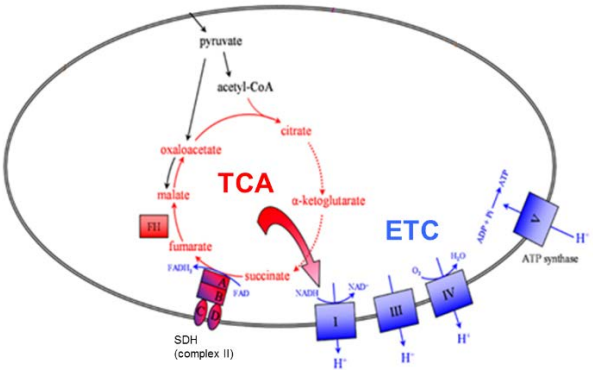

Figure 1. SDH plays a dual role in aerobic respiration by linking the TCA cycle to the ETC (King, Selak, and Gottlieb 2006).

1.3. SDH subunits are encoded by nuclear genome

The four subunits of the SDH complex are nuclear encoded unlike the other ETC complexes, which are encoded by the nuclear and mitochondrial genomes. *SDHA* is located on chromosome 5p15.33 with a known pseudogene on chromosome 3q29. *SDHB* and *SDHC* are located on chromosome 1, at 1p36.1-p35 and 1q23.3, respectively. *SDHD* is

located on chromosome 11q23.1. All four subunits are nuclear encoded and translated in the cytosol. The precursor proteins are then targeted to the mitochondria where the targeting sequence is cleaved allowing the proteins to mature and assembly into the SDH complex which is comprised of two soluble subunits and two membrane bound subunits (described in more detail in **Section 1.6.1**).

1.4. SDH is regulated by post-translational modification and active site inhibition

Post-translational phosphorylation, acetylation, and active site inhibition regulate SDH abundance and activity. Most of the known regulation pathways affect the flavoprotein, SDHA. The phosphorylation of SDHA results in decreased activity of the SDH complex (Tomitsuka, Kita, and Esumi 2009). Unfortunately, the specific sites of phosphorylation were not determined. Instead the authors described a global phosphorylation phenotype involving tyrosine, serine, and threonine residues. More recently it has been described that ROS (reactive oxygen species) trigger the phosphorylation on tyrosine residues of SDHA by FGR kinase to decrease SDH complex activity (Acín-Pérez et al. 2014).

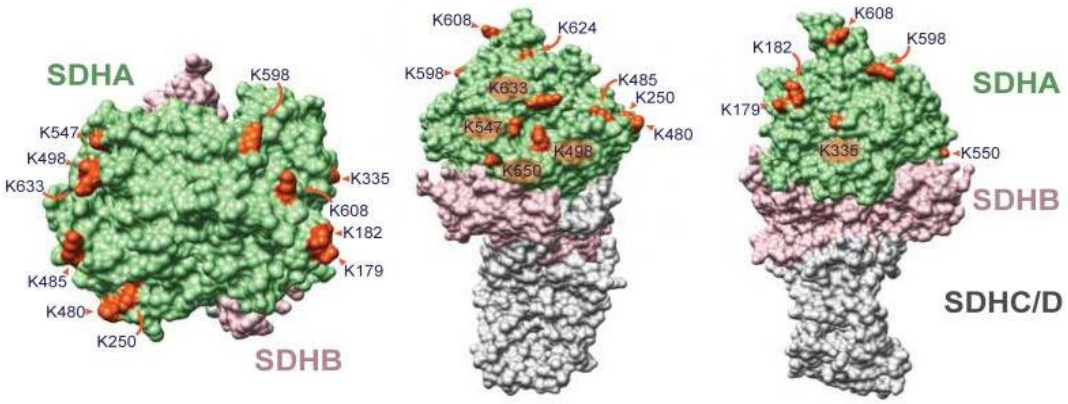

Figure 2. 13 residues are acetylated on SDHA (Finley et al. 2011).
Avian complex II crystal structure with 13 acetylated lysines identified.

Additionally, SdhA (mouse homolog of human SDHA) is a substrate of the mitochondrial deacetylase, SIRT3 [sirtuin (silent mating type information regulation two homologs)]. Deacetylation of several lysine residues on SdhA increases the activity of the SDH complex (Cimen et al. 2010). SDHA is the only known SDH subunit with lysine-acetylation, and thus far, 13 acetylated residues have been identified (Finley et al. 2011) (**Figure 2**). The deacetylation of SDHA by SIRT3 increases SDH enzyme activity. As seen in **Figure 2,** every acetylation site is solute-accessible and there is no acetylation on the SDHA/SDHB interface suggesting this modification may happen after SDH complex assembly. It is still unclear how acetylation influences SDH activity, what regulates the acetylation/deacetylation of SDHA, and which residues are necessary for controlling SDH complex activity.

Oxaloacetate, a TCA cycle intermediate, inhibits SDHA by binding to the active site for succinate oxidation. This inhibition is part of the regulation of the TCA cycle that allows it to respond to the metabolic needs of the cell.

It is interesting to note that acetylation/deacetylation, phosphorylation, and substrate inhibition by oxaloacetate do not seem to be regulated by the same overarching mechanism, suggesting that multiple modifications are used for fine-tuning the activity of SDH. Also, there are no described mechanisms that change the protein abundance of SDHA, other than loss-of-function mutations in the SDHx subunits which I will discuss at length below.

1.5. Complex II Superfamily of enzymes

The Complex II superfamily is composed of enzymes from all species that have two distinct but coordinated catalytic reactions. These Complex II enzymes use a reversible oxidoreduction of succinate and fumarate and pair it with the reversible oxidoreduction of quinol and quinone. Depending on the species, some members of the family will have increased reaction rates when catalyzing the reaction in one direction versus the other. For example, SDH (also referred to as SQR, succinate: ubiquinone reductase) is architecturally skewed to oxidize succinate and reduce quinone as described above for the ETC and TCA cycle. Alternatively, bacteria have an enzyme (QFR, fumarate:menaquinol oxidoreductase) that is skewed to catalyze the reverse reaction, the oxidation of quinol and the reduction of fumarate (Maklashina, Cecchini, and Dikanov 2013) (**Figure 3).**

Regardless of the enzymatic direction, all Complex II Superfamily members have a very similar structure for the soluble subunits which are comprised of a large flavoprotein (SDHA or FrdA, in the case of bacteria), and an iron-sulfur protein (SDHB or FrdB). However, the membrane-bound subunits differ across the superfamily and are divided

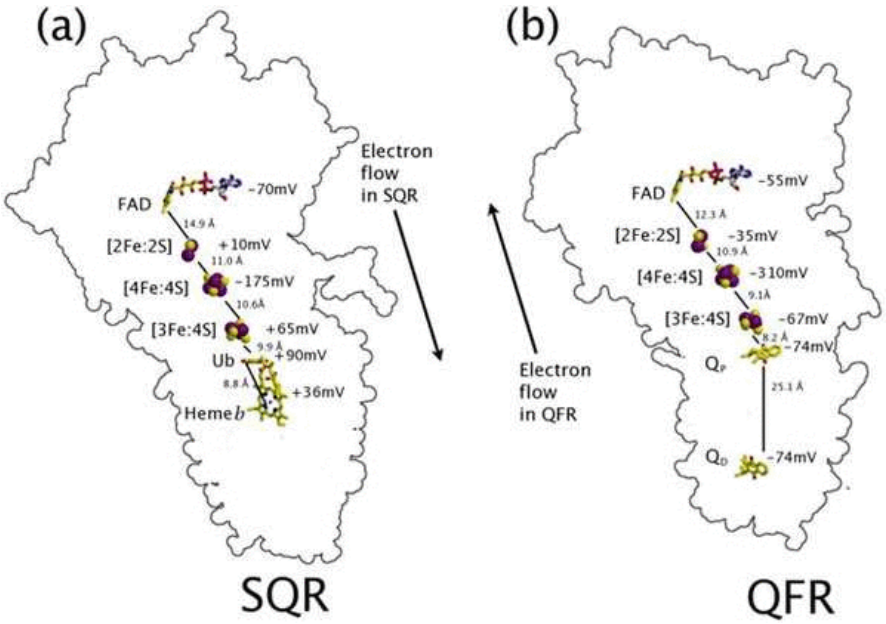

Figure 3. Electron flow between two Complex II Superfamily members, SQR and QFR (Tomasiak, Cecchini, and Iverson 2007).

into subfamilies (types A-E) (Hagerhall and Hederstedt 1996). For our purposes, we will focus on the similarities in the catalytic flavoprotein across Complex II Superfamily species to examine the structure/function relationship of specific amino acids that are involved in protein stability and catalytic function of SDHA.

1.6. SDH protein structure and catalytic function

The crystal structure of porcine SDH shows two parts comprising the complex, a hydrophilic portion that protrudes into the mitochondrial matrix and a hydrophobic portion that anchors the complex into the membrane (**Figure 4**) (Sun et al. 2005).

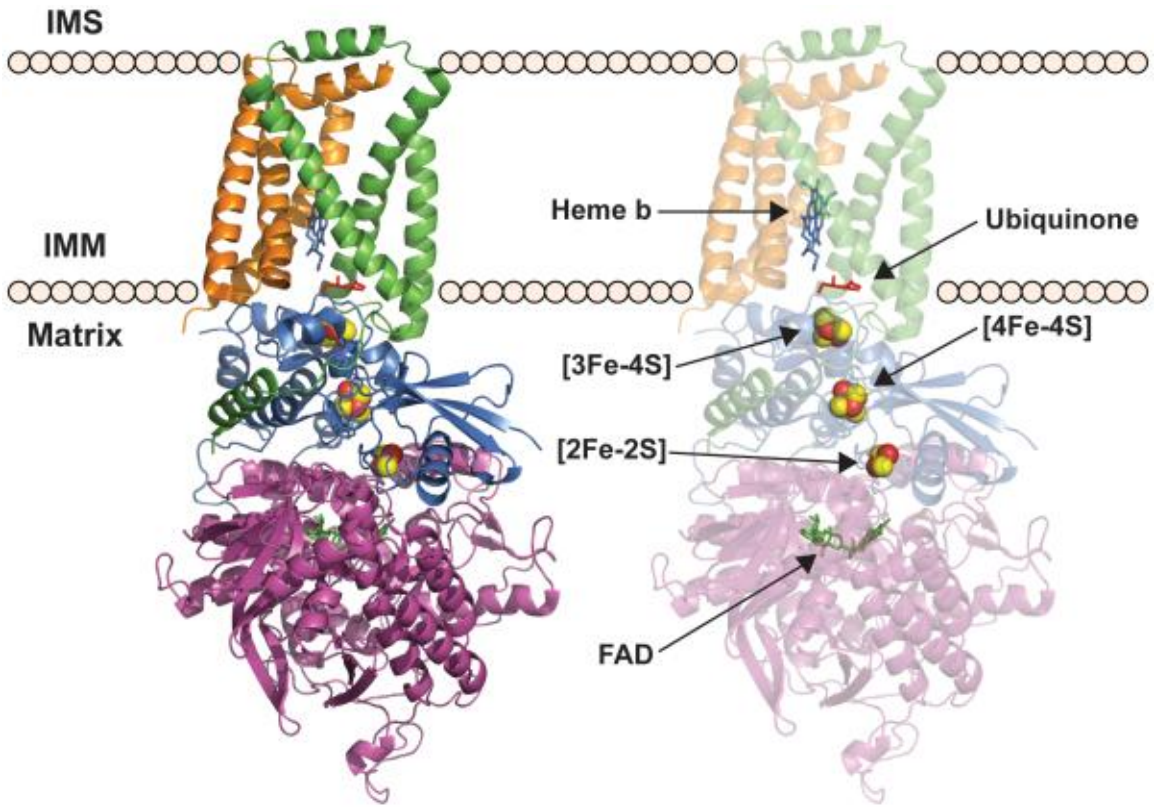

Figure 4. Porcine SDH crystal structure showing four subunits SDHA (purple), SDHB (blue), SDHC (green) and SDHD (orange) and there associate cofactors (Van Vranken et al. 2015).

The hydrophilic portion is composed of SDHA and SDHB. SDHA is the catalytic subunit of the complex responsible for the oxidation of succinate to fumarate. Based on crystal structures from multiple Complex II Superfamily members including porcine, SDHA has a Rossmann-type fold with four domains; a FAD binding domain, a capping domain, a helical domain and a C-terminal domain (**Figure 5)**.

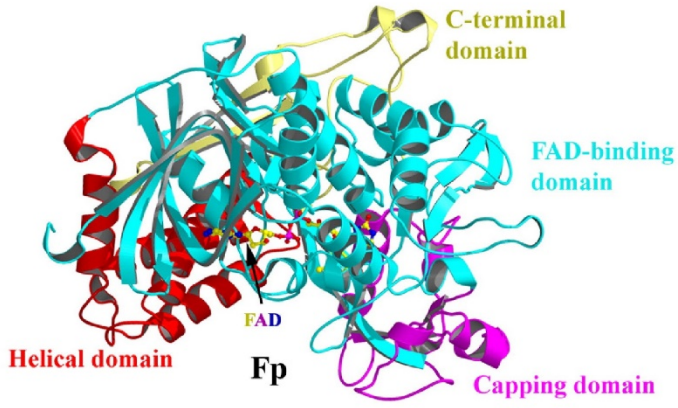

Figure 5. SDHA Rossmann-type fold with four domains; an FAD binding domain (teal), a capping domain (pink), a helical domain (red) and a C-terminal domain (yellow) (Sun et al. 2005).

SDHA contains the succinate binding domain, as well as a covalently bound flavoprotein, FAD (flavin adenine dinucleotide). FAD accepts two electrons, one at a time, during the oxidation of succinate to fumarate. The flavin sequentially passes the electrons to the [2Fe–2S], [4Fe–4S], and [3Fe–4S] clusters in SDHB (**Figure 6)** to reduce ubiquinone. SDHB acts as the neck of the complex, holding together SDHA and the membrane-bound part of the complex. Both the C-terminal and N-terminal domain of SDHB interact with SDHA and the SDHB C-terminal interacts with SDHC and SDHD providing amino acids residues that interact with the ubiquinone binding site in SDHC/D.

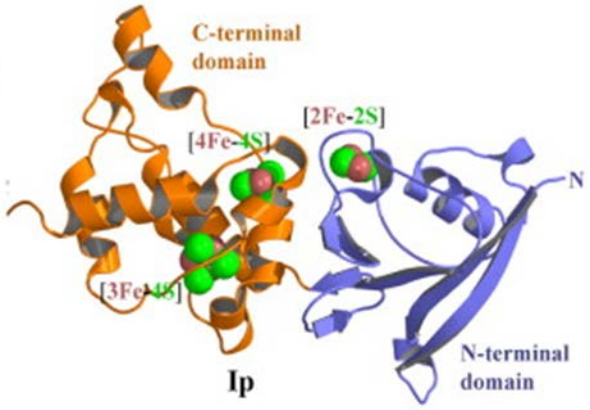

Figure 6. SDHB is composed of two domains that house three iron-sulfur groups involved in the transfer of electrons of succinate to ubiquinone (Sun et al. 2005).

The hydrophobic or membrane bound portion of the complex consists of SDHC and SDHD. These two subunits both interact with a heme whose role in catalysis is not clear. There are two ubiquinone-binding sites identified in the mammalian SDH complex, proximal (Qp) and distal (Qd). The Qp site is a higher affinity ubiquinone-binding site and is composed of residues from SDHB, SDHC, and SDHD. The Qp site stabilizes the

highly reactive semiquinone formed by the transfer of single electrons that reduce ubiquinone in two steps (Yankovskaya et al. 2003). Less is known about the Qd site which is located close to the intermembrane space. The *b* heme sandwiched in-between SDHC and SDHD may play a role in electron transfer to ubiquinone in the Qd site, but the mechanism has not been fully elucidated (Oyedotun, Sit, and Lemire 2007).

1.6.1. Yeast is a valuable model system for understanding mitochondria

Yeast, particularly *Saccharomyces cerevisiae,* are a powerful model system for studying cellular biology but play an even more valuable role in understanding mitochondrial biology (**Figure 7**). Yeast models have played a vital role in understanding mitochondrial protein import (Dudek, Rehling, and van der Laan 2013), quality control (Fischer, Hamann, and Osiewacz 2012), mitochondrial signaling (Fontanesi et al. 2006) and ETC complexes (Lasserre et al. 2015).Further, mitochondrial processes are highly conserved from yeast to human so most of the basic science discoveries are applicable for human mitochondrial diseases.

Perhaps the largest differentiator of yeast as a model system when studying mitochondrial diseases is their ability to survive on a fermentable carbon source in the absence of functional mitochondria (**Figure 8**). This combined with the ability to easily manipulate their genome, allows researchers to insert loss-of-function (pathogenic) mutations in mitochondrial proteins. As long as a fermentable carbon source is available,

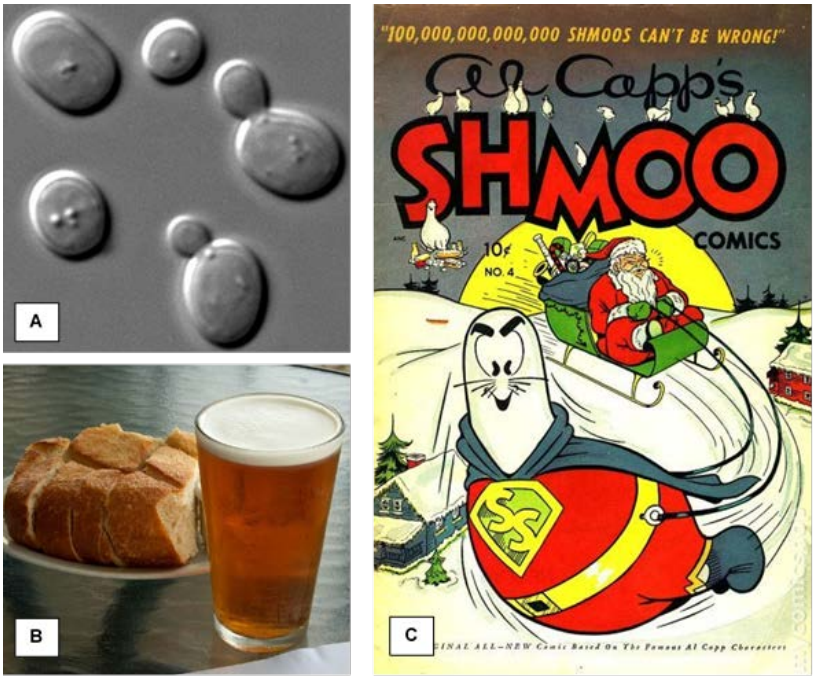

Figure 7. The multiple benefits of yeast as a model system.
A. *Saccharomyces cerevisiae* under a microscope. Note the budding yeast also referred to as a shmoo. B. The best feature of yeast is the snacks they make for when you need a science break. C. Al Capp's famous character the shmoo in his cartoon Li'l Abner. Scientists adopted the term "shmoo" because of the similarity of the beloved cartoon character to budding yeast. As you continue reading remember "100,000,000,000,000 shmoos can't be wrong!"

these mutations have no negative biologic effects because the breakdown of glucose to pyruvate generates ATP regardless of mitochondrial function (**Figure 8**). In contrast, a non-fermentable carbon source must utilize the mitochondria to produce ATP. This difference in energy metabolism allows researchers to easily differentiate between a loss-of-function mutation and one that does not affect mitochondrial function by manipulating carbon sources and measuring the yeasts' ability to grow (this assay is used in **Section 2.5**). More information on the yeast model in relation to SDH mutations is found in **Section 1.7.4** and **Chapter 2**.

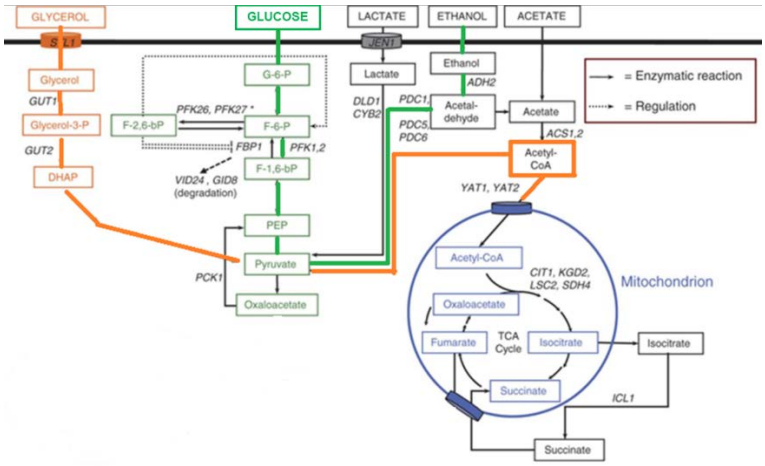

Figure 8. Yeast metabolic pathways.
Yeast are able to bypass mitochondrial function (shown in blue) in the presence of a fermentable carbon source, glucose (shown in green) but must use their mitochondria for energy production with a non-fermentable carbon source, glycerol (shown in orange).

1.6.2. Assembly of SDH complex requires assembly factors and cofactors

The complexes of the ETC require helper proteins to properly coordinate assembly of the multiple subunits that make up these complexes; these are known as assembly factors. SDH (Complex II) assembly is not as well understood as the other complexes. Only recently has the field identified the detailed, multistep assembly process where the four subunits of SDH are encoded by the nuclear genome, synthesized in the cytosol, transferred to the mitochondria, and independently mature before they can be assembled into the complex. This process involves the SDH subunits, cofactors (FAD, Fe-S clusters), SDH-specific assembly factors (currently SDHAF1-4 have been identified), as well as other more general mitochondrial assembly factors. The stepwise processing of each SDHx subunit into the mature SDH complex is described below (**Figure 9, Table 1**).

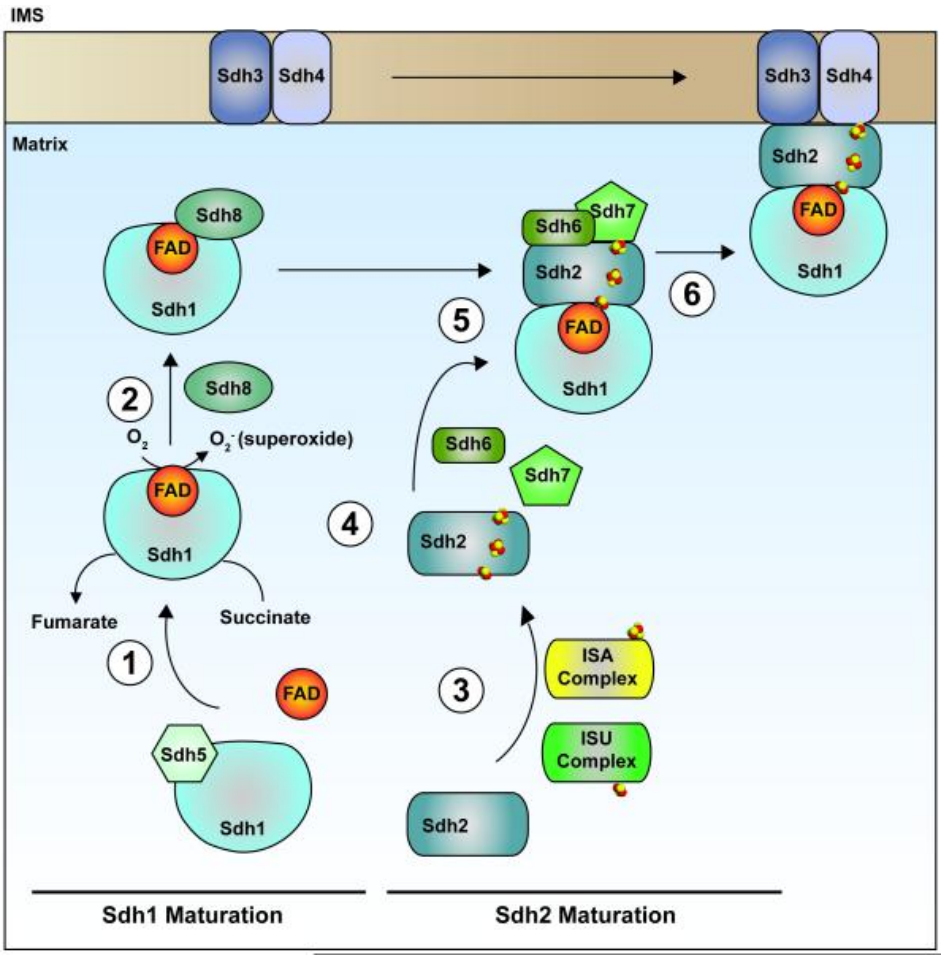

Figure 9. Assembly of SDH with cofactors and assembly factors in yeast (Van Vranken et al. 2015). Human orthologs are defined in Table 1. ISA (iron sulfur assembly), ISU (iron sulfur cluster unit)

Yeast protein	Human ortholog	Description/function
Sdh1	SDHA	Flavoprotein and succinate catalysis
Sdh2	SDHB	Iron-sulfur protein
Sdh3	SDHC	Membrane anchor and ubiquinone catalysis
Sdh4	SDHD	Membrane anchor and ubiquinone catalysis
Sdh5	SDHAF2	FAD insertion
Sdh6	SDHAF1	Facilitates transfer and insertion of iron-sulfur clusters
Sdh7	SDHAF3	Chaperone of iron-sulfur protein
Sdh8	SDHAF4	Chaperone of flavoprotein

Table 1. Yeast and human orthologs for major players in SDH complex assembly.

1.6.3. SDHA – the catalytic subunit - with help from FAD, SDHAF2, and SDHAF4

SDHA houses the catalytic active site for the oxidation of succinate to fumarate. Importantly there is a covalent bond between SDHA (His99 in humans) and the flavin group. Early research using a yeast model identified the covalent flavin was necessary for the oxidation of succinate (Robinson et al. 1994). The mechanism of covalent attachment is still unknown, but it likely involves the assembly factor SDHAF2 (Sdh5 in yeast; **Table 1**). A yeast screen of uncharacterized and highly conserved mitochondrial proteins identified Sdh5. Yeast cells with a *Sdh5* deletion have a respiratory defect due to the lack of SDH function associated with unflavinated Sdh1 (SDHA in humans, **Table 1)** leading researchers to believe Sdh5 is necessary and sufficient to covalently attach flavin to Sdh1 (Hao et al. 2009). However, recent studies have shown covalent flavination of SDHA does not require SDHAF2 in all model systems. For example, *Arabidopsis* and thermophilic bacteria lacking the SDHAF2 ortholog still have flavinated SDHA (Huang et al. 2013; Kounosu 2014). It is important to note that both of these studies did show a substantial increase in the amount of flavinated SDHA in the presence of the assembly factor and are only used as examples to show that SDHAF2 might not be essential for covalent flavination, but instead could just increase the kinetics of the reaction. It was recently shown that knockout of SDHAF2 in a breast cancer cell line did not inhibit covalent attachment of flavin to SDHA (Bezawork-Geleta et al. 2016). Studies of SDHAF2 in mammalian cell culture are limited, so this unexpected result, could point to an alternative mechanism for flavination in more complex species. Almost directly contradicting this idea is the observation of loss-of-function mutations in *SDHAF2* causing

paraganglioma due to decreased SDH function (to be discussed further in later sections) (Bausch et al. 2017). Taken together these data illustrate both the importance of SDHAF2 for proper SDH activity and the confusion surrounding the mechanism of SDHAF2's role in covalent attachment of flavin to SDHA.

Following flavination, the SDHA apo-protein forms a hetero-dimer with SDHB. However, there is unbound SDHA in the mitochondrial matrix. Again, a yeast model was used to identify Sdh8 (SDHAF4 in humans) as a subunit-specific chaperone. *Sdh8* deletion in yeast cells causes a slow growth on nonfermentable carbon sources characterized as a decreased respiration phenotype (Van Vranken et al. 2014). In both yeast cells and *Drosophila* mutants, there is a block in the TCA cycle at SDH. However, this phenotype is not as severe as the phenotype seen in cells lacking one of the four SDH subunits or SDHAF2, suggesting that SDHAF4 plays a role but is not required in the assembly of the SDH complex.

1.6.4. SDHB – the electron wire - with help from FE-S clusters (x3), ISU, ISA, SDHAF1, and SDHAF3

The SDHB subunit houses the three iron-sulfur (Fe-S) groups and acts as an electron wire transferring the electrons from the FAD in SDHA to the ubiquinone in SDHC/D. Obviously, proper assembly and function of SDHB are reliant on correct insertion of the Fe-S clusters. Assembly occurs using both general assembly factors (for Fe-S biogenesis) and the known SDH-specific assembly factors (SDHAF1 and SDHAF3) (**Figure 9**).

Fe-S clusters play roles in electron transfer in multiple organelles throughout cells, including the mitochondria, endoplasmic reticulum, cytosol and the nucleus. Due to their role in a multitude of cellular processes, the biogenesis and delivery of Fe-S clusters is well understood (Braymer and Lill 2017). The mitochondrial biogenesis and delivery of Fe-S clusters involve 18 known assembly proteins (Lill et al. 2012). The Fe-S clusters are formed on the scaffold protein complex ISU (iron sulfur cluster unit) and the first step in delivery to SDH is facilitated by the ISA (iron sulfur assembly) complex. From there it is theorized a series of chaperone proteins stabilize and insert the Fe-S clusters into SDHB.

The dedicated SDH assembly factor, SDHAF1, was identified due to an inherited disease characterized by leukoencephalopathy with decreased SDH activity (Bugiani et al. 2006). More about this disease and others caused by mutations in SDHAF1 is discussed below. Using genome-wide linkage analysis, researchers found homozygous mutations in a previously undefined gene (Ghezzi et al. 2009). The gene encodes the protein now known as SDHAF1, which is a small, soluble protein necessary for normal SDH function. Using a yeast model, the deletion of *SDHAF1* was shown to decrease SDH activity without affecting other components of the ETC (Ghezzi et al. 2009). The exact role of SDHAF1 is still not completely understood, but based on its predicted structure it is thought to be a chaperone protein. Detailed work in yeast and Drosophila models found that Sdh6 interacts with an SDH assembly intermediate (Sdh1/2 dimer) and partially stabilizes Sdh2 in the presence of a nonfunctioning Sdh1 (Na et al. 2014). However, the yeast and drosophila models were unable to elucidate the exact role and timing of Sdh6's importance in Sdh2 maturation (Na et al. 2014). Using cell lines derived from patients with missense *SDHAF1* mutations, it has been found that SDHAF1 recruits Fe-S cluster transfer

protein to the C-terminus of SDHB through its LYR motif, which binds to a co-chaperone HSC20 (Maio et al. 2014; Maio et al. 2016).

The final SDHB assembly factor is the mitochondrial matrix protein SDHAF3 (Sdh7 in yeast). In yeast and Drosophila models, SDHAF3 plays a similar role to SDHAF1. However, there are currently no SDHAF3-deficient cell lines, so its exact role in SDHB maturation is still largely unknown. Knockdown of *SDHAF3* in yeast yielded a respiratory-deficient phenotype and caused an increase in succinate, suggesting a role unique to SDH (Na et al. 2014).

1.6.5. SDHC and SDHD – the anchor – with help from heme (maybe?)

SDHC and SDHD are the hydrophobic subunits that anchor the SDH complex to the mitochondrial membrane. In yeast, SDHC/D are translated in the cytosol and imported into the mitochondria through the TOM (translocase of the other membrane) complex. There is not a lot known about the assembly of SDHC and SDHD but when SDHD is deleted, levels of SDHC dramatically decrease. There is a type-b heme cofactor nestled between the two subunits, but there is no information on the insertion of that heme and more importantly on the role of the heme (Sun et al. 2005; Oyedotun and Lemire 2004; Oyedotun, Sit, and Lemire 2007). It does not seem to be involved in the catalytic function of the transfer of electrons between the last Fe-S cluster and the ubiquinone as mentioned in an earlier section. However, this heme cofactor is present in SDH complexes from simple organisms like *E. coli* to higher organisms like pigs (*Sus scrofa*), suggesting an important role, such as stabilization.

1.7. Role in human disease

SDH plays a vital role in ATP production, as it is part of both the ETC and the TCA cycle. Therefore loss-of-function defects in SDH cause human disease. There are two main categories of disease associated with defects in SDH; Complex II deficiency and cancer.

1.7.1. Complex II deficiency

Complex II deficiency is a rare, genetic cause of mitochondrial respiratory chain defects (Parfait et al. 2000; Vladutiu and Heffner 2000; Ghezzi et al. 2009). Similar to other diseases of energy metabolism, the phenotype of Complex II deficiency is not well-defined, but symptoms tend to group in organs that heavily rely on ATP production such as the central nervous system (CNS), heart, muscle, and eyes. It also affects the liver, kidneys, and causes dysmorphic features. See **Table 2** for common clinical symptoms seen in patients with Complex II deficiency.

	# of patients	**% of patients**
Neurological involvement	29	85%
Total evaluated	34	
Hypotonia	8	
Spasticity	13	
Ataxia	8	
Seizures	3	
Irritability	3	

Normal	5	
Abnormal brain imaging	20	80%
Total evaluated	25	
Leukoencephalopathy	10	
Leigh disease	8	
Cerebellar atrophy	2	
Normal	5	
Cardiac abnormality	9	50%
Total evaluated	18	
Hypertrophic cardiomyopathy	5	
Conduction defect	2	
Dilated cardiomyopathy with non-compaction	2	
Muscle involvement	9	53%
Total evaluated	17	
Eye abnormality	8	53%
Total evaluated	15	
Abnormal development	25	78%
Total evaluated	32	
Failure to thrive	9	28%
Total evaluated	32	
Elevated lactic acid	13	52%
Total evaluated	25	

Table 2. Clinical symptoms seen in patients with Complex II Deficiency (Jain-Ghai et al. 2013).

Leigh syndrome and leukoencephalopathy are the most common disorders associated with Complex II deficiency. Below is a more detailed description of these disorders and their relation to SDH mutations. In addition, rare mutations in SDHx have been linked to late onset neurodegenerative disease (Birch-Machin et al. 2000; Taylor et al. 1996), cardiomyopathy (Levitas et al. 2010; Davili et al. 2007), encephalopathy (Jackson et al. 2014; Ardissone et al. 2015; Ma et al. 2014) and leukodystrophy (Alston et al. 2012).

1.7.1.1. Leigh syndrome

Leigh syndrome, also known as infantile subacute necrotizing encephalomyelopathy, is a progressive neurodegenerative disorder characterized by focal, bilateral lesions in one or more areas of the CNS and is most often caused by homozygous or compound heterozygous mutations affecting the function of Complex I-V in the ETC or their assembly factors. The most commonly mutated gene is the *SURF1* gene, which encodes an assembly factor protein for proper assembly of Complex IV.

Patients with Leigh syndrome often present with symptoms in their infancy. These symptoms include vomiting, seizures, developmental delay, and lactic acidosis. Also, patients present with bilateral symmetric lesions in basal ganglia and subcortical brain regions thought to be due to apoptotic cells that were not able to produce enough ATP for proper cell function. Because there is no effective treatment for this disease patients often die within several months of their diagnosis.

In addition to other mutated metabolic enzymes, loss-of-function homozygous or compound heterozygous mutations in *SDHA* are implicated in causing Leigh syndrome. The first described case of Leigh syndrome with an *SDHA* mutation was seen in two siblings whose parents are first cousins (Bourgeron et al. 1995). The affected children were homozygous for an Arg554Trp substitution in SDHA that was absent in 120 controls and decreased SDH function in a yeast model (Bourgeron et al. 1995). Since then, there have been several reports on patients with SDH-deficient Leigh syndrome showing either homozygous or compound heterozygous mutations in *SDHA* (Parfait et al. 2000; Van Coster et al. 2003; Horvath et al. 2006).

1.7.1.2. Infantile leukoencephalopathy

Leukoencephalopathy refers to a disease or condition that causes defects in the white matter of the brain. These abnormal lesions can be detected in the brain using magnetic resonance imaging (MRI). Symptoms include lack of speech development, spastic quadriparesis, loss of mental function, and seizures. Although no functional studies were done, after observing the symptoms in two groups of families with multiple affected children, researchers established the connection between *SDHAF1* mutations and infantile leukoencephalopathy. These children, likely born of related parents, had loss-of-function mutations in the gene now known as *SDHAF1* (Ghezzi et al. 2009). Other studies have solidified the link between *SDHAF1* mutations and leukoencephalopathy (Ohlenbusch et al. 2012).

1.7.2. SDH-deficient cancer

1.7.2.1. Current mechanistic understanding of tumorigenesis

Potential roles for SDH in tumorigenesis have been proposed **(Figure 10**), but the mechanisms by which SDH-deficiency initiates the formation of cancer are incompletely understood.

First, a lack of SDH function inhibits the complex from passing electrons into the ETC. Instead, they are passed to oxygen or water to produce ROS (**Figure 10A**). The increase in ROS causes oxidative stress and possible DNA damage (Pollard et al. 2005), although the significance of genomic damage from the increased ROS has been disputed in the field

(Smith, Janknecht, and Maher 2007). While this mechanism may play some role, it may not be the major driver of tumorigenesis.

More relevant is that loss-of-function mutations in SDHx prevent the conversion of succinate to fumarate, which leads to accumulation of succinate both *in vitro* and clinically (Pollard et al. 2005; Lendvai et al. 2014). Succinate belongs to a new class of tumor initiators called oncometabolites (Yang and Pollard 2013). Other oncometabolites include fumarate, from fumarate hydratase loss of function, and 2-hydroxyglutarate (2-HG), from isocitrate dehydrogenase change in function. These oncometabolites share similar structures with one another and with alpha-ketoglutarate (α-KG), a substrate for a family of α-KG-dependent dioxygenase enzymes. Due to their similarity with alpha-ketoglutarate (α-KG) (**Figure 11**), oncometabolites act as competitive inhibitors to a family of α-KG-dependent dioxygenases (Xiao et al. 2012; MacKenzie et al.

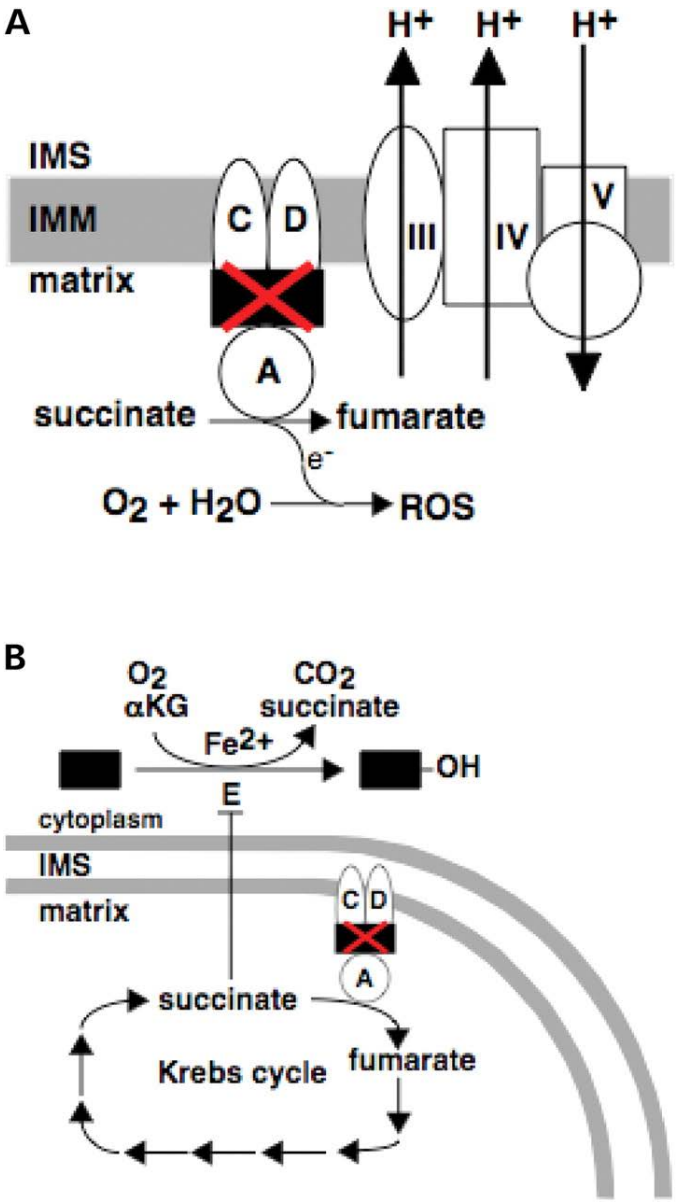

Figure 10. Potential mechanisms of tumorigenesis in SDH-deficient cells (Smith, Janknecht, and Maher 2007).

2007).

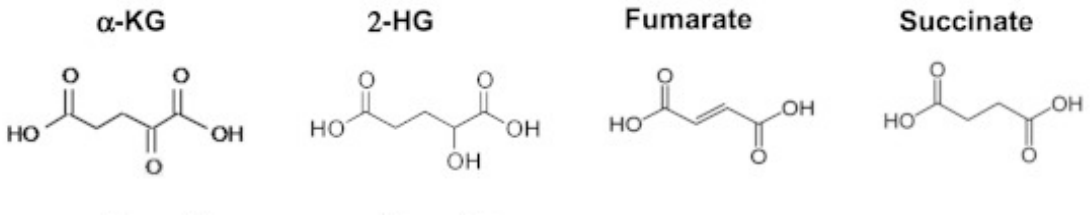

Figure 11. Structural comparison of oncometabolites (2-HG, fumarate, and succinate) to α-KG. (Xiao et al. 2012)

This dysregulation of α-KG-dependent dioxygenases has been connected to two mechanisms of cancer pathogenesis, as shown in **Figure 12**: 1) inhibition of prolyl hydroxylase, which leads to the accumulation of the transcription factor HIF1α; and 2) inhibition of demethylases, resulting in DNA and histone hypermethylation and gene deregulation.

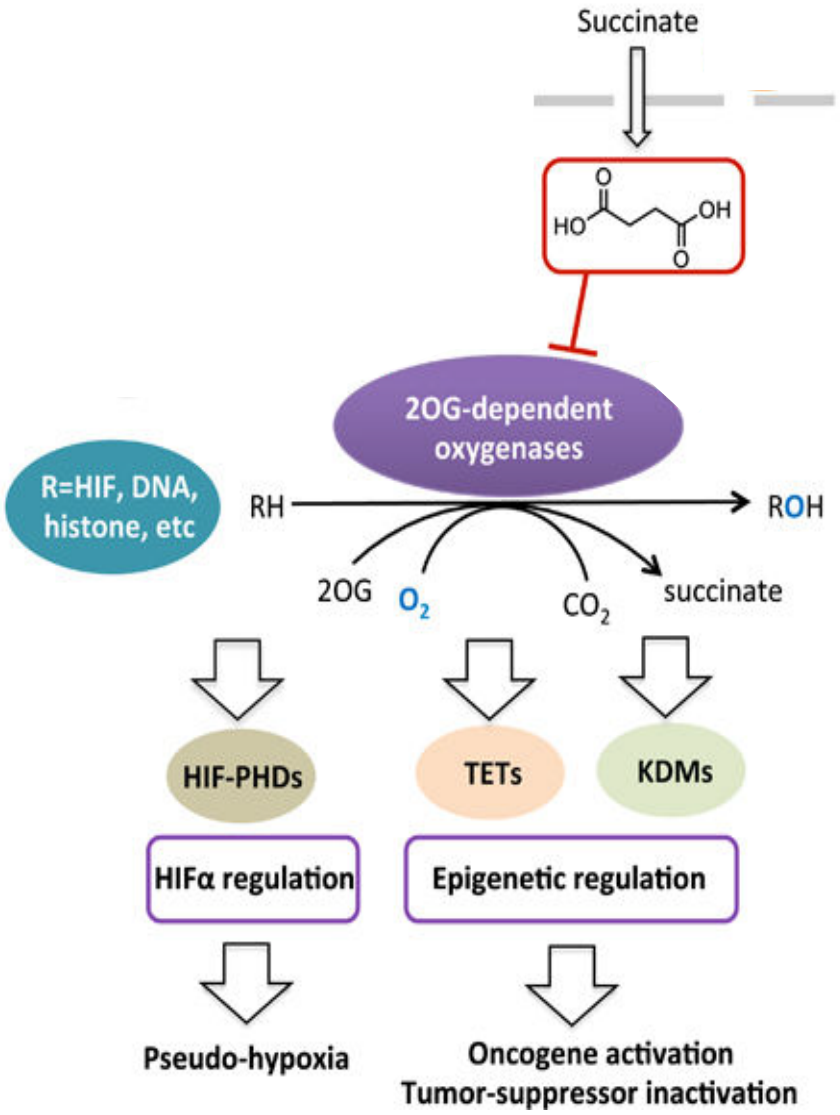

Figure 12. Succinate inhibits α-KG-dependent dioxygenases causing HIF1α and epigenetic dysregulation that promotes tumorigenesis (Adam et al. 2014).

The α-KG-dependent family of enzymes includes prolyl hydroxylase (PHD), which is responsible for the degradation of hypoxia-inducible factor alpha (HIFα) under normal cellular respiration. When the cell is hypoxic, or pseudo-hypoxic due to the inhibition of PHD by succinate, HIFα increases the transcription of several genes potentially involved

in tumorigenesis including angiogenesis, extracellular matrix elements, glucose metabolism, and survival (Pollard et al. 2005; Selak et al. 2005). Paragangliomas with SDH mutations show an increase in HIFα, providing supportive evidence that HIFα may be important in tumor progression (Pollard et al. 2005; Pollard et al. 2006).

In addition to inhibiting HIFα degradation, succinate inhibits histone demethylation, by histone demethylases and the TET (ten-eleven translocation) family of 5-methylcytosine (5mC) hydroxylases (Xiao et al. 2012). This is supported by a global hypermethylation pattern in gastrointestinal stromal tumors (GISTs) with SDH-deficiency, but not in GISTs that have tyrosine kinase mutations (Killian et al. 2013). The hypermethylation has also been observed in paragangliomas with SDHx mutations (Letouze et al. 2013). In a mouse Sdhb-deficient cell line which is used to model paragangliomas, hypermethylation promotes epithelial–mesenchymal transition while blocking differentiation. Exciting preliminary data suggest that the increased migratory capacity of the Sdhb-deficient cell line is repressed after treatment with DNA demethylating agents (Letouze et al. 2013).

Currently, no therapeutic strategies directly target SDH-deficient cancer cells, but based on the above observations there may be several opportunities to target SDH-deficient cells vs. wildtype (WT), including the changes in metabolism or epigenetics.

1.7.2.2. Gastrointestinal stromal tumors

GISTs are the most common mesenchymal tumor of the gastrointestinal (GI) tract. Most GISTs are driven by gain-of-function mutations in *KIT* or *PDGFRA* receptor tyrosine

kinase genes. However, 15% of GIST in adults and 85% in children lack mutations in either of these receptor genes; these are referred to as 'wild-type' GIST. Recently, a subset of WT GIST was found to carry various mutations in the *SDHx* genes. These are germline mutations or rare somatic mutations, accompanied by loss of heterozygosity in the WT allele, that impair or destroy enzymatic activity of SDH. Unlike KIT- and PDGFRA-mutant GIST, SDH-deficient GIST do not respond to tyrosine kinase inhibitors and, due to their inherent resistance to chemotherapy and radiation, there are no effective treatment options for these patients.

Please note **Chapter 4** will discuss, in detail, the multiple molecular classifications of GIST and the current therapeutic strategies based on molecular subtype. Below is a very brief description of the two categories of SDH-deficient GIST, syndromic and sporadic.

1.7.2.2.1. Syndromic GIST- Carney triad and Carney-Stratakis

Carney triad describes a nonhereditary SDH-deficient syndrome associated with the clinical triad of GIST, paraganglioma, and pulmonary chondroma (Carney et al. 1977). The syndrome mostly affects young females. Only very recently have SDHx mutations been identified in these patients but this is extremely rare (Boikos, Xekouki, et al. 2016). Promoter hypermethylation resulting in a loss of SDHC gene transcription is thought to be the tumor-initiating event in these patients (Haller et al. 2014).

During the process of investigating the etiology of Carney triad, another syndrome designated as Carney-Stratakis was recognized. Carney-Stratakis patients have a hereditary susceptibility to GIST and paragangliomas (Carney and Stratakis 2002).

Inherited mutations in *SDHA*/*B*/*C*/*D* are found in these patients along with a loss of heterozygosity event or second mutation in the second allele. Carney-Stratakis affects both males and females equally. Despite the genetic differences in Carney-Stratakis and Carney Triad, GISTs both of these syndromes present with similar clinical characteristics. These patients develop multifocal gastric tumors with epithelioid histology that frequently metastasize to the lymph nodes. In contrast, KIT- and PDGFRA- GIST are not restricted to gastric origin, have a spindle cell morphology, and rarely metastasize to lymph nodes. Given that GIST and paraganglioma both characterize Carney-Stratakis syndrome and Carney Triad, it is challenging to determine which condition is responsible for the development of these tumors in a given patient without appropriate molecular testing.

1.7.2.2.2. Sporadic GIST

In addition to syndromic SDH-deficient GISTs, sporadic SDH-deficient GISTs can arise. These GISTs share the same clinical characteristics as those SDH-deficient GIST described above. Both hypermethylation of *SDHC* and mutations in the SDHx subunits can cause GIST. Mutations in *SDHA* are the most common in sporadic SDH-deficient GIST.

As mentioned above, SDH-deficient GISTs are a separate subset of tumors than the tyrosine kinase-mutated GISTs, however, there is one reported example of SDH-deficiency in a PDGFRA-mutant GIST (Belinsky et al. 2017). This notable exception is an interesting tumor where the two distinct mechanisms of tumorigenesis overlap.

1.7.2.3. Paragangliomas and pheochromocytomas

Similar to GIST, there are hereditary paraganglioma-pheochromocytoma (PGL-PC) syndromes. Spontaneous PGL or PC is rare in the population, with the risk being approximately 1 in 30,000 (Petropoulos et al. 2000). However, patients with a mutation in one of the *SDHx* genes have a lifetime tumor rate of greater than 70% (Pasini and Stratakis 2009). PGLs are neuroendocrine tumors that can occur in a variety of places from the base of the skull to the pelvis, but the most common location is the head and neck. PCs arise from the adrenal medulla. PGL and PC tumors are heterogeneous; some secrete catecholamines while others do not. Also, they are described based on their location- adrenal or extra-adrenal. The clinical classification (PGL1, PGL2, etc.) relies on which SDH-associated gene is mutated. As with GIST, *SDHx* mutations identified in the tumors are homozygous or compound heterozygous loss-of-function mutations.

1.7.2.3.1. PGL1- *SDHD* mutations

Mutations in *SDHD* predispose patients to head and neck PGLs and less commonly adrenal PCs. These are usually multifocal tumors but are rarely malignant. Also, they rarely secrete catecholamines (Baysal et al. 2000). There are a variety of different loss-of-function mutations seen in *SDHD,* including frameshift, nonsense, and splicing mutations (Pasini and Stratakis 2009).

1.7.2.3.2. PGL2- SDHAF2 mutations

PGL2 has been recognized for decades, affecting Dutch families with multiple head and neck paragangliomas (van Baars et al. 1982). It was only recently shown to be due to a mutation in *SDHAF2*, one of the SDH assembly factors (Hao et al. 2009). Mutations of chromosome 11 are associated with both PGL1 and PGL2. Interestingly, these syndromes more often affect the offspring of male carriers versus female carriers, indicating there could be some maternal imprinting (Baysal 2004).

1.7.2.3.3. PGL3- SDHC mutations

Patients with *SDHC* mutations are categorized as having PGL3. These mutations cause head and neck paragangliomas and extremely rarely adrenal or extra-adrenal PCs. These tumors have been known to secrete catecholamines but since this is such a rare type of PGL the phenotype is not very well established (Niemann et al. 2003).

1.7.2.3.4. PGL4- SDHB mutations

Mutations in *SDHB* are associated with PGL4 (Astuti et al. 2001). These tumors are most often extra-adrenal PCs that secrete catecholamines. Also, these PCs tend to proliferate rapidly and have a higher risk of metastasis (King et al. 2011). PGL4 patients have an average age of diagnosis between 27 and 42, with the youngest reported case being three years old (Ricketts et al. 2010).

1.7.2.3.5. PGL5- SDHA mutation

SDHA mutations were not associated with PGL until 2010 when a woman presented with a germline SDHA mutation and PGL (Burnichon et al. 2010). Since then, more cases of PGL have been identified, but it is still a rare subtype of PGL (Korpershoek et al. 2011).

1.7.2.4. Other tumor types

In addition to the more common SDH-deficient tumors, GIST and PGL/PC, the increased availability and ease of sequencing technology has identified other tumor types that albeit rarely present with SDH mutations.

Cowden syndrome is associated with hamartomas, noncancerous growths of the skin and mucous membranes, as well as a variety of cancers including breast, thyroid, and endometrial neoplasia. Although not a common cause of Cowden syndrome, *SDHB* and *SDHD* mutations, occur in a subset of these patients (Ni et al. 2008). Cowden syndrome patients with *SDHB* and *SDHD* mutations have elevated succinate in their plasma, which could be a useful diagnostic tool for all cancers associated with SDH-deficiency (Hobert et al. 2012).

A family with known germline *SDHB* mutations had two family members diagnosed with renal cell carcinoma in addition to paraganglioma tumors (Vanharanta et al. 2004). The renal cell carcinoma showed loss of heterozygosity for *SDH,* as would be expected. Although this is a rare phenomenon, the presence of other SDH-deficient renal cell carcinomas has been confirmed. In fact, SDH-deficient renal cell carcinomas have unique clinicopathologic features such as a homogeneous population of cells with eosinophilic

cytoplasm, cytoplasmic inclusions of flocculent or eosinophilic material, and solid or nested architecture (Williamson et al. 2015). Correctly classifying these tumors as SDH-deficient would be helpful in evaluating the patient's risk for other SDH-deficient tumors described in this review.

A subset of pituitary tumors with a previously unexplained genetic were recently found to be SDH-deficient. These tumors have a unique phenotype that presents as prolactin-producing macroadenomas in young males. However, this genotype-phenotype correlation will be better understood as more patients are diagnosed with SDH-deficient pituitary tumors (Gill 2014).

1.7.3. Inconsistent phenotype and penetrance

It is curious that mutations in the different subunits of SDH give different phenotypes, both for Complex II deficiency and cancer. In Complex II deficiency, two sisters with the same SDHB mutations had different Complex II deficiency phenotypes even though their protein levels were similarly drastically reduced compared to normal controls (Ardissone et al. 2015). Other evidence includes the case study of a patient with homozygous SDHA mutation and relatively mild Leigh syndrome despite greater than 50% reduction in Complex II activity (Pagnamenta et al. 2006). It was noted after a review of multiple patients that the percent reduction in Complex II activity did not correlate with severity of disease (Jain-Ghai et al. 2013). This correlation could be an artifact of different laboratory assays, or it could be a clue as to why or how different mutations result in different disease outcomes.

Similarly, inherited mutations in the different SDH subunits have different lifetime cancer risks and penetrance in PGL. For example, *SDHB* mutations carriers have a 76% lifetime risk of cancer with 50% penetrance by age 35 compared to *SDHD* mutations carriers who have a 100% lifetime risk of cancer with 86% penetrance by age 50 (Pasini and Stratakis 2009). *SDHA* mutations, which until recently were thought not to predispose patients to PGL, have a penetrance of 13-39% at age 40 (Bausch et al. 2017). The tumor phenotype of different *SDHx* mutations also is significantly varied as shown in **Figure 13.**

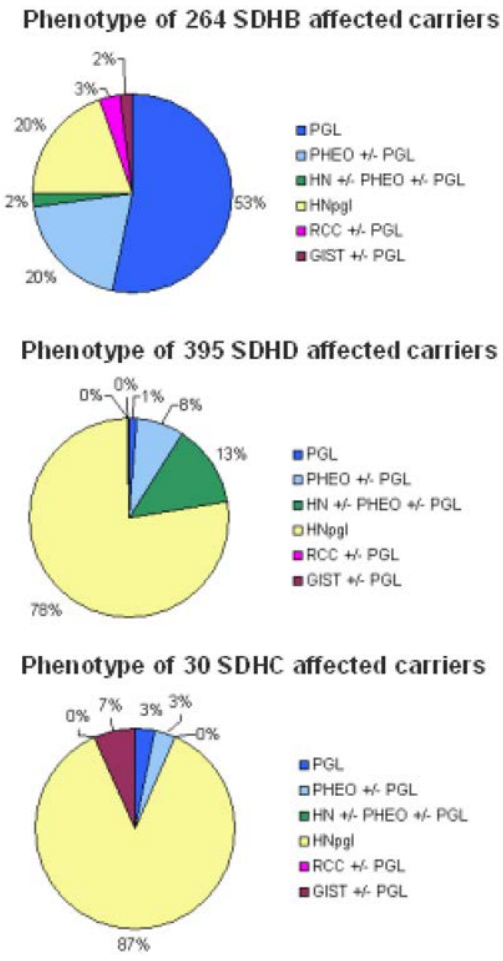

Figure 13. Different phenotypes in SDHx mutation carriers (Pasini and Stratakis 2009).

Potentially related is work showing that loss of SDHB, but not SDHA, triggers ROS-dependent HIF activation and tumorigenesis (Guzy et al. 2008). More studies need to be done to see if there is indeed a difference in ROS production when specific subunits are mutated and how that relates to pathogenicity in both Complex II deficiency and cancer.

1.7.4. Variants of unknown significance

Due to the substantial increase use of targeted sequencing panels, more patients are now being found to harbor *SDHx* germline mutations. These germline mutations can be categorized as causing a loss of function (pathogenic), having no effect (non-pathogenic), or as a variant of unknown significance (VUS). Often variants will only be classified as loss of function (pathogenic) if they cause protein truncation (e.g. an early stop codon or frame shift) or if there is an established family history. The first two categories of variants, loss of function and no effect, are relatively straightforward regarding genetic counseling for patients (see **Section 1.7.5**). However, by definition VUS have an unknown effect on protein function, meaning we do not understand if these VUS will predispose patients to the cancers described above. Additionally, for patients with GIST, understanding the genetic driver, either the SDH VUS or an unknown cause, will dictate their medical treatment (see **Chapter 4**). Importantly, several tumors and tumor syndromes that can arise are from inherited *SDHx* mutations, so these patients and their family members are potentially at risk. Currently, if a patient has a VUS it is assumed not to affect protein function and tumor screening for either the patient or family members is not

recommended. *It is important to first identify whether or not the variants affect function before giving screening recommendations to patients and their families.*

Specifically, for SDH, the medical genetics field recognizes the importance of classifying these VUS as loss of function or no effect. Several approaches, including genotype-phenotype correlation and bioinformatic analyses, have attempted to classify these VUS but has many disadvantages. The most popular approach is to establish genotype-phenotype correlations from patients that present with a SDH VUS. This can be done by looking at the number of times a specific mutation has been identified in a tumor across the population. Several databases are useful for collecting these variants and the associated tumor. The most relevant for SDH are the Leiden Open source Variation Database (LOVD) and ClinVar (Fokkema et al. 2011; Landrum et al. 2016). Unfortunately, since these are rare tumor types, usually the variant has only been reported once. Another approach to genotype-phenotype correlation is assessing SDHB and SDHA protein expression by immunohistochemistry (IHC) and classifying the mutation based on protein expression. Regrettably, IHC for these proteins is not widely applied and the results are sometimes inconclusive. Also, there are instances where a patient presents with an *SDHx* VUS and normal SDH expression as assessed by IHC. Finally, bioinformatic approaches like using SIFT, Polyphen, and MutationAssessor have been used to predict which amino acids changes would likely decrease protein function (Vaser et al. 2016; Adzhubei et al. 2010; Reva, Antipin, and Sander 2011). These approaches do not always agree with one another making the results difficult to interpret. Overall, there is agreement that functional studies are necessary to classify these variants. Several groups have turned to a yeast model to investigate the functional consequences of these VUS (Panizza et al. 2013;

Alston et al. 2012; Goffrini et al. 2009; Kim et al. 2012; Burnichon et al. 2010). See **Chapter 2** for our integrated approach to classifying SDH VUS.

1.7.5. Genetic counseling and tumor screening recommendations

Unfortunately, there are no evidence-based genetic counseling guidelines for patients with known pathogenic *SDHx* mutations, however several experts agree that tumor surveillance screening is an important tool for disease management in these patients (Raygada et al. 2014; Lenders et al. 2014; Tufton et al. 2016; Bausch et al. 2017; Pasini and Stratakis 2009; Prodanov et al. 2009; King et al. 2011). In general, these reports agree on the screening protocol for patients with loss-of-function (pathogenic) *SDHx* mutations. However, our incomplete understanding of penetrance and overall risk for patients with VUS make it difficult to know how often to perform and at what age to start screening procedures (Raygada et al. 2014). Early detection of PGL/PC requires whole-body imaging, done by MRI from pelvis to neck every 2-3 years (Lenders et al. 2014). Additionally, annual urine analysis for catecholamines (epinephrine, norepinephrine, dopamine and vanillylmandellic acid) produced by some of these PGL is advised (Pasini and Stratakis 2009). Since MRI is not the best screening tool for gastric GIST detection, regular endoscopies are also recommended. A significant number of patients under the age of 10 have been diagnosed with these tumors. Therefore screening is recommended to start at age 5-7 especially in patients with *SDHB* mutations (Raygada et al. 2014; Prodanov et al. 2009; King et al. 2011).

2. CHAPTER TWO: Biochemical, Molecular, and Clinical Characterization of Succinate Dehydrogenase Subunit A Variants of Unknown Significance

Amber E. Bannon, Jason D. Kent, Isaac Forquer, Ajia Town, Lillian R. Klug, Kelly E. McCann, Carol Beadling, Oliver Harismendy, Jason K. Sicklick, Christopher L. Corless, Ujwal Shinde, and Michael C. Heinrich

2.1. Preface

There is a clear link between loss of SDH function and cancer development. However, in the case of germline *SDHx* variants with unknown significance, it is unclear how to counsel such patients about enhanced cancer surveillance procedures and testing of other family members to determine the risk of having a cancer susceptibility syndrome.

SDHA is the most commonly mutated SDH subunit in WT GISTs. Despite this, the vast majority of clinically observed *SDHA* variants have not been functionally characterized and are of uncertain significance. Mutations of uncertain clinical significance make it difficult to know if tumorigenesis is driven by a deficiency in SDH or a different oncogenic pathway, even in the cases of tumors that are known to be SDH-deficient due to severely reduced or absent expression of SDHB. Understanding which pathway is abnormal in GIST affects many treatment decisions such as targeted therapies as well as counseling patients on their risk of future disease. Patients with clinically significant, germline SDHA mutations are at high risk for acquiring other cancers that are associated with SDH-deficiency. Thankfully, if we understand which patients have loss-of-

function mutations, we can screen for the development of tumors, allowing early detection and surgical removal which is essentially curative. *To optimize clinical care of these patients, we first need to understand which SDHA mutations are pathogenic vs. non-pathogenic.*

This manuscript which was published in *Clinical Cancer Research* (Bannon, Kent, et al. 2017) categorizes these VUS as loss-of-function (pathogenic) or not affecting function (non-pathogenic) using data from clinical observations, a functional yeast model, and a computational model.

2.2. Abstract

Purpose:

Patients who inherit a pathogenic loss-of-function genetic variant involving one of the four succinate dehydrogenase (SDH) subunit genes have up to an 86% chance of developing one or more cancers by the age of 50. If tumors are identified and removed early in these high-risk patients, they have a higher potential for cure. Unfortunately, many alterations identified in these genes are variants of unknown significance (VUS), confounding the identification of high-risk patients. If we could identify misclassified SDH VUS as benign or pathogenic SDH mutations, we could better select patients for cancer screening procedures and remove tumors at earlier stages.

Experimental Design:

In this study, we combine data from clinical observations, a functional yeast model, and a computational model to determine the pathogenicity of 22 *SDHA* VUS. We gathered *SDHA* VUS from two primary sources: The OHSU Knight Diagnostics Laboratory

and the literature. We used a yeast model to identify the functional effect of a VUS on mitochondrial function with a variety of biochemical assays. The computational model was used to visualize variants' effect on protein structure.

Results:

We were able to conclude functional effects of variants using our three-prong approach to understanding VUS. We determined that 16 (73%) of the alterations are pathogenic, causing loss of SDH function, and six (27%) have no effect upon SDH function.

Conclusions:

We report the reclassification of the majority of the VUS tested as pathogenic, and highlight the need for more thorough functional assessment of inherited SDH variants.

2.3. Translational relevance

Molecular testing plays an important role in the clinical management of GIST, including decision making about the most appropriate medical or surgical therapy. As the routine use of multi-gene sequencing panels has expanded, there has also been an increase in reported variants of unknown significance (VUS) of the *SDHA* gene. In many cases, these *SDHA* VUS are present in the germline and are therefore potentially heritable by other family members. In order to understand the functional consequences of these variants, we combined clinical observations, data from a functional yeast model, and computational modeling to classify these *SDHA* VUS as having no effect or causing loss of function. These results will be helpful for appropriate genetic counseling of individuals

with these germline variants. In addition, our data highlight the limitations of SDHA immunohistochemistry in clinical testing of tumors with SDHA VUS.

2.4. Introduction

SDH, succinate dehydrogenase, also known as complex II of the electron transport chain (ETC), is a four-subunit complex encoded by nuclear genes (SDHA, SDHB, SDHC, and SDHD, collectively referred to as SDHx). The assembled SDH complex localizes to the inner membrane of the mitochondria and links the tricarboxylic acid (TCA) cycle to the ETC, making SDH function critical for aerobic respiration (Bezawork-Geleta et al. 2017).

Loss-of-function mutations affecting the SDH complex predispose patients to develop multiple cancers, including GIST, paraganglioma, pheochromocytoma, renal cell carcinoma, Hodgkin lymphoma, chronic lymphocytic leukemia, thyroid cancer, pituitary adenomas, and neuroendocrine tumors of the pancreas (Janeway et al. 2011; Burnichon et al. 2012; Baysal 2007; Beamer 2014; Niemeijer et al. 2015). Tumor formation due to SDH-deficiency requires the complete loss of function of at least one SDHx subunit (e.g. A, B, C, or D), causing destabilization and loss of enzymatic function of the entire SDH complex (van Nederveen et al. 2009). There are several genetic mechanisms that can lead to SDH-deficiency. Typically, loss of function of an SDHx subunit is the result of a combination of an inactivating germline mutation (first hit) with a somatic loss of heterozygosity or other inactivating mutation affecting the other allele (second hit). Less commonly, loss of SDH complex occurs due to somatic inactivation of both alleles of a given complex subunit or SDH assembly factor. Finally, SDH-deficiency can be caused by an *SDHC* epimutation, defined as hypermethylation of the *SDHC* promoter, which leads to repression of SDHC

transcription and depletion of SDHC protein levels, without a known underlying heritable cause (Killian et al. 2014).

Importantly, germline loss-of-function genetic *SDHx* variants are associated with a high lifetime risk of developing the aforementioned malignancies. For example, the chance of a patient with germline loss-of-function *SDHD* variant of developing one or more primary tumors by the age of 50 was reported to be 86% (Ricketts et al. 2010; Neumann et al. 2004). Therefore, if we could identify high-risk patients through genetic testing and follow them serially with specialized screening tests, early tumor detection may lead to curative surgical resection before the tumors are metastatic/incurable. Early detection is crucial since there are no effective medical treatments for patients with advanced SDH-deficient cancers.

Currently, an SDH-deficient tumor is identified by measuring SDHB protein abundance using immunohistochemistry (IHC); absence of SDHB protein is indicative of loss of SDH function. However, it can be challenging to determine the underlying cause of SDH-deficiency in a tumor lacking SDHB expression. Clinical sequencing panels may turn up missense mutations in SDHx genes, but many of these are VUS. In addition, such panels can miss large intragenic deletions, and are not designed to identify epigenetic silencing of the *SDHC* promoter. Some SDHB, C, and D VUS have been functionally characterized to determine their effect on function, and thus their pathogenicity in tumors like paraganglioma and pheochromocytoma. However, the study of the functional consequences of SDHA VUS has lagged behind that of other SDHx subunits (van Nederveen et al. 2009).

GIST is a heterogeneous group of tumors that arise from the interstitial cells of Cajal (ICC). However there are several different driver genes that when mutated give rise to GIST (Bannon, Klug, et al. 2017). The molecular classification of GIST is especially important because of the treatment implications of the different genetic drivers. The majority of GISTs have an activating receptor tyrosine kinase (RTK) mutation but about 13% of GIST lack RTK mutations (RTK-WT). Most RTK-WT GIST are SDH-deficient as assessed by immunohistochemistry (IHC) for SDHB. *SDHA* pathogenic variants are found in 47% of SDH-deficient GIST, and the majority of these *SDHA* mutations are germline, and thus heritable, variants (Evenepoel et al. 2015). However, some of the *SDHA* variants we find in GIST are VUS. A universal problem in the field is that these variants are rarely seen with a complete clinical and pathogenic annotation making it difficult to draw conclusions on functional effect from clinical data alone. Our study gathered these VUS from two primary sources; OHSU and the literature (Evenepoel et al. 2015). We then combine data from clinical observations, a functional yeast model, and a computational model to understand the effects of *SDHA* VUS identified in GIST specimens on SDH complex function. Historically, yeast have been a robust system for identifying the assembly and enzymatic activity of SDH (Hao et al. 2009; Van Vranken et al. 2014; Na et al. 2014). In addition, yeast have proven to be an ideal model to study the functional effect of *SDHB*/*C*/*D* variants on SDH complex activity (Panizza et al. 2013; Goffrini et al. 2009; Szeto et al. 2007; Alston et al. 2015). Yeast are able to survive without functional mitochondria (e.g. lacking SDH complex activity) if they are provided a fermentable carbon source; thus, they provide a unique model system to study the biochemical effects of *SDHA* VUS (Fontanesi, Diaz, and Barrientos 2009).

Based on our findings, we discriminated between *SDHA* VUS that affected or did not affect SDH complex activity, and thus, their potential for pathogenicity. These data will aid clinicians' ability to provide genetic counseling and tumor surveillance to patients with germline inheritance of these specific *SDHA* variants.

2.5. Materials and methods

Yeast strains and vectors. All *Saccharomyces cerevisiae* strains used in this study were derivatives of BY4741 (MATa *his3Δ1 leu2Δ0 met15Δ0 ura3Δ0*). The *SDH1* (yeast homolog to *SDHA*) deletion strain (*sdh1Δ)* was purchased from ATCC (catalog #4004998). The *sdh1Δ* was constructed as part of the *Saccharomyces* Genome Deletion Project by homologous recombination using the *KanMX4* cassette (Winzeler et al. 1999). We verified the deletion of *SDH1* using PCR mapping of the *SDH1* locus with primer pairs recommended by the *Saccharomyces* Genome Deletion Project.

An amplicon containing the WT *SDH1* (including the native *SDH1* promoter and 3' UTR) was generated from WT BY4741 and cloned into the pRS416 plasmid (Sikorski and Hieter 1989) (ATCC) and expressed in the *sdh1Δ* strain. The *SDH1* point mutations were introduced by QuikChange mutagenesis PCR system (Agilent Technology, cat #200521). All mutations were confirmed by Sanger sequencing. Yeast strains were transformed using Frozen EZ Yeast Transformation II (Zymo Research, catalog # T2001). Strains were grown in synthetic complete medium lacking uracil to maintain plasmid selection with either 2% glucose or 3% glycerol as the carbon source.

Alignment of multiple species' succinate dehydrogenase flavoprotein subunit. Cluster Omega was used to align the protein sequences of SDH flavoproteins including *E. coli* (P0AC41), yeast (Q00711), human (P31040), and pig (Q0QF01).

Immunoblotting. Intact mitochondria were isolated using a previously described method (Muller, Crofts, and Kramer 2002). Steady-state levels of mitochondrial proteins were resolved on SDS-PAGE, transferred to nitrocellulose membrane, probed using the indicated primary antibodies and visualized using Amersham enhanced chemiluminescence (ECL) Western Blotting Detection Reagent (GE life sciences, catalog #RPN2106) with horseradish peroxidase-conjugated secondary antibodies (BioRad, catalog #1662408EDU). We used previously described polyclonal rabbit antibodies for immunodetection of Sdh1 and Sdh2 (Kim et al. 2012). Anti-porin was purchased from ThermoFisher Scientific (catalog # 459500).

Analysis of Sdh1-bound flavin adenine dinucleotide (FAD) and total mitochondrial FAD. Levels of FAD covalently bound to Sdh1 were analyzed as previously described (Hao et al. 2009; Bafunno et al. 2004). Briefly, mitochondrial proteins were resolved on SDS-PAGE and the gel was placed in a 10% acetic acid solution for 20 minutes to oxidize flavin. FAD was visualized upon exposure to UV light using a Bio-Rad ChemiDoc MP Imaging System.

Oxygen consumption assay. Yeast strains were grown to confluency in glucose-based media and then switched to glycerol-based media for 12 hours. Two million cells were plated onto commercially available microplates with oxygen sensors (Oxoplate; PreSens catalog #OP96U) (Kitanovic et al. 2012). Kinetic reading of oxygen consumption was measured using a spectrofluorometer. A Student's t-test was used to determine statistical significance between a variant of interest and yeast complemented with WT Sdh1.

Computational modeling of Sdh1 variants. A model of yeast Sdh1 (Q00711) from the Swiss Model repository was refined using Yasara Homology Modelling to include the liganded flavin adenine dinucleotide (FAD) interactions with the peptide chain, followed by optimization of the loop and side-chains interactions. Side-chain rotamers were fine-tuned considering electrostatic and knowledge-based packing interactions as well as solvation effects. An unrestrained high-resolution refinement with explicit solvent molecules was run, using YAMBER, a second-generation self-parameterizing force field derived from the AMBER force field. Clinically identified variants were introduced in the homology model, and the structures were minimized as described earlier. The variants were compared with the wild-type (WT) model of *E. coli* or yeast Sdh1 using PYMOL.

FoldX analysis. FoldX was used to measure the effect of point mutations on the stability of the Sdh1 yeast model (Schymkowitz et al. 2005). Except as noted, we used the default software settings. The move neighbors setting was turned off, and the average ΔΔG was calculated after three runs.

Mutation analysis. We gathered *SDHA* VUS from two primary sources: The OHSU Knight Diagnostics Laboratory (Portland, OR) and the literature (Evenepoel et al. 2015). The majority of the variants pulled from the literature were found in a review highlighting the need for a functional model to characterize *SDHx* variants of unknown significance (Evenepoel et al. 2015). The remaining literature variants are from a paper identifying novel causes of GIST that were WT for any known oncogenic driver of GIST (Shi et al. 2016). A collaboration with the OHSU Knight Diagnostics Laboratory, which offers a targeted exome panel to identify genetic drivers in GIST which includes all four SDHx subunits (GeneTrails GIST panel), lead to identification of several novel variants. All of the

variants came from tumor samples that lacked any known oncogenic driver of GIST (e.g. no KIT mutations).

2.6. Results

2.6.1. Clinical analysis

All the known clinical information on the *SDHA* VUS identified in this study including SDHA/B IHC, tumor mutant allele fraction, other disease references, population data from the ExAC database (Lek et al. 2016), and ClinVar clinical significance (Landrum et al. 2016) is listed in **Table 3**. Unfortunately, there were few variants with complete clinical and pathological annotation, emphasizing the challenge of trying to understand the functional effects of these variants from available clinical data alone. Currently, SDHx subunit testing remains uncommon for GIST and only a limited number of reference laboratories offer this testing. However, these laboratories usually do not have access to full clinical annotation and/or prior SDHB IHC testing results. This limitation applies to the published cases as well as the cases from the Knight Diagnostic laboratory. We listed all available additional clinical information for tumors with VUS **Table 4**.

hSDHA mutation	ySdh1 mutation	Source	SDHB/ SDHA IHC	Tumor mutant allele fraction	Other disease references	Allele frequency from EXAC database	ClinVar clinical significance	Conclusions drawn
R31X	R19X	Control	Neg/neg (Italiano et al. 2012)	N/A	GIST (Italiano et al. 2012; Pantaleo et al. 2011) Paraganglioma (Korpershoek et al. 2011)	1.647×10^{-4}	Pathogenic/ Likely pathogenic	LOF (control)
H99S	H90S	Control (Hao et al. 2009)	N/A	N/A	None	N/A	N/A (H99Y Likely pathogenic)	LOF (control)
G106R	G97R	OHSU	N/A	92%	Novel	N/A	N/A	LOF
N118S	N109S	OHSU	N/A	50.7%	Novel	N/A	N/A	No effect
T143M	T134M	Literature (Shi et al. 2016)	N/A	22%	Novel	N/A (T143R reported 8.31×10^{-6})	Uncertain significance	LOF
R171H	R162H	OHSU	N/A	34%	Novel	8.24×10^{-6}	Uncertain significance	No effect
R171H	R162H	OHSU	N/A	40.3%	Novel	8.24×10^{-6}	Uncertain significance	No effect

R188W	R179W	Literature (Evenepoel et al. 2015)	Neg/pos [30]	N/A	None	N/A (R188Q reported 1.65×10^{-5})	N/A	LOF
R195W	R186W	OHSU	Neg/ND	66.7%	GIST (Miettinen et al. 2013)	N/A (R195Q reported 8.23×10^{-6})	N/A	No effect
G260R	G251R	Literature (Evenepoel et al. 2015)	Pos/pos [32]	N/A	None	N/A	Uncertain significance	LOF
H296Y	H287Y	Literature (Shi et al. 2016)	N/A	87%	Novel	N/A	N/A	LOF
R312C	R303C	OHSU	N/A	34.5%	Novel	N/A	N/A (R312P Uncertain significance)	LOF
R408C	Y399C	OHSU	N/A	52.8%	GIST(Heinrich et al. 2017); late onset neurodegenerative disease (Birch-Machin et al. 2000)	N/A	N/A	LOF
G419R	G410R	OHSU	N/A	77%	GIST (Pantaleo et al. 2014)	N/A	N/A	LOF
C438F	C431F	OHSU	N/A	48.5%	Novel	N/A	N/A	LOF
G439E	G432E	OHSU	N/A	87.6%	Novel	N/A	N/A	LOF

R451C	R444C	Literature (Shi et al. 2016)	N/A	18%	Complex II deficiency (Birch-Machin et al. 2000)	N/A (R451H reported 8.23×10^{-6})	N/A	LOF
R451H	R444H	OHSU	N/A	47.5%	Novel	8.23×10^{-6}	N/A	LOF
R451H	R444H	OHSU	N/A	39.5%	Novel	8.23×10^{-6}	N/A	LOF
A454E	A447E	Literature (Evenepoel et al. 2015)	Neg/pos [31]	N/A	None	N/A	N/A (A454T Uncertain significance)	LOF
R465W	R458W	OHSU	N/A	50%	Novel	8.23×10^{-6}	Uncertain significance	LOF
T508I	T501I	OHSU	N/A	50.6%	Cardiomyopathy and Leukodystrophy (Alston et al. 2012)	7.60×10^{-4}	Conflicting interpretations of pathogenicity	No effect
R589G	R582G	OHSU	N/A	40.2%	Paraganglioma (Burnichon et al. 2010)	8.29×10^{-6}	Uncertain significance	LOF
H625W	H601Y	Literature (Evenepoel et al. 2015)	Neg/neg [39]	N/A	Pituitary adenoma and Pheochromocytoma/paraganglioma	N/A	N/A	LOF
Y629F	W605F	OHSU	N/A	99.6%		1.52×10^{-1}	Benign/likely benign	No effect
V657I	V633I	OHSU	N/A	95.1%	Not pathogenic (Baysal, Lawrence, and Ferrell 2007)	1.30×10^{-1}	Likely benign	No effect

Table 3. Clinical variants of human SDHA with unknown significance.
All of the genetic variants were found in GIST, except for hG260R which was found in a paraganglioma. A summary of available clinical data for each variant is listed, including source of the variant, clinical IHC results for SDHB/SDHA, frequency of the variant in tumor, other SDHA variants found in the same tumor, information on functional effect of other variants in the tumor, other disease references to the variant of interest in the literature, population allele frequency, and results from our yeast model. The no effect variants are highlighted in grey for clarity. Loss of function (LOF); Not available (N/A); Not Done (ND); neg (negative- SDHx absent); pos (positive- SDHx expression).

hSDHA mutation	**ySdh1 mutation**	**Frequency of mutation in tumor**	**Info on other mutations**	**Conclusions drawn**
R31X	R19X	N/A	N/A	LOF
H99S	H90S	N/A	N/A	LOF
G106R	G97R	1. G106R (92%)	N/A	LOF
N118S	N109S	1. N118S (50.7%) 2. V657I (45.3%) germline	V657- no effect in this yeast model	No effect Tumor cause unknown
T143M	T134M	1. T134M (22%)	N/A	LOF Tumor cause unknown
R171H	R162H	1. R171H (34%) 2. R31X (~50%)	R31X (used as neg control in yeast model) Known pathogenic (Italiano et al. 2012) (Korpershoek et al. 2011)	No effect Tumor cause unknown
R171H	R162H	1. R171H (40.3%)	N/A	No effect Tumor cause unknown
R188W	R179W	N/A	N/A	LOF
R195W	R186W	1. R195W (66.7%)	N/A	No effect Tumor cause unknown
G260R	G251R	N/A	N/A	LOF
H296Y	H287Y	1. H296Y (87%)	N/A	LOF
R312C	R303C	1. R312C (34.5%)	D38V- likely pathogenic (Italiano et al. 2012)	LOF

		2. D38V (45%) germline		
R408C	Y399C	1. Y408C (52.8%) 2. R451H (47.5%) somatic	R451H- likely pathogenic (Boikos, Pappo, et al. 2016)	LOF
G419R	G410R	1. G419R (77%)	N/A	LOF
C438F	C431F	1. C438F (48.5%) 2. R589W (40.2%)	R589W- likely pathogenic	LOF
G439E	G432E	1. G439E (87.6%)	N/A	LOF
R451C	R444C	1. R451C (18%) 2. R171H (49%)	R171H- no effect in this yeast model	LOF Tumor cause unknown (R171H)
R451H	R444H	1. R451H (47.5%) 2. Y408C (52.8%) somatic	Y408C- LOF in this yeast model	LOF
R451H	R444H	1. R188W (52%) 2. R451H (39.5%) germline 3. V657I (45%). germline 4. Y629F (61.5%) germline	R188W- LOF in this yeast model V657I and Y629F- no effect in this yeast model	LOF
A454E	A447E	N/A	N/A	LOF
R465W	R458W	1. R465W (50%) 2. V657I (95.1%) germline	V657- no effect in this yeast model	LOF Tumor cause unknown
T508I	T501I	1. T508I (50.6%) 2. V657I (49.2%)	V657- no effect in this yeast model	No effect Tumor cause unknown
R589G	R582G	1. R589G (40.2%) 2. R312H (38%) somatic	R312H- R312C caused LOF in yeast model	LOF
H625W	H601Y	N/A	N/A	LOF
Y629F	W605F	1. Y629F (99.6%) germline	N/A	No effect Tumor cause unknown

V657I	V633I	1. R465W (50%) 2. V657I (95.1%) germline	R465W- LOF in this yeast model	No effect Tumor cause unknown

Table 4. Additional clinical information on tumors with variants characterized in this study

2.6.2. Functional studies in yeast

To understand the functional consequences of VUS in human *SDHA*, we used complementation studies in a yeast strain lacking Sdh1 (*sdh1Δ*). The flavoprotein subunit of the SDH complex is highly conserved across all species, including yeast Sdh1 (ySdh1) and human SDHA (hSDHA) (**Figure 14**). For simplicity, we use yeast nomenclature throughout this study and reference the corresponding human variant in all of the tables.

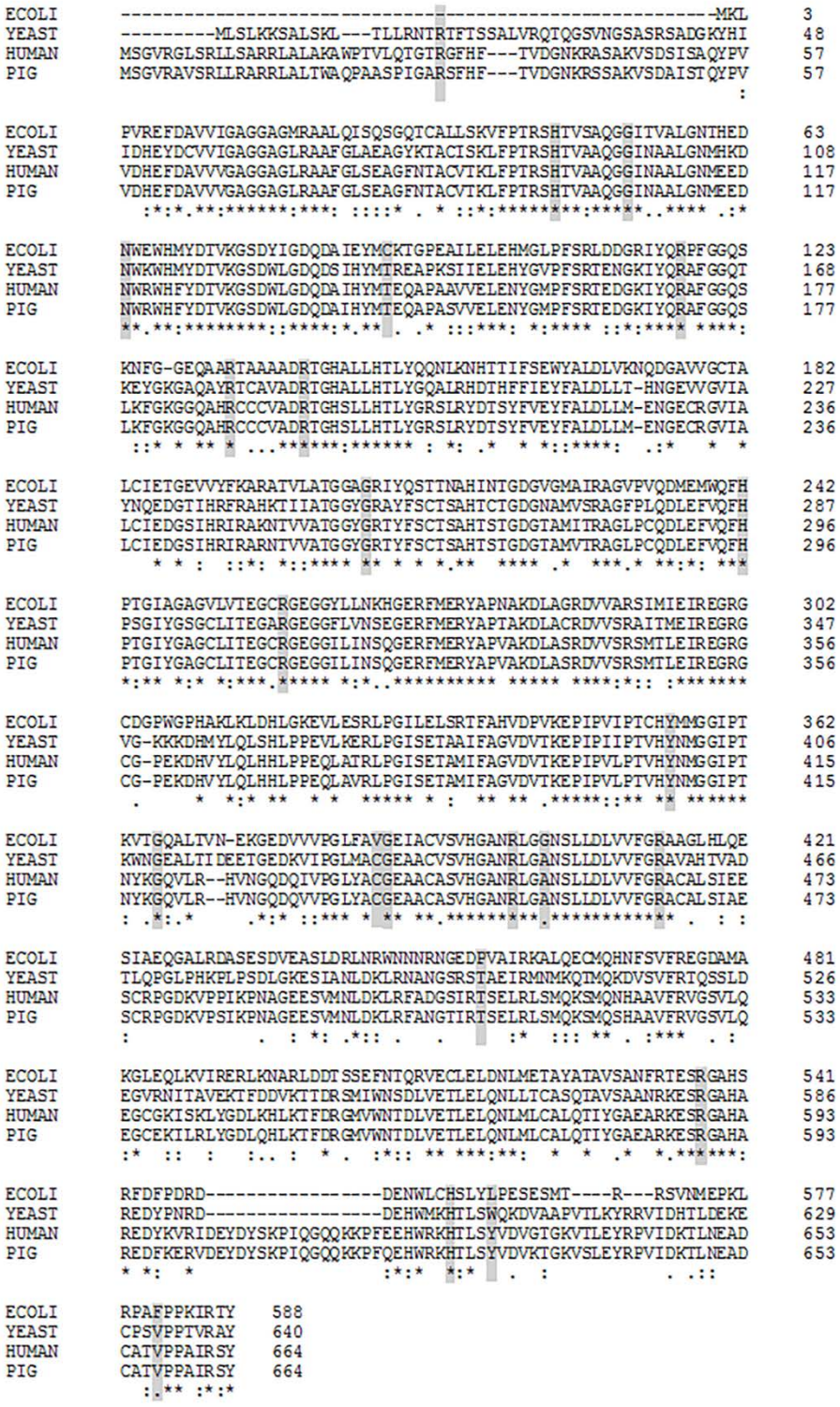

Figure 14. Alignment of SDH flavoprotein across multiple species.

WT variants that are used in this study are highlighted using a gray box. Consensus analysis using the standard Clustal Omega key is shown under each group of residues.

As a positive control, we generated a WT *SDH1* amplicon from BY4741 that included the promoter and the 3' UTR which was cloned into a pRS416 plasmid and expressed in *sdh1Δ* yeast. We used *sdh1*Δ as our negative control. S*dh1*Δ do not have a functional SDH complex and were unable to utilize their mitochondria for canonical TCA or ETC pathways, allowing growth on a fermentable carbon source (glucose), but preventing growth with a non-fermentable carbon source such as glycerol (**Figure 15**).

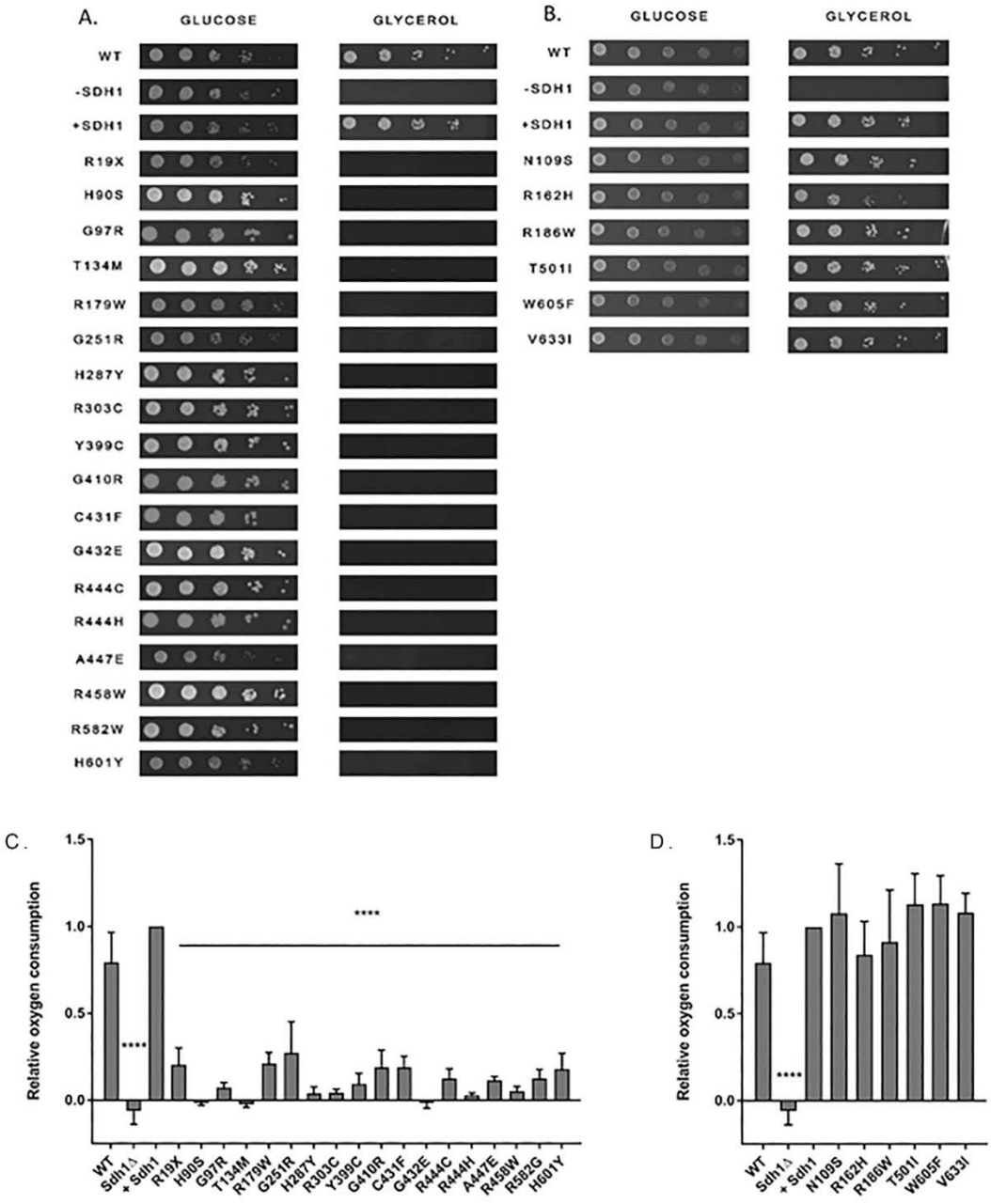

Figure 15. ySdh1 variants causing loss of function are unable to use glycerol as a sole carbon source or consume oxygen.

Yeast were grown to a confluency of 2 x 10^7/mL and then serially diluted and plated onto either glucose or glycerol media plates (Left to right: highest to lowest). All variants, regardless of SDH complex function, can grow on glucose but only those variants that complement *sdh1Δ* and restore SDH complex activity are able to grow on glycerol and consume oxygen. A. Loss-of-function variants that are unable to grow with glycerol as their sole carbon source. B. Variants with no effect are able to grow with glycerol as their sole carbon source. C. Sdh1 variants that consume significantly less oxygen than cells complemented with WT Sdh1

(+Sdh1 control). D. Variants that consume oxygen at a similar rate to the +Sdh1 control. **** p-value <0.0001

Complementation with WT *SDH1* (+Sdh1) restored growth on glycerol (**Figure 15**). Using this strategy, we tested the ability of plasmids encoding individual VUS to complement the *sdh1Δ* strain and restore a normal growth phenotype. The two loss-of-function controls (yR19X and yH90S), as well as 16 of the variants shown in **Figure 15** (yG97R, yT134M, yR179W, yG251R, yH287Y, yR303C, yY399C, yG410R, yC431F, yG432E, yR444C, yR444H, yA447E, yR458W, yR582G, yH601Y) were unable to grow on glycerol, indicating that these variants result in loss of oxidative phosphorylation (**Figure 15A**). In contrast, six of the variants (yN109S, yR162H, yR186W, yT501I, yW605FF, yV633I) were able to grow on glycerol, indicating these variants had no effect on the Sdh1 function as their phenotype was the same as WT Sdh1 (**Figure 15B**).

As a secondary measure of SDH complex activity, we measured oxygen consumption to assess oxidative phosphorylation, a surrogate for measuring the ability of the SDH complex to transfer electrons to the ETC. In concordance with our previous results, the same 18 variants that were unable to grow on glycerol consumed significantly less ($p<0.0001$) oxygen than WT Sdh1 (**Figure 15C**). Variants that grew on glycerol had similar oxygen consumption to WT Sdh1, confirming that these variants do not disrupt the ETC (**Figure 15D**). To ensure oxygen consumption was due to the ETC, azide was added to each cell strain, and this promptly abolished oxygen consumption for all controls and variants.

To better understand how each variant affects Sdh1 protein function, we measured the covalent attachment of FAD to Sdh1, a process known as flavination. We also measured the protein abundance of Sdh1 and Sdh2 (**Figure 16**). Sdh1 flavination is critical for the catalytic activity of Sdh1; without covalent attachment of flavin, the Sdh1 protein is unable to oxidize succinate (Hao et al. 2009). As a positive control for a variant that inhibited insertion of FAD into Sdh1, we used the previously described Sdh1 H90S variant (Hao et al. 2009). Variants that complemented *sdh1*Δ yeast in our functional assays had similar levels of flavinated Sdh1, total Sdh1, and total Sdh2 as yeast complemented with WT Sdh1 (**Figure 16D**). However, variants that were unable to perform oxidative phosphorylation had differential effects on the levels of flavinated Sdh1 and total Sdh1 protein (**Figure 16A-C**). Some loss-of-function variants inhibited flavination without affecting the abundance of Sdh1 (H90S, G97R, T134M, R444C, H601Y) while others caused a marked decrease in Sdh1 protein abundance (R179W, G251R, H287Y, R303C, Y399C, G410R, C431F, G432E, R444H, A447E, R458W, R582G). All of the loss-of-function variants resulted in a decrease in Sdh2 protein abundance, consistent with loss of a functional SDH complex as described previously (Kim et al. 2012). In a subset of no effect and loss-of-function variants, we confirmed that Sdh1 mRNA expression was not significantly different from WT.

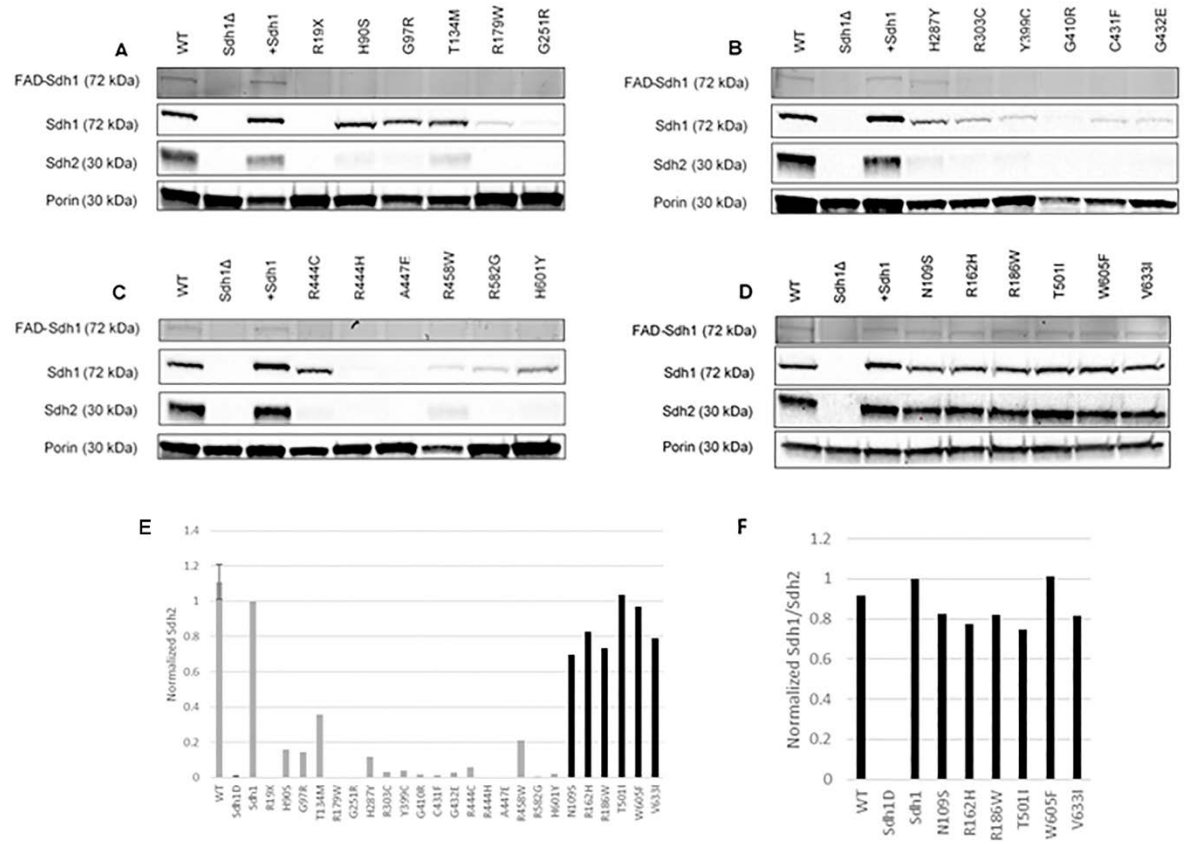

Figure 16. Abundance of flavinated Sdh1, total Sdh1, and total Sdh2 in mitochondrial lysates from yeast expressing each variant.
Western blotting of mitochondrial lysates from each variant are shown. Positive and negative control lanes are included on each western blot (WT, SDH1Δ, +SDH1). WT and +Sdh1 show bands at expected size for each protein. Sdh1Δ does not show bands for Sdh1-FAD, Sdh1, or Sdh2, but does have normal expression of the mitochondrial marker, porin. A-C. Loss-of-function variants are shown in numerical order by altered amino acid residue. D. No effect variants are shown in numerical order by altered amino acid residue and have with no reduction in flavin, Sdh1, or Sdh2 expression compared to WT controls. E. Sdh2 protein abundance was calculated relative to Sdh1 and then normalized to porin (control for mitochondrial protein loading). The no effect variants are labeled in black, while the loss-of-function variants are in gray. No effect variants have Sdh2 protein abundance more similar to complemented Sdh1 and loss-of-function variants have decreased Sdh2 similar to *sdh1Δ*. F. Ratio of Sdh1/Sdh2 protein abundance in no effect variants.

Based on all of the above results, we characterized 16 variants (73%) as causing loss of function and six variants (27%) as having no effect on SDH function (**Table 5**). All the loss-of-function variants were unable to grow on glycerol, had decreased oxygen

consumption, and showed decreased Sdh2 protein abundance. In contrast, the no effect group had similar results to cells complemented with WT Sdh1 protein in these assays.

hSDHA mutation	ySdh1 mutation	Growth phenotype on glycerol	Oxygen consumption (% of complemented)	Sdh2 protein (% of complemented)	Structural implications of variants	Group name
R31X (control)	R19X (control)	Unable to grow	Decreased (20%)	Decreased (0%)	Truncates mitochondrial targeting sequence (Chapman, Solomon, and Boeke 1992)	Loss-of-function (control)
H99S (control)	H90S (control)	Unable to grow	Decreased (-2%)	Decreased (15%)	Inhibits covalent bond to FAD (Hao et al. 2009)	Loss-of-function (control)
G106R	G97R	Unable to grow	Decreased (7%)	Decreased (14%)	Distorts the active site (Iverson 2013)	Loss-of-function
N118S	N109S	Growth	Similar (108%)	Similar (83%)	Surface of protein	No effect
T143M	T134M	Unable to grow	Decreased (3%)	Decreased (35%)	No obvious disturbances but causes loss of function	Loss-of-function
R171H	R162H	Growth	Similar (84%)	Similar (78%)	Surface of protein	No effect
R188W	R179W	Unable to grow	Decreased (21%)	Decreased (0%)	Disrupts salt bridge with D108	Loss-of-function
R195W	R186W	Growth	Similar (91%)	Similar (82%)	Surface of protein	No effect
G260R	G251R	Unable to grow	Decreased (27%)	Decreased (0%)	Obstructs flavin binding pocket	Loss-of-function

H296Y	H287Y	Unable to grow	Decreased (4%)	Decreased (11%)	Inhibits succinate binding (Iverson 2013)	Loss-of-function
R312C	R303C	Unable to grow	Decreased (4%)	Decreased (3%)	Contributes to proper orientation and activation of the flavin isoalloxazine ring to facilitate formation of the covalent FAD bond and disrupts salt bridge (Cecchini et al. 2002)	Loss-of-function
R408C	Y399C	Unable to grow	Decreased (9%)	Decreased (4%)	In flavin binding site	Loss-of-function
G419R	G410R	Unable to grow	Decreased (19%)	Decreased (2%)	Distorts helix	Loss-of-function
C438F	C431F	Unable to grow	Decreased (19%)	Decreased (2%)	Bulky change disrupts helix	Loss-of-function
G439E	G432E	Unable to grow	Decreased (-2%)	Decreased (3%)	Obstructs flavin binding pocket	Loss-of-function
R451C	R444C	Unable to grow	Decreased (12%)	Decreased (6%)	Disrupts flavin binding, succinate binding and proton shuttle necessary for catalytic activity (Iverson 2013)	Loss-of-function
R451H	R444H	Unable to grow	Decreased (3%)	Decreased (0%)	Disrupts flavin binding,	Loss-of-function

					succinate binding and proton shuttle necessary for catalytic activity (Iverson 2013)	
A454E	A447E	Unable to grow	Decreased (11%)	Decreased (0%)	Lines succinate binding site (Iverson 2013)	Loss-of-function
R465W	R458W	Unable to grow	Decreased (5%)	Decreased (21%)	Disrupts salt bridge with E136	Loss-of-function
T508I	T501I	Growth	Similar (113%)	Similar (75%)	Surface of protein	No effect
R589G	R582G	Unable to grow	Decreased (12%)	Decreased (0%)	Inhibits C-terminal flavination (Kim et al. 2012)	Loss-of-function
H625W	H601Y	Unable to grow	Decreased (18%)	Decreased (2%)	Inhibits C-terminal flavination	Loss-of-function
Y629F	W605F	Growth	Similar (113%)	Similar (101%)	Surface of protein	No effect
V657I	V633I	Growth	Similar (108%)	Similar (82%)	Surface of protein	No effect

Table 5. Consistent findings across multiple functional assays for each variant in our yeast model.
A summary of results including the growth on glycerol, oxygen consumption, Sdh2 protein abundance, consequences of changing the WT amino acid using computational modeling and literature search for studies in other species' flavoprotein are tabulated along with our classification of each variant based on our yeast model. The no effect variants are highlighted in grey for clarity. Numerical values for oxygen consumption were taken from Figure 15 C and D. Numerical values for Sdh2 protein were taken from Figure 16 E.

2.6.3. Computational modeling

We next performed computational modeling to predict the potential structural implications of each variant. Using the two groups (loss-of-function and no effect) identified in our yeast model, we further characterized each variant by visualizing the location in the Sdh1 protein. Both groups, loss-of-function and no effect, were located throughout the four domains of Sdh1, suggesting that there are not "hotspot" areas or domains for pathogenic variants, unlike the situation for some proteins. Within the loss-of-function group, 12 variants (yH90S (loss-of-function control), yG97R, yG251R, yH287Y, yR303C, yY399C, yG432E, yR444C, yR444H, yA447E, yR582G, yH601Y) were identified as being involved in cofactor (FAD) or substrate (succinate) binding in the Sdh1 active site (Figure 17 **Table 5,** and **Video 1**). Structural studies from the homologous protein quinol:fumarate reductase (QFR) in *E. coli* suggests an important catalytic function for most of these amino acids (Iverson 2013). In addition to the amino acids directly interacting with the flavin binding pocket, it has been previously shown that the C-terminal domain of Sdh1 is crucial for the flavination of Sdh1 (Kim et al. 2012). Two variants located in the C-terminal domain of Sdh1, yR582G and yH601Y, both inhibited flavination of Sdh1. To visualize the substrate (succinate) and cofactor (FAD), which were not visualized using the yeast structure, these Sdh1 variants were modeled using the *E. Coli* crystal structure of Sdh1.

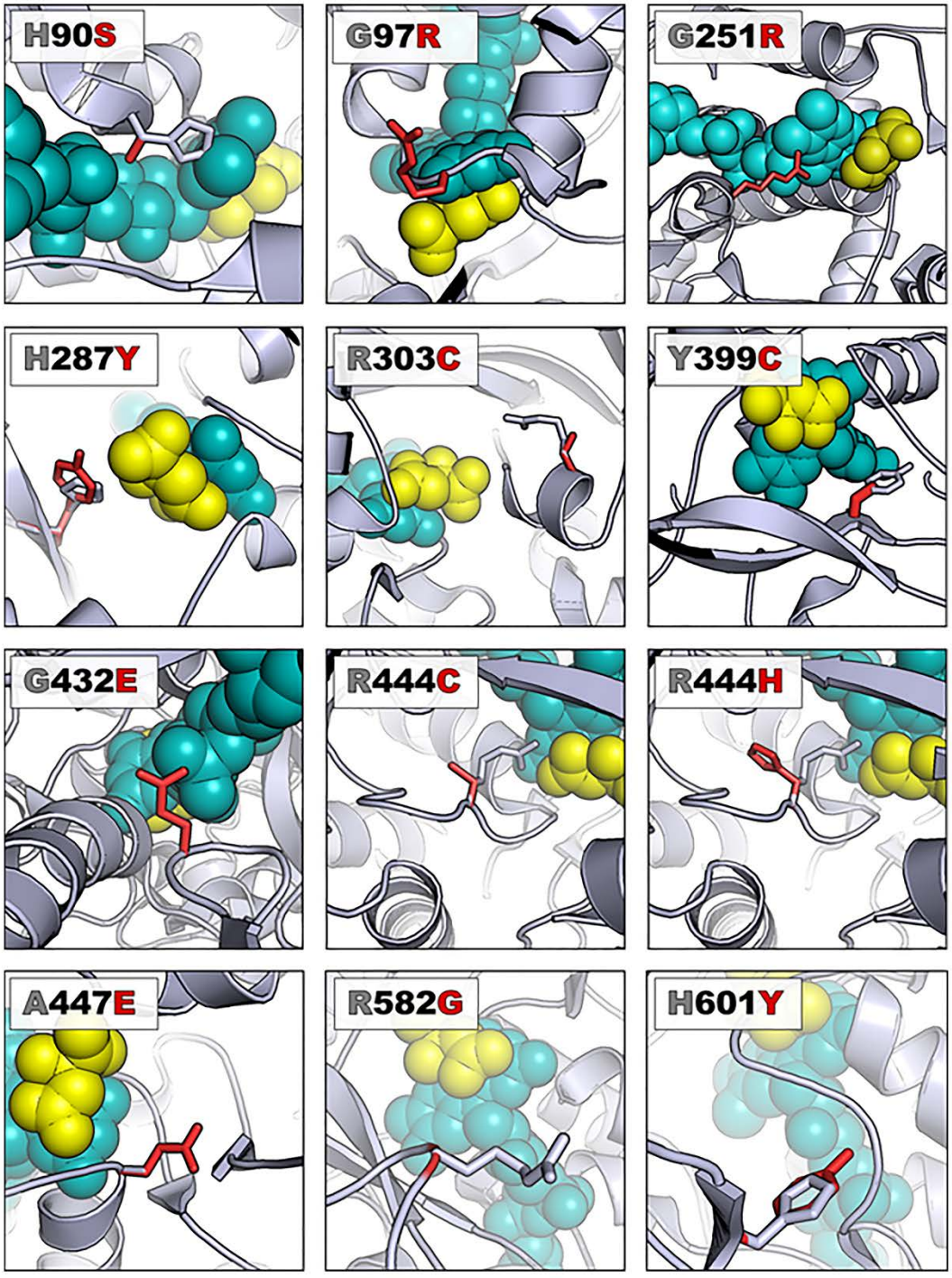

Figure 17. Variants involving the active site cause loss of Sdh1 function.
A ribbon representation of Sdh1 (*E. coli* model PBD file 2WP9) is shown with WT protein carbons colored gray and the variant carbons colored red. The FAD is shown as teal-colored spheres while the dicarboxylic acid substrate (succinate analog) is depicted with yellow-colored spheres. In each case, the view has been

rotated so that residues of interest are clearly observed. References detailing structural implications of each variant can be found in Table 2.

The other six loss-of-function variants (yR19X (control- not picture in computational models because it is an early truncation of the protein), yT134M, yR179W, yG410R, yG431F, yR458W) are not located in the active site of Sdh1. Changes in protein structure based on each of these variants are visualized in **Figure 18A** and **Video 1.** Further, FoldX analyses of the variants compared to WT provided insight on how the variants affect stability (**Table 6**) (Schymkowitz et al. 2005). yT134M, yR179W, yG410R, and yG431F all have positive ΔΔG (change in free energy) indicating these changes are highly destabilizing. Some of these also were associated with decreased Sdh1 protein abundance (**Figure 16**).

Interestingly, all the variants with no functional effects were localized to the surface of the protein (**Figure 18B, Video 1**) where it would be predicted that they would be less likely to affect protein structure and function. Notably, these mutations did not map into any of the known critical domains of Sdh1 or predicted Sdh2 interaction sites.

Video 1. VUS modeled in SDH complex (yeast model PBD file 1ORZ).
Video 1 can be viewed here through Clinical Cancer Research
This movie is designed to complement Figures 3 and 4, where the WT residues have been mutated to model the specific variant of interest. Only WT residues are shown in this model.
The four WT subunits of SDH are individually colored; Sdh1, Sdh2, Sdh3, Sdh4, and FAD are shown in grey, green, orange, purple, and teal, respectively. In the first part of the movie, we zoom in to show the location of residues (depicted in red) surrounding the active site that result in loss of function when mutated. The viewer should note that succinate (substrate) is not depicted, but would also bind in the active site in close approximation to FAD. Later in the movie, we zoom out from the active site to show variants causing loss of function but not involving the active site (also depicted in red). Specifically, the location of potential salt bridge interactions that may be disrupted by mutation of the WT residue are featured.
Finally, the no effect variant residues are shown in yellow. These residues are localized to the surface of Sdh1 and do not interact with Sdh2 (green structure).

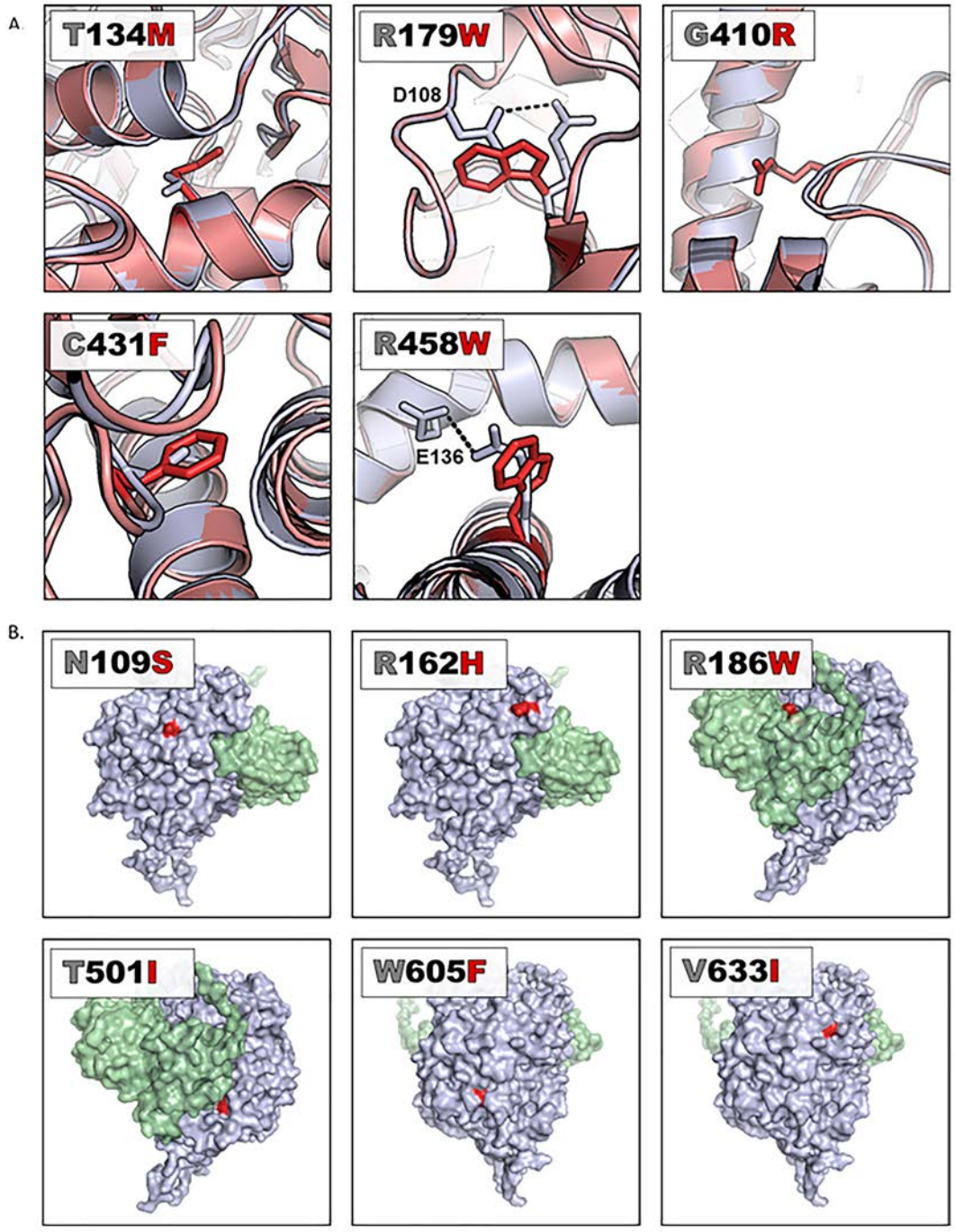

Figure 18. Structural consequences of variants visualized in a yeast model (yeast model PBD file 1ORZ). A. Variants not in the active site causing loss-of-function. WT Sdh1 protein is represented as a gray ribbon with the amino acid of interest labeled as a gray stick and the re-folded variant Sdh1 protein as a red ribbon with the amino acid of interest indicated by a red stick. In each case, the view has been rotated such that residues of interest are clearly observed. Potential structural implications of each variant can be found in Table 2. B. Variants that do not affect protein function are located on the surface of Sdh1. The surface area

of WT Sdh1 is shown in gray, the variant residue is labeled red, and the surface area of Sdh2 is labeled in green. In each case, the view has been rotated such that residues of interest are clearly observed.

hSDHA mutation	**ySdh1 mutation**	**ΔΔG (kcal/mol)**	**Readout**
R31X	R19X	N/A	N/A
H99S	H90S	-0.54	Slightly stabilizing
G106R	G97R	63.07	Highly destabilizing
N118S	N109S	-0.04	Neutral
T143M	T134M	20.58	Highly destabilizing
R171H	R162H	2.38	Highly destabilizing
R188W	R179W	61.94	Highly destabilizing
R195W	R186W	-0.35	Neutral
G260R	G251R	57.42	Highly destabilizing
H296Y	H287Y	50.00	Highly destabilizing
R312C	R303C	0.91	Slightly destabilizing
R408C	Y399C	1.21	Destabilizing
G419R	G410R	72.76	Highly destabilizing
C438F	C431F	49.07	Highly destabilizing
G439E	G432E	8.81	Highly destabilizing
R451C	R444C	-8.15	Highly stabilizing
R451H	R444H	16.98	Highly destabilizing
A454E	A447E	27.20	Highly destabilizing
R465W	R458W	-1.76	Stabilizing
T508I	T501I	1.77	Destabilizing
R589G	R582G	7.66	Highly destabilizing
H625W	H601Y	8.48	Highly destabilizing
Y629F	W605F	0.71	Slightly destabilizing
V657I	V633I	-0.75	Slightly stabilizing

Table 6. FoldX table showing ΔΔG for variants compared to yeast WT.

2.7. Discussion

Molecular testing plays an important role in the clinical management of GIST, including decision making about appropriate medical and surgical therapy. SDH deficiency is a potential cause of GIST in tumors lacking known oncogenic drivers such as gain-of-function KIT mutations. To attempt to identify the cause of SDH deficiency in such GIST, it is necessary to use multi-gene sequencing panels to search for SDHx pathogenic mutations, however, as the routine use of multi-gene sequencing panels has expanded, there has also been an increase in reported VUS. Due to the multiple potential causes of SDH-deficiency, it is difficult to determine if a newly discovered VUS is responsible for the defect, or if a different genetic mechanism is responsible for the loss of SDH complex activity. This problem is exacerbated in GIST as loss of SDHA protein is the most common cause of SDH deficiency in GIST, but SDHA variants have not been extensively characterized at the functional level. Finally, many SDHA VUS are also found in the germline, meaning that they can be inherited. Knowing a patient has a loss-of-function *SDHA* variant in a tumor dramatically changes clinical decision making concerning screening recommendations for tumor syndromes, which affects both the patient and other family members. Since there are no effective medical treatments for advanced SDH-deficient tumors, early detection of tumors allowing curative surgical resection is crucial.

A major problem in the field has been the lack of a validated model system to assess the biochemical function of *SDHA* VUS. Currently, there are no human SDHA-deficient cell lines and assessing SDH complex activity in tumor samples is difficult. Previously it has been shown that a yeast model can be used to evaluate the pathogenic

significance of *SDHB* mutations (Panizza et al. 2013; Goffrini et al. 2009). Extending these studies, we report the successful use of a yeast model to characterize *SDHA* variants found in GIST tumors as either causing loss of function or having no biochemical consequence. Together with computational modeling, structural homology, and patient data, we have drawn conclusions on how and why the *SDHA* variants we studied affect SDH function, providing clinicians with information to guide genetic counseling of patients and family members who harbor one of these germline VUS.

Using our yeast model, we characterized variants as either causing loss of protein function or having no effect. All variants in the loss-of-function group were unable to grow on a non-fermentable carbon source (glycerol). In addition, these variants also failed to consume oxygen, indicating defective oxidative phosphorylation. Interestingly, these variants had differential effects on Sdh1 flavination and/or protein abundance. As a group, all of the loss-of-function variants were associated with a dramatic decrease in Sdh2 protein abundance, which is in concordance with current clinical testing to determine SDH-deficiency in tumors - assessment of SDHB (human equivalent to ySdh2) expression using IHC (Boikos, Pappo, et al. 2016; Gill et al. 2011; Gill et al. 2010; Gaal et al. 2011; Janeway et al. 2011; Doyle et al. 2012). Our data provides further evidence supporting the role of SDHB IHC as the most reliable clinical test to identify SDH deficiency in a tumor. Notably, we identified four novel loss-of-function variants that did not affect Sdh1 protein abundance (yG97R, yT134M, yR444C, yH601Y). These variants prevent flavination of Sdh1 making Sdh1 dysfunctional but still expressed at normal levels. Our findings are consistent with previous reports where SDHA expression was retained in some *SDHA*-mutant tumors that lack SDHB expression (Miettinen et al. 2013), confirming that not all dysfunctional

SDHA (or Sdh1) variants lead to decreased protein expression of this subunit. There are three clinical samples (R188W, G260R, A454E) that we characterized as loss-of-function variants but are associated with normal sdh1 in our yeast model. Based on these results and coupled with the fact the SDHA IHC is not universally available, we advocate for the use of SDHB IHC to identify tumors that are SDH-deficient.

The conclusions drawn from our yeast model are largely supported by our computational modeling results. For many variants, we could find confirmatory structural modeling evidence that the amino acids affected by these mutations played a role in the catalytic site of Sdh1. The computational model and energy minimization also allowed us to explain why some variants could reduce Sdh1 protein abundance. Furthermore, all the variants that did not affect protein function were on the surface of the protein as visualized by our computational model, suggesting that they would not interact with the catalytic mechanism of Sdh1.

Based on our biochemical data, there are still several tumors that have no known mechanism for loss of SDH activity (**Table 3**). One of these tumors had the hR195W (yR186W) variant with an allele frequency of 66.7% and negative SDHB IHC. This tumor is likely driven by a different mechanism of SDH-deficiency. The rest of the unexplained tumors had no IHC data available, so it is possible that these GISTs are not driven by SDH-deficiency and instead belong to a different subtype of GIST (Bannon, Klug, et al. 2017). Alternatively, these GISTs may be SDH-deficient by a different genetic mechanism than the *SDHA* variant identified using targeted exome sequencing. There are several weaknesses of various targeted exome sequencing panels including potential lack of coverage for regions of certain *SDHx* genes, failure to detect large genomic deletions

involving SDHx subunits, as well as the inability to measure hypermethylation of the *SDHC* promoter. In addition, mutations that inactivate newly identified SDH assembly factors (SDHAF3, 4) are typically not included in clinical cancer gene sequencing panels (Na et al. 2014; Van Vranken et al. 2014). Given the limitations of using de-identified results from clinical testing, we did not have access to residual tumor samples to perform additional IHC or genomic testing.

We used a yeast model to characterize 22 *SDHA* VUS. These data revealed 16 (73%) of SDHA VUS as loss-of-function (and therefore pathogenic), highlighting the importance of understanding such variants to provide better clinical recommendations for genetic counselors concerning family screening and early detection protocols. However, our approach using a functional yeast model paired with computational modeling can distinguish between *SDHA* VUS that cause loss of function and those that have no biochemical effect, allowing us to discriminate between pathogenic and non-pathogenic variants.

2.8. Acknowledgements

Thank you to Arin McKinley, Diana Griffith, Janice Patterson, and Ashley Young for their constant support during the completion of this project. The advice and feedback from Amanda McCullough, Maureen Hoatlin, and David Koeller were extremely beneficial for experimental design and interpretation of results. Also, thank you to Dennis Winge for his generous gift of primary antibodies for Sdh1 and Sdh2.

3. CHAPTER THREE: Identifying novel causes of SDH-deficiency

3.1. Preface

There is a subset of GISTs that have no identifiable molecular driver. Some of these tumors are SDH-deficient as assessed by SDHB IHC without having a loss-of-function mutation in any of the SDH subunits using our currently available GIST sequencing panel. As explained in **Chapter 4,** GIST is a paradigm for understanding the molecular cause of a tumor and translating that knowledge into the clinic by guiding the selection of appropriate therapies. In addition to selecting appropriate therapies, patients with SDH-deficient GISTs should be screened for a variety of other cancers. And if the cause of the SDH-deficiency is hereditary due to a germline SDHx mutation versus non-hereditary due to *SDHC* promoter hypermethylation (see **Section 1.7.2**) then it is important for their family members to undergo genetic counseling.

We hypothesized that there are novel causes of SDH-deficiency in GIST that are currently not identified. These could include mutations in recently identified SDH assembly factors, hypermethylation or mutation of the promoters for genes involved in SDH activity, and other metabolic oncogenes (*FH, IDH*) that are not yet associated with GIST. This chapter describes the design and testing of a custom next generation sequencing (NGS) AmpliSeq panel for genes involved in SDH assembly and function.

3.2. Introduction

GIST is a heterogeneous disease with several known molecular drivers (See **Chapter 4**). One subset of GIST is SDH-deficient, usually caused by homozygous or compound

heterozygous loss-of-function mutations in one of the SDHx subunits. There is a subset of these tumors that are SDH-deficient for unknown reasons. Some of the SDH-deficient tumors have an *SDHx* VUS, as described in **Chapter 2,** while others have no molecular abnormalities in the sequenced *SDHx* genes. Patients with known loss-of-function (pathogenic) *SDHx* mutations are at risk for a variety of cancers and cancer syndromes, so routine screening protocols are recommended (**Section 1.7.5**). However, if the cause of SDH-deficiency is unknown, it is difficult to counsel these patients and their families.

SDH genes (including *SDHA, SDHB, SDHC, SDHD,* and the SDH assembly factor *SDHAF2)* are classic tumor suppressor genes. Loss-of-function germline mutations in these genes coupled with a second hit result in a decrease in SDH activity that is associated with the development of tumors. Additionally, mutations in *SDHAF1* have been shown to cause human disease, specifically leukoencephalopathy, but have not yet been linked to cancer. *SDHAF1* and *SDHAF2* demonstrate that mutations in SDH assembly factors have similar consequences in human disease as mutations in the SDH subunits. For this reason, *SDHAF1* and *SDHAF2* are both included in the clinically available GIST genome screening panel.

New SDH assembly factors (SDHAF3, SDHAF4) have been identified in playing important roles in proper maturation of SDH (see **Section 1.6.2**). The leader in this field, Dr. Jared Rutter, identified two new proteins (NDUFAB1, DARS2) involved in the proper function of SDH (unpublished data). Through collaboration, Dr. Rutter kindly identified these novel, potential SDH assembly factors and allowed us to put these genes on our SDH panel for their possible role in SDH-deficient disease. Currently, these SDH assembly

factors ($SDHAF_3$, $SDHAF_4$, NDUFAB1, $DARS_2$) are not sequenced on the clinically available GIST sequencing panel.

Mutations and epimutations are also found in the promoters of *SDH* genes. One well-documented case of SDH-deficiency is through hypermethylation of the *SDHC* promoter (Killian et al. 2014; Haller et al. 2014). Tumors with *SDHC* epimutation have decreased *SDHC* mRNA expression compared with healthy controls (Killian et al. 2014). Decreased SDHC protein expression leads to SDH complex instability and the secondary loss of SDHB protein expression as assessed by IHC. All known cases of GIST with an *SDHC* epimutation are SDHB-deficient. The mechanisms leading to increased *SDHC* promoter hypermethylation remain unknown at this time but are likely post-zygotic because the risk of these tumors is not inherited (Killian et al. 2014). Patients with *SDHC* epimutation often manifest Carney Triad, which consists of gastric GIST, paraganglioma, and pulmonary chondroma. Based on this evidence it is plausible that the other SDH-related genes could have hypermethylation of their promoters that would lead to decreased SDH activity.

Point mutations in transcription binding sites on the *SDHD* promoter are found in 4-10% of melanoma (Weinhold et al. 2014; Scholz et al. 2015). These mutations occurred in a TTCC response element that is highly conserved for E26 transformation-specific (ETS) transcription factors. SDHD mRNA expression was lower in the SDHD promoter mutated-tumor samples compared to WT SDHD promoter tumor samples (Weinhold et al. 2014). Unfortunately, SDHB IHC was not done during this study, so it is unknown if these tumors are truly SDH-deficient. Non-protein coding regions in SDH-related genes, such as

promoters, are not usually tested in SDH-deficient GIST but may represent a novel mechanism of SDH-deficiency.

We hypothesize that there are new causes of SDH-deficiency potentially including hypermethylation of SDHx gene promoters, genomic mutations in SDHx gene promoters that result in decrease SDHx protein expression, or genomic mutations in recently identified SDH assembly factors. We have designed a custom NGS AmpliSeq panel, validated the panel with normal spleen samples, and tested nine GIST samples with no known molecular drivers.

3.3. Materials and methods

Designing the AmpliSeq panel. A custom gene panel has been developed using Ion AmpliSeq Designer. Each gene was individually added by the Ion Torrent program which pulled the DNA regions of interest from the UCSC genome browser and also included the 3' untranslated region. The promoters for each gene were manually entered to add the 1 kb upstream of the gene of interest. The known IDH1/2 DNA hotspot regions that are associated with cancer were also manually entered.

Tumor samples. Formalin fixed parafin embedded (FFPE) tumor tissues that have an unknown molecular driver mutation were used for mutation analysis. These tumors were WT for all mutations on the Knight Diagnostic Laboratories GeneTrails GIST genotyping panel which includes the following genes: AKT1, AKT2, AKT3, ATM, BRAF, CDKN2A, HRAS, KIT, KRAS, MAP2K1, NF1, NRAS, PDGFRA, PIK3CA, PTEN, PTPN11, SDHA, SDHAF1, SDHAF2, SDHB, SDHC, SDHD, and TP52. Additionally, SDHB IHC and gene

fusion testing were done on a subset of these samples as previously described (Beadling et al. 2013).

Sequencing protocol. DNA was extracted and purified from these tumors as previously described (Beadling et al. 2013). The DNA was sequenced on the Ion Torrent PGM, using the standard Ion Torrent AmpliSeq library prep protocol (Beadling et al. 2013).

3.4. Results

3.4.1. SDH-related gene panel

The custom SDH-related gene panel has 386 amplicons covering 36.99 kb with an overall coverage of 87.66%. Coverage for genes varied based on the repetitive regions and GC content in the region specified (**Table 7**). The amplicon range within each target region is 125-175 bp.

Name	Chromosome	Start	End	Amplicons	Coverage (%)
SDHA	Chr5			35	95.55
SDHB	Chr1			19	100
SDHC	Chr1			35	98.75
SDHD	Chr11			20	93.35
SDHAF1	Chr19			16	100
SDHAF2	Chr11			17	100
SDHAF3	Chr7			26	98.99
SDHAF4	Ch6			7	90.45
NDUFAB1	Chr16			11	100
DARS	Chr1			52	96.45
FH	Chr1			30	100
SDHA promoter	Chr5	217356	218356	8	81.7
SDHB promoter	Chr1	17380665	17381665	7	74
SDHC promoter	Chr1	161283166	161284166	10	100
SDHD promoter	Chr11	111956548	111957548	10	100

SDHAF1 promoter	Chr19	36485090	36486090	10	94.8
SDHAF2 promoter	Chr11	61196597	61197597	11	98.3
SDHAF3 promoter	Chr7	96744905	96745905	11	100
SDHAF4 promoter	Chr6	71275625	71276625	11	99.9
NDUFAB1 promoter	Chr16	23607639	23608639	8	76.5
DARS promoter	Chr1	173792797	173793797	11	100
FH promoter	Chr1	241683085	241684085	13	100
IDH1 hotspot (R132)	Chr2	209113111	209113113	1	100
IDH2 hotspot (R140)	Chr15	90631934	90631936	1	100
IDH2 hotspot (R172)	Chr15	90631837	90631839	1	100

Table 7. Gene name and coverage of SDH-related genes and promoters on the custom NexGen panel.

3.4.2. Molecular findings in tumor samples

Nine GIST samples with no identified molecular mechanism were run on the panel (**Table 8**). All of these samples were run on the clinically available GIST panel and showed no mutations. A subset of these samples had SDHB IHC. A negative SDHB IHC result is indicative of loss of SDHB protein expression found within the tumor; a positive SDHB IHC result means the SDHB protein expression is found within the tumor. Testing for gene fusions (see **Section 4.6.3.3.2**) which would not show up on the currently available GIST screening panel were done in a subset of tumors but were all negative. Finally, it is worth noting that 67% of these GISTs were found in the stomach which is often associated with SDH-deficient GISTs.

Sample number	Type	Current GIST panel	SDHB IHC	Fusion	Tumor origin
1	GIST	No mutation	Negative	N/A	Stomach
2	GIST	No mutation	N/A	N/A	Stomach
3	GIST	No mutation	Negative	N/A	Stomach
4	GIST	No mutation	Positive	N/A	Small intestine
5	GIST	No mutation	Negative	Not detected	Stomach
6	GIST	No mutation	N/A	Not detected	Stomach
7	GIST	No mutation	Positive	Not detected	Small intestine
8	GIST	No mutation	Positive	Not detected	Unknown
9	GIST	No mutation	Negative	N/A	Stomach

Table 8. Results from previous assays attempting to identify the molecular driver for the nine GISTs that were run on the SDH-related gene panel.
SDHB IHC Negative= no SDHB protein expression, SDHB IHC Positive=normal expression of SDHB. N/A=not available

Two novel variants were identified in the nine GIST samples after being sequenced with the new SDH-related gene panel (**Table 9**). Unfortunately, the clinical interpretation of these variants is unclear.

Sample #	Protein	Variant freq	Mutation	Copy #	Polyphen	SIFT	EXAC (allele freq)	ClinVar
2	C6orf57 (SDHAF 4)	46.7	Q46R	2.26	Benign	Damaging	0.18	N/A
5	SDHA	51.0	G184R	1.86	Damaging	Damaging	0.0015	Benign/likely benign

Table 9. Results of new NGS SDH-related gene panel.

3.5. Discussion

Successful treatment of a heterogeneous cancer like GIST requires a thorough understanding of the molecular mechanism that drives cancer. However, there is still a small subset of GISTs that are WT for all known causes of GISTs including *KIT, PDGFRA, SDH*, RAS-pathway, and RTK translocations (see **Chapter 4**). Additionally, there are a subset of SDH-deficient GISTs with no identified cause of SDH-deficiency. We hypothesize that there are novel causes of SDH-deficiency potentially including hypermethylation of SDHx gene promoters, genomic mutations in SDHx gene promoters that result in decrease SDHx expression, or genomic mutations in recently identified SDH assembly factors. We have designed a custom NGS AmpliSeq panel, validated the panel

with normal spleen samples, and tested nine GIST samples with no known molecular drivers.

Our results identified variants in two samples that might be responsible for SDH-deficiency. Sample 2 is a gastric GIST but has unknown SDHB protein expression since IHC was not performed. This sample contains the mutation Q46R at a frequency of 47.% in SDHAF4. Polyphen and SIFT have contradictory reports on whether or not this amino acid change will affect protein function. The Exac database shows a high allele frequency in the population indicating this variant would not predispose patients to cancer especially because despite a high population frequency, this mutation is not documented in ClinVar. However, most clinical sequencing panels would not include this gene, so mutation of this gene in association with cancer remains poorly described and understudied.

Sample 5, a gastric GIST with negative SDHB protein expression by IHC is shown to have a heterozygous G184R mutation in SDHA. Again our analysis tools give contradictory information on the functional effect of this mutation. Polyphen and SIFT both predict it to be damaging due to the large change in amino acid structure. The Exac database has a low population frequency for this variant which is hard to interpret. Moreover, ClinVar has reported the variant as benign/likely benign. This variant is the perfect candidate for functional screening using the yeast model and computational analysis as described in **Chapter 2**. However even if this variant was proven to be loss of function since it is a heterozygous mutation, there is still something to be learned about the cause of SDH-deficiency in this tumor.

Unfortunately, we were unable to clearly identify any mutations in these tumors that would be solely responsible for SDH-deficiency. However, we believe this project has long term potential. Future directions for this project include hypermethylation analysis, large genome deletion testing using microarrays, increasing sample number and type, and using our panel to test for new variants that might influence prevalence for families with known loss-of-function germline mutations in SDHx. These ideas are further discussed in **Chapter 5.2**.

4. CHAPTER FOUR: Using Molecular Diagnosis to Personalize the Treatment of Patients with Gastrointestinal Stromal Tumors

Amber E. Bannon, Lillian R. Klug, Christopher L. Corless, Michael C. Heinrich

4.1. Preface

The previous chapters have focused on the role of SDH loss-of-function variants in GIST pathogenesis, however SDH-deficient GIST comprise only a small subset of GIST. This manuscript which was published May 2017 in *Expert Reviews in Molecular Diagnostics* (Volume 17, Issue 5, Pages 445-457) (Bannon, Klug, et al. 2017) describes the various molecular subtypes of GIST and the clinical implications of each known driver mutation in GIST, specifically how it affects clinical treatment of GIST. As the oncology field continues to search for biomarkers that will predict treatment response to targeted therapy, GIST should be used as the gold standard to show the power of understanding genetic drivers and the proper therapeutic approach both with choosing a drug and dosing.

4.2. Summary

Gastrointestinal stromal tumors are a model system for use of molecular diagnosis to guide the selection of appropriate therapy. Multiple principal driver genes have been identified, dividing GISTs into molecularly distinct groups that require different therapies, and in some cases different dosing. This review focuses on the evolution of our understanding of the molecular basis of GIST and how modern molecular diagnostics should be used to optimize the therapeutic approach.

4.3. Keywords

Gastrointestinal stromal tumors, receptor tyrosine kinases, KIT, PDGFRA, SDH, BRAF, KRAS, NF1, RTK Translocations, imatinib, sunitinib, regorafenib

4.4. Introduction

Although not widely recognized before 1998, gastrointestinal stromal tumor (GIST) now represents the most common mesenchymal tumor of the gastrointestinal tract, with more than 5000 new cases diagnosed annually in the United States (Demetri et al. 2010). GISTs have become a paradigm for the use of molecular diagnostics and targeted therapy. The molecular classification of a patient's GIST informs therapeutic decision-making and predicts treatment responses. Unfortunately, less than 15% of patients have their tumors genotyped, potentially leading to suboptimal care (Barrios et al. 2015).

Most GISTs are driven by activating mutations in either of two receptor tyrosine kinases (RTKs), KIT or platelet derived growth factor receptor alpha (PDGFRA). Following the discovery of these mutations as tumor drivers, GIST was the first solid tumor to be successfully treated with small molecule tyrosine kinase inhibitors (TKIs). We now know that there are other molecular drivers of GIST pathogenesis including deficiency of succinate dehydrogenase (SDH) or NF1, activating mutations in the RAS/RAF/MEK pathway, and translocations involving the kinase domain of RTKs other than KIT/PDGFRA (e.g. NTRK3). Optimal treatment of patients with GIST requires molecular

subclassification. This review focuses on advances in the diagnosis and characterization of GIST and how molecular testing should be used to achieve the best patient care.

4.5. Initial diagnosis using immunohistochemistry

GISTs most commonly arise in the stomach (60%), but can also be found in the small intestine (25%), rectum (5%) and elsewhere in the gastrointestinal tract, including esophagus, colon, appendix, and gallbladder. Occasionally, GISTs arise outside the wall of the gut, designated extra-intestinal GIST. Even more rare are reports of primary GISTs that originate outside the abdominal cavity, including reports of a primary GIST of the pleura or pericardium (Long et al. 2010; Zhang et al. 2016; Arpaci et al. 2015).

Historically, GISTs were classified as smooth muscle tumors (leiomyoma or leiomyosarcoma) because of their predominantly spindle cell morphology and their association with the muscularis propria of the bowel wall. However, studies using electron microscopy and immunohistochemistry differentiated these tumors from classic leiomyosarcoma, leading Mazur and Clark to propose the term 'stromal tumor' in 1983 (Mazur and Clark 1983). The subsequent discovery that most stromal tumors arising in the GI tract are CD34-positive provided further evidence for their distinction from CD34-negative leiomyosarcoma.

During the 1990s, several investigators noted similarities between GIST cells and a unique population of cells in the gut wall known as the interstitial cells of Cajal (ICC). ICC are the pacemaker cells of the gut, responsible for coordinated peristalsis. Normal ICC express KIT (CD117) and are developmentally dependent on the expression of both KIT

and its cognate ligand, stem cell factor (SCF). Mice deficient in KIT or SCF expression have a marked reduction in certain populations of ICC (Isozaki et al. 1995). In 1998, two separate groups reported that GISTs commonly express CD117 (Hirota et al. 1998; Kindblom et al. 1998). It is now well established that 95% of GISTs are immunohistochemically positive for CD117.

In 2004, another highly specific marker for GISTs was described. ANO1 (anoctamin-1 or DOG1) is a calcium-activated chloride channel that is highly expressed in ICC and in 98% of GIST, regardless of CD117 expression levels (Liegl et al. 2009). Conveniently, only a small number of non-GIST sarcomas express ANO1. The combination of CD117 and ANO1 expression by an abdominal sarcoma is essentially diagnostic of GIST (Liegl et al. 2009; West et al. 2004).

The use of CD117 and ANO1 has helped define the full range of cellular morphology associated with GIST (see **Table 10**). Although most GISTs consist of a uniform population of spindled cells, some cases have an epithelioid appearance and others are a mixture of spindled and epithelioid cells. Tumor cellularity varies widely among GISTs. Low-grade lesions may show areas of central calcification, or demonstrate band-like alignment of nuclei mimicking a schwannoma. High-grade tumors often ulcerate the overlying mucosa and may undergo significant hemorrhagic necrosis. This variety in GIST histology dictates a broad morphologic differential diagnosis; therefore judicious use of CD117 and ANO1 immunohistochemistry is key to making an accurate diagnosis.

Diagnosis	KIT	DOG1	SDHB	SDHA	Desmin	S-100
KIT, BRAF, NF1 mutant GIST	Positive	Positive	Positive	Positive Positive	Negative	Negative
PDGFRA mutant GIST	Sometimes low*	Positive	Positive	Positive	Negative	Negative
SDHB-D mutant GIST	Positive	Positive	Negative	Positive	Negative	Negative
SDHA mutant GIST	Positive	Positive	Negative	Negative or positive	Negative	Negative
RTK-WT/ SDHB positive	Positive	Positive	Positive	Positive	Negative	Negative
Quintuple WT	Positive	Positive	Positive	Positive	Negative	Negative
Leiomyoma	Negative	Negative	Positive	Positive	Positive and uniform	Negative
Leiomyosarcoma	Negative	Negative	Positive	Positive	Usually positive	Negative
Schwannoma	Negative	Negative	Positive	Positive	Negative	Positive and uniform
Desmoid Fibromatosis	Negative	Negative	Positive	Positive	Negative	Negative

Table 10. Immunohistochemistry in differential diagnosis of GIST.
Multiple immunohistochemical markers can be used in the differential diagnosis of GIST. However, the combination of CD117 (KIT) and ANO1 expression by an abdominal sarcoma is essentially diagnostic of GIST. SDH IHC is useful in further distinguishing subtypes of GIST.
ANO1: anoctamin-1; GIST: gastrointestinal stromal tumor; NF1: neurofibromatosis type I; PDGFRA: platelet-derived growth factor receptor alpha; RTK: receptor tyrosine kinase; SDH: succinate dehydrogenase; SDHA: succinate dehydrogenase subunit A; SDHB: succinate dehydrogenase subunit B; WT: wild type.
*Weak KIT indicates a *PDGFRA* mutation but *PDGFRA* mutation can also be present when KIT is positive
**Absent SDHA indicates an *SDHA* mutation but *SDHA* mutation can also be present when SDHA is retained. *SDHA* mutation is always accompanied by SDHB-deficiency.

In 2008, a subset of GISTs were found to be immunohistochemically negative for the expression of succinate dehydrogenase subunit B (SDHB) (van Nederveen et al. 2009). An additional subset of SDHB-deficient tumors also lacks succinate dehydrogenase subunit A (SDHA) expression. The implications and importance of these findings are discussed below. An overview of IHC markers used in the differential diagnosis of GIST is summarized in **Table 10.**

4.6. Molecular classification

The vast majority of GISTs (75-80%) harbor gain-of-function *KIT* mutations (Hirota et al. 1998). The second most common mutations, representing 5-10% of GIST, affect PDGFRA, an RTK homologous to KIT. The remaining 10-15% of GISTs do not have mutations in *KIT* nor *PDGFRA*; these tumors historically have been referred to as wild type (WT) GIST (**Figure 19**).

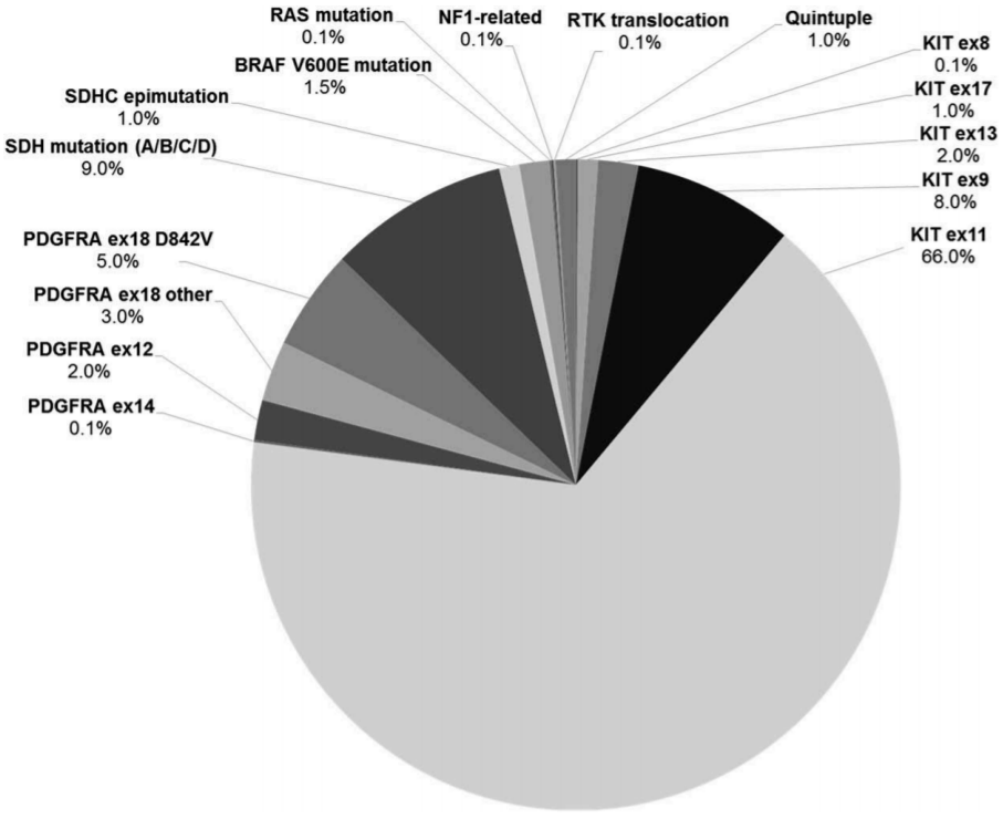

Figure 19. Mutational subclassification of GIST.
The percentage of GIST cases within each mutation-based subclass is depicted.

Increasingly, the term of WT GIST is confusing, as modern testing can actually identify a pathogenic mutation in most of these cases. An updated molecular classification of GIST summarized in **Table 11** may be helpful for diagnostic, prognostic, and treatment planning purposes.

Molecular Classification	**Relative Frequency (%)**	**Clinical features**	**Treatment or notable features**
KIT mutation	77		
Exon 8	Rare	Small bowel	Rare, reports of favorable response to imatinib
Exon 9	8	Small bowel, colon	Better responses with high-dose imatinib (800mg per day) or sunitinib than with standard dose imatinib
Exon 11	67	All sites	Sensitive to imatinib (400mg per day), no advantage to higher dose therapy
Exon 13	1	All sites	Sensitive to imatinib but limited treatment data; need for higher doses than 400 mg
Exon 17	1	All sites	Some are sensitive to imatinib, consider dose escalation if no response to imatinib 400 mg
PDGFRA mutation	10		
Exon 12	1	All sites	Sensitive to imatinib
Exon 14	<1	Stomach	Sensitive to imatinib
Exon 18 D842V	7	Stomach, mesentery, omentum	Resistant to all agents approved for GIST, consider clinical study
Exon 18 other	1	All sites	Most are sensitive to imatinib (D842V is resistant)
RTK-WT	13	All sites	
RTK-WT/SDHB negative			Treat with standard paradigm of imatinib--> sunitinib--> regorafenib. Needs closer follow up than kinase mutation GIST as this is much less likely to respond to conventional GIST TKIs.
SDH mutation (A/B/C/D)	9	Stomach only; Some cases with germline mutations (Carney-Stratakis), rarely Carney Triad	Carney-Stratakis syndrome; rarely Carney triad

SDHC epimutation	<1	Stomach only, Carney Triad (not heritable) or sporadic	Carney triad, not heritable
RTK-WT/SDHB positive			
BRAF V600E mutation	<1	All sites	May respond to BRAF inhibitor +/- MEK inhibitor
RAS mutation	<1	Stomach	No established therapy for advanced medical disease. Consider clinical study of MEK inhibitor or other investigational approaches
NF1-related	~1	Small bowel	Multiple lesions, rarely malignant. No established medical therapy for advanced disease
RTK translocation	<1	Non-gastric	Reports of response of an NTRK3 translocated GIST to an investigational NTRK3 TKI. Other forms may respond to appropriate inhibitors for the translocated kinase. Enrollment in a clinical study of an appropriate kinase inhibitor is recommended.
Quintuple WT	<1	All sites	Response to standard GIST therapy is poorly described. Reasonable to try one or more approved GIST agents in cases of advanced disease. As this entity becomes better understood, additional options may emerge.

Table 11. Molecular classification of GIST.
An updated classification of GIST subtypes, including relative frequency, clinical presentation, treatment, and notable features, is provided. GIST: gastrointestinal stromal tumor; PDGFRA: platelet-derived growth factor receptor alpha; RTK: receptor tyrosine kinase; WT: wild type; SDHB: succinate dehydrogenase subunit B; SDH: succinate dehydrogenase; SDHC: succinate dehydrogenase subunit C; TKI: tyrosine kinase inhibitor.

4.6.1. *KIT*-mutant GIST

KIT is a type III RTK, belonging to the family that also includes PDGFRA, PDGFRB, CSF1R, and FLT3. Upon binding its cognate ligand, stem cell factor (SCF), two KIT polypeptides dimerize and transactivate each other by tyrosine phosphorylation. The resultant fully activated kinase complex initiates downstream signaling through multiple pro-proliferative and pro-survival pathways, including PI3K/AKT and RAS/RAF/MEK.

The functional importance of *KIT* mutations in GIST pathogenesis is supported by multiple lines of evidence. First, phosphorylated KIT, indicative of activated KIT, is readily detected in extracts from clinical GIST specimens and GIST cell lines (Rubin et al. 2001). Second, mutant KIT can transform BA/F3 cells, supporting their growth in nude mice (Hirota et al. 1998). Third, mice engineered to express KIT with activating mutations like those found in human GISTs develop diffuse ICC hyperplasia of the stomach and intestines and can develop GIST-like tumors (Rubin et al. 2005; Sommer et al. 2003). The histologic pattern of diffuse ICC hyperplasia and focal GIST formation in these mice is similar to that seen in individuals who inherit germline KIT-activating mutations (Chen et al. 2002; O'Riain et al. 2005). Fourth, when exogenously expressed in cell lines, mutant forms of KIT show constitutive kinase activity in the absence of SCF, as shown by auto-phosphorylation and activation of downstream signaling pathways (Hirota et al. 1998; Heinrich et al. 2000; Tuveson et al. 2001). Fifth, treatment of GIST cell lines or primary GIST cell cultures with KIT kinase inhibitors or interfering RNA against *KIT* results in decreased proliferation and apoptosis (Tuveson et al. 2001; Heinrich et al. 2006). Finally, TKI-resistant *KIT*-mutant GIST typically harbor secondary *KIT* mutations that confer drug resistance but maintain kinase activity, suggesting that even in the advanced state, GISTs

require maintenance of KIT signaling (see below for additional discussion of resistance mutations) (Heinrich et al. 2006).

4.6.1.1. KIT exon 11 mutations

Mutations in *KIT* exon 11 are the most common type of oncogenic mutation found in GIST, occurring in approximately 67% of cases. These mutations include point mutations, in-frame deletions and/or insertions. Exon 11 encodes the juxtamembrane portion of KIT that prevents the kinase activation loop from swinging into the active state, thus favoring the auto-inhibited conformation. Mutations of *KIT* exon 11 disrupt this auto-inhibition, allowing spontaneous kinase activation in the absence of SCF ligand (Mol et al. 2004).

KIT exon 11-mutant GISTs arise throughout the GI tract, but the most common site is the stomach. Tumors with *KIT* exon 11 mutations typically have spindled cell morphology, rather than epithelioid. After complete resection, these tumors have a higher rate of recurrence than other genotypically-defined GIST subgroups. Correspondingly, GISTs with *KIT* exon 11 deletions, particularly deletions involving codons 557 and/or 558, have a worse prognosis than those with exon 11 point mutations (Martin et al. 2005).

4.6.1.2. KIT exon 9 mutations

The second most common class of mutations affects *KIT* exon 9 (8%–10% of GISTs), which encodes the KIT proximal extracellular domain. More than 95% of GIST-associated *KIT* exon 9 mutations consist of an insertion of 6 nucleotides, resulting in

duplication of amino acids 502 and 503. Rare cases of amino acid substitutions involving codon 476 have also been reported (Corless, Barnett, and Heinrich 2011). Most GISTs harboring a *KIT* exon 9 mutation arise from the small or large bowel and *KIT* exon 9-mutant tumors make up 25-30% of intestinal GISTs. In contrast, *KIT* exon 9 mutations make up less than 2% of gastric GISTs (Corless, Barnett, and Heinrich 2011). *KIT* exon 9 mutations result in constitutive kinase activation by mimicking the conformational change that the extracellular domain undergoes after ligand binding. The kinase domain conformation in exon 9-mutant KIT is believed to be the same as for WT KIT.

4.6.1.3. Other KIT mutations

Primary mutation of *KIT* exon 13, which encodes part of the kinase adenosine triphosphate (ATP)-binding pocket, occurs in approximately 1% of GISTs. The substitution K642E accounts for the vast majority of primary *KIT* exon 13 mutations. *KIT* exon 13-mutant GISTs are most commonly found in the stomach but can arise throughout the GI tract. *KIT* exon 13-mutant tumors typically have a spindle cell appearance, but occasionally have epithelioid or mixed histology.

Primary mutations affecting *KIT* exon 17, which encodes the kinase activation loop, are found in approximately 1% of GISTs. Substitutions at codons 820, 822, or 823 are the most common mutation sites in this exon. Almost all of these tumors have a spindle cell appearance and most are located in the small bowel, but can arise in the stomach as well (Lasota et al. 2008).

Mutations can also occur in *KIT* exon 8, which encodes part of the KIT extracellular domain. The majority of these GISTs occur outside of the stomach, in the duodenum or small intestine (Ito et al. 2014).

4.6.2. *PDGFRA*-mutant GIST

Mutations in *PDGFRA* are the most common non-*KIT* oncogenic mutations associated with GIST. PDGFRA is a close homolog of KIT and uses similar downstream signaling pathways to drive proliferation. *PDGFRA* mutations found in GIST result in constitutive kinase activation and are mutually exclusive with *KIT* mutations (Heinrich, Corless, Duensing, et al. 2003; Hirota et al. 2003). The most common location for *PDGFRA*-mutant GISTs is the stomach, but they can arise in the small or large intestine. Histologically, *PDGFRA*-mutant GISTs usually have an epithelioid or mixed epithelioid/spindle appearance, commonly accompanied by a myxoid stroma (Lasota, Stachura, and Miettinen 2006). Some, but not all, *PDGFRA*-mutant GIST express low or undetectable levels of KIT as assessed by IHC (so called KIT-negative GIST); however, these tumors retain expression of ANO1. Other similarities between *PDGFRA*-mutant and *KIT*-mutant GISTs include expression of PKC-theta and activation of the RAS/MAPK and PI3K pathways (Corless, Barnett, and Heinrich 2011). In addition, these tumors tend to have similar cytogenetic abnormalities, including monosomy of chromosome 14 (Heinrich, Corless, Duensing, et al. 2003). However, gene expression profiling of *KIT*-mutant and *PDGFRA*-mutant GISTs has shown subtle differences that may relate to some of the differences in clinical behavior (Subramanian et al. 2004). In a population-based series of 492 primary GISTs in France, the frequency of *PDGFRA* mutations was 15%, whereas only

2% of cases in two large clinical series of metastatic GIST were driven by *PDGFRA* mutations (Emile et al. 2012). These observations, which have been confirmed in other series, suggest that *PDGFRA*-mutant GISTs generally have a lower risk of recurrence than *KIT*-mutant GIST. As with *KIT* mutations, rare families with germline *PDGFRA* mutations and susceptibility to developing GIST have been reported (de Raedt et al. 2006).

4.6.2.1. PDGFRA exon 18 mutations

The most common *PDGFRA* mutations in GIST involve exon 18, and are thought to stabilize the kinase activation loop in a conformation that favors kinase activation (Dibb, Dilworth, and Mol 2004). A single mutation, D842V, accounts for at least 70% of all *PDGFRA* mutations seen in GIST (Corless et al. 2005). Curiously, D842V mutations are found only in tumors arising in the stomach, omentum and mesentery.

4.6.2.2. PDGFRA exon 12 mutations

Mutations affecting exon 12 of *PDGFRA* are found in approximately 1% of GISTs (Emile et al. 2012; Corless et al. 2005). *PDGFRA* exon-12 is homologous to *KIT* exon-11 and point mutations or in-frame insertion/deletion mutations of this region lead to loss of the auto-inhibitory function of the juxtamembrane domain (Corless, Barnett, and Heinrich 2011; Dibb, Dilworth, and Mol 2004).

4.6.2.3. PDGFRA exon 14 mutations

Less than 1% of GISTs have activating mutations in *PDGFRA* exon-14, making these tumors some of the rarest types of RTK-mutant GIST. By homology with *KIT* exon 13, mutations in *PDGFRA* exon 14 may interfere with the auto-inhibitory function of the juxtamembrane domain.

4.6.3. RTK-WT GIST

4.6.3.1. Historical perspective

Beginning in 1998, GISTs were classified as *KIT*-mutant versus WT, based on the original description of *KIT* exon 11 mutations. When *PDGFRA*-mutant GISTs were identified in 2003, the definition of WT GIST was revised to mean those tumors lacking *KIT* or *PDGFRA* mutations. As detailed below, other gain- or loss-of-function pathogenic mutations have since been discovered in GIST lacking *KIT* or *PDGFRA* mutations. In light of these newer mutations, categorizing GISTs as WT has become confusing and misleading. They are perhaps better referred to as RTK-WT with further sub-classification dependent on the results of additional molecular testing, as discussed below (see *Table 11*).

4.6.3.2. SDHB-deficient, RTK-WT GIST

A major breakthrough in the understanding of non-RTK oncogenic mechanisms in GIST arose from studies of patients with Carney-Stratakis syndrome. This autosomal-dominant syndrome manifests as a susceptibility to develop both paraganglioma and GIST. Previous studies of familial paraganglioma syndromes revealed germline

inactivating mutations in the genes encoding the succinate dehydrogenase (SDH) complex, which is composed of four subunits: SDHA, SDHB, SDHC, SDHD (collectively termed SDHx) (Burnichon et al. 2009; Pasini et al. 2008). The *SDHx* genes are classic tumor suppressor genes, requiring inactivation of both alleles of a specific SDH subunit for loss of SDH activity. Typically, this is the result of a combination of an inactivating germline mutation (first hit) with a somatic loss of heterozygosity or other inactivating mutation affecting the other allele (second hit). Inactivation of any of the SDHx subunits causes destabilization and loss of enzymatic function of the entire complex, resulting in SDH deficiency (van Nederveen et al. 2009).

The mechanisms by which SDH-deficiency initiates the formation of GIST are incompletely understood. Loss of SDH activity prevents the conversion of succinate to fumarate, which leads to accumulation of succinate - an oncometabolite that has been connected to two mechanisms of cancer pathogenesis: 1) inhibition of prolyl hydroxylase, which leads to the accumulation of the transcription factor HIF1α; and 2) inhibition of DNA demethylases, resulting in DNA hypermethylation and gene de-regulation. Oncometabolite initiation of GIST is believed to be independent of KIT signaling and this has implications for treatment of SDH-deficient GIST as noted below.

Several investigators have shown that absence of immunohistochemical staining for SDHB is a reliable method to identify SDH-deficient GIST (Gill et al. 2011; Gaal et al. 2011; Janeway et al. 2011; Miettinen et al. 2011). Overall, SDHB-deficient GISTs have distinct clinical and pathologic characteristics, including gastric origin, epithelioid morphology, a multifocal nodular growth pattern, and frequent involvement of local lymph nodes (Doyle et al. 2012; Miettinen et al. 2013). Miettinen and colleagues reported that 7.5% of 756

gastric GIST were SDHB immunonegative, but no cases of SDHB deficiency were found among 378 non-gastric GISTs (Miettinen et al. 2011). Many SDHB-deficient GISTs arise in patients younger than 20 years. In contrast, gastric GIST diagnosed in patients older than 40 years are rarely SDHB-deficient (Janeway et al. 2011; Miettinen et al. 2011). SDHB staining is retained in GIST with *KIT* or *PDGFRA* mutations and in GISTs with other oncogenic mutations, as discussed below and in **Table 10**.

Absence of SDHA immunostaining generally correlates with loss-of-function SDHA mutations, most of which seem to be inherited (Miettinen et al. 2013; Oudijk et al. 2013; Belinsky et al. 2013; Dwight et al. 2013; Wagner et al. 2013). In rare cases, SDHA staining is retained in an *SDHA*-mutant tumor that lacks SDHB staining (Miettinen et al. 2013); presumably, this is because the mutant-SDHA protein, although dysfunctional, is not degraded. Of 127 SDHB-deficient gastric GISTs, 28% also lacked SDHA expression, suggesting that *SDHA* mutations account for more than a quarter of SDH-deficient GISTs (Miettinen et al. 2013). In contrast, 0 of 556 cases of SDHB-positive GISTs lacked SDHA protein expression. Compared to patients with SDHA-positive/SDHB-negative GISTs, those with SDHA-negative/SDHB-negative GISTs have an older median age (34 vs 21 years), lower female/male ratio, and a slower course of disease, despite a slightly higher rate of liver metastases.

Unlike mutations in *KIT* and *PDGFRA*, the mutations seen in *SDHx* are varied. Loss-of-function mutations are found throughout the coding regions and do not cluster around specific amino acids. Indeed, one of the challenges in evaluating *SDHx* variants in SDH-deficient tumors is determining which ones are responsible for the disease. Functional assays to determine their effects on SDH complex activity would be useful to

guide genetic counseling for these patients and their families (Evenepoel et al. 2015; Panizza et al. 2013).

A subset of SDHB-deficient GISTs have no detectable *SDHx* mutations. The majority of these are thought to have *SDHC* promoter-specific CpG island hypermethylation, referred to as *SDHC* epimutation. Tumors with *SDHC* epimutation have decreased *SDHC* mRNA expression compared with normal controls (Killian et al. 2014). Decreased SDHC protein expression leads to SDH complex instability and the secondary loss of SDHB protein expression as assessed by IHC. All known cases of GIST with an *SDHC* epimutation are SDHB-deficient. The mechanisms leading to increased *SDHC* promoter hypermethylation remain unknown at this time, but are likely post-zygotic because the risk for these tumors is not inherited (Killian et al. 2014). Patients with *SDHC* epimutation often manifest Carney Triad, which consists of gastric GIST, paraganglioma, and pulmonary chondroma. Given that both Carney-Stratakis syndrome and Carney Triad are characterized by GIST and paraganglioma, it is challenging to determine which condition is responsible for development of these tumors in a given patient without appropriate molecular testing.

Identification of SDHB immunonegative GISTs is important for several reasons. First, given the increased frequency of *SDHx* mutations in these tumors, genotyping can be used to guide subsequent testing for the presence of germline mutations (Carney-Stratakis syndrome). Clinical screening guidelines have been described for patients with familial paraganglioma/GIST (Buffet et al. 2012). Second, conventional risk stratification of SDHB-deficient tumors using tumor size and mitotic index is poorly predictive of tumor behavior. These tumors frequently metastasize but often have an indolent clinical course.

In addition, lymph node metastases are common in SDHB-deficient tumors, but extremely rare in SDHB-positive tumors (Doyle et al. 2012; Celestino et al. 2013).

4.6.3.3. RTK-WT/SDHB-positive GIST

4.6.3.3.1. RAS/RAF/MAPK

GISTs that are RTK-WT and SDHB-positive are uncommon, but nevertheless comprise a genetically diverse group. Some harbor alterations that hyperactivate the RAS/RAF/MAPK pathway. Among these are mutations in the gene neurofibromatosis type I (*NF1*), which encodes the tumor suppressor neurofibromin that serves as a negative regulator of the activity of the RAS pathway. Approximately 7% of patients with germline *NF1* mutations develop RTK-WT GIST (frequently multiple) of the small bowel (Andersson et al. 2005; Kinoshita et al. 2004). As expected, *NF1*-associated GISTs are uniformly SDHB positive (Wang, Lasota, and Miettinen 2011). Interestingly, there have been reports of sporadic *KIT*-mutant GISTs in patients with type I neurofibromatosis, and this has treatment implications, as discussed below (Yantiss et al. 2005).

BRAF V600E mutations have been reported in 7-15% of RTK-WT GISTs, but comprise less than 2% of overall GIST diagnoses (Daniels et al. 2011; Agaram et al. 2008; Hostein et al. 2010). There do not seem to be any common anatomic or pathologic associations for *BRAF*-mutant GIST. Rare cases of *RAS*-mutant GIST have also been described (Corless, Barnett, and Heinrich 2011; Miranda et al. 2012).

4.6.3.3.2. RTK Translocations

Approximately 5% of GISTs lack mutations in all genes currently linked to GIST development (*KIT, PDGFRA, SDHx*, RAS pathway). These GISTs have been termed quadruple wild type (Pantaleo et al. 2015). In 2016, two groups identified oncogenic RTK translocations in a subset of quadruple WT GISTs. Brenca *et al*. used transcriptome sequencing to identify the fusion of exon 4 of *ETV6* to exon 14 of *NTRK3* in one quadruple WT GIST that arose in the rectum (Brenca et al. 2016). The Heinrich group analyzed five quadruple WT GIST using an amplicon-based gene fusion panel covering 19 driver genes and 94 partners. Two out of five tumors were positive for oncogenic RTK translocations; one tumor showed an *ETV6-NTRK3* fusion and another harbored a *FGFR1-TACC1* fusion. Notably, the *ETV6-NTRK3* fusion was in a colon primary, and the *FGFR1-TACC1* was in a small intestine primary (Shi et al. 2016). Together these three cases represent a new subset of non-gastric GIST. Given the small size of the reported series, it is possible that other gene fusions of these or other kinases may be involved in GIST pathogenesis.

4.6.3.3.3. Quintuple wild type

As outlined above, it is imperative that the molecular classification of GIST be defined during the diagnostic process to better define therapeutic options for individual patients. However, there is still a small subset of GIST that is WT for all known causes of GIST including *KIT, PDGFRA, SDH*, RAS-pathway, and RTK translocations. We propose that these GISTs be termed 'quintuple wild type' GIST. This group likely represents only 1% of GISTs (Shi et al. 2016).

4.7. Using molecular classification to optimize clinical treatment

There are three treatment scenarios in which molecular classification of GIST is important: therapy for advanced disease, adjuvant therapy following primary GIST resection, and primary/secondary resistance. Although molecular classification is beneficial in all three circumstances, it is the most powerful for optimizing clinical treatment in advanced disease (**Table 11**). The relevance of molecular classification in each scenario is discussed below.

4.7.1. Therapy for Advanced Disease

While many GISTs are controlled by surgery with or without adjuvant imatinib, treatment of GIST in the advanced setting has improved greatly when patients are stratified by molecular subtype. Pre-clinical and clinical data demonstrate therapeutic responses differ significantly between GISTs with different molecular defects or advanced disease, there are currently three approved small molecule therapies to treat GIST of any classification: imatinib (first line), sunitinib (second line), and regorafenib (third line); all are tyrosine kinase inhibitor (TKI) small molecules that have variable potency against mutations in KIT or PDGFRA. In general, these treatments have been shown to be most effective in RTK mutant GIST. As we further understand what drives these tumors, we are able to effectively inhibit their growth. The preclinical and clinical studies that inform the treatment of each GIST subtype are summarized below (see also **Table 10**).

4.7.1.1. KIT-mutant GIST

KIT exon 11-mutant GISTs have the most robust and durable response to front-line treatment with imatinib compared with other types of GIST. *In vitro* assays of *KIT* exon 11-mutant kinases have confirmed that mutations found in GIST tumors are 10-fold more sensitive to KIT inhibitors, such as imatinib, than the WT isoform (Heinrich, Maki, et al. 2008). These *in vitro* findings are reflected in the clinic, where primary resistance to imatinib treatment (defined by progression within the first 6 months of therapy) is seen in only 5% of cases of advanced *KIT* exon 11-mutant GIST, compared with 16% of *KIT* exon-9 mutant and 43% of *KIT*/*PDGFRA* WT cases (Heinrich, Corless, Demetri, et al. 2003; Heinrich, Owzar, et al. 2008). Correspondingly, the objective response rate to imatinib is 67-83% for *KIT* exon 11-mutant GIST versus 35-48% for *KIT* exon 9-mutant GIST (Heinrich, Owzar, et al. 2008). The median time to progression on first-line imatinib therapy for *KIT* exon 11-mutant GIST is approximately 25 months, and the current median overall survival for patients with *KIT* exon 11-mutant GIST is at least 60 months. The molecular mechanisms leading to secondary drug resistance in *KIT* exon 11-mutant GISTs are discussed below.

Exon 9 mutant- *KIT* shows decreased *in vitro* sensitivity to imatinib compared with exon 11-mutant *KIT* (Yuzawa et al. 2007; Heinrich, Marino-Enriquez, et al. 2012). In agreement with these data, results from randomized phase 3 studies showed that patients with *KIT* exon 9-mutant GIST had a significantly improved progression-free survival, approximately 1 year longer, when treated with a higher total daily dose of 800 mg of imatinib compared with patients treated with 400 mg ('Comparison of two doses of imatinib for the treatment of unresectable or metastatic gastrointestinal stromal tumors: a

meta-analysis of 1,640 patients' 2010). Sunitinib, the second-line KIT inhibitor approved for GIST, has a greater potency than imatinib against *KIT* exon 9 mutant kinases. Consistent with this, patients with *KIT* exon 9-mutant GIST represent the most likely subset of patients with imatinib-resistant tumors to benefit from second line sunitinib therapy (Heinrich, Maki, et al. 2008).

Treatment of GIST with mutations in *KIT* exons 13 and 17 can be informed by preclinical and clinical observations as well. *In vitro* data indicate that *KIT* exon 13 and 17 are sensitive to imatinib, but perhaps less so than *KIT* exon 11 mutant kinases (Heinrich, Corless, Demetri, et al. 2003; Corless, Barnett, and Heinrich 2011; Lasota et al. 2008; Lux et al. 2000). If there is no response to imatinib at 400 mg/day, it is reasonable to consider dose escalation to 800 mg/day, if tolerated.

4.7.1.2. PDGFRA-mutant GIST

The mutations seen in *PDGFRA* exon 18 differ markedly in their imatinib sensitivity (Corless et al. 2005; Heinrich, Griffith, et al. 2012). D842V confers resistance to imatinib and all other approved KIT TKIs *in vitro* (Heinrich, Corless, Demetri, et al. 2003). After D842V, the next most common mutation of exon 18 is deletion of codons 842 to 845, which is imatinib-sensitive (Heinrich, Griffith, et al. 2012; Corless et al. 2005). Other more rare mutations in exon 18 are imatinib-resistant, including D846Y, N848K, and Y849K.

While the majority of *PDGFRA* exon 18 mutations are resistant to imatinib and other approved KIT TKIs, a novel PDGFRA selective kinase inhibitor, crenolanib, was found to have *in vitro* potency against D842V and other imatinib-resistant *PDGFRA* mutations.

Based in part on these results, a phase 3 clinical study of this agent to treat advanced GIST with the *PDGFRA* D842V mutation has been initiated (Heinrich, Griffith, et al. 2012) (Clincaltrials.gov identifier NCT02847429). Even more promising, BLU-285 has demonstrated higher potency and specificity against *PDGFRA* exon 18 mutants than any existing small molecule inhibitors, including crenolanib. Early results from a phase 1 clinical trial of this agent reported an impressive objective response rate of this agent for *PDGFRA* D842V-mutant metastatic GIST (Heinrich et al. 2016). Further study is needed to confirm these results and determine the durability of the reported responses. Based on the lack of response of PDGFRA D842V-mutant GIST to conventional agents, consideration of referral to an appropriate clinical study should be strongly considered, even in untreated patients.

In vitro, *PDGFRA* exon-12 mutant kinases are as sensitive to imatinib as *KIT* exon-11 mutant kinases. While there are only rare reports of clinical outcomes for patients with metastatic *PDGFRA* exon-12 mutant GISTs treated with imatinib, the available clinical data suggest that patients have high response rates and durable disease control (Heinrich, Corless, Demetri, et al. 2003; Heinrich, Owzar, et al. 2008; Hirota et al. 2003; Corless et al. 2005). *In vitro* and clinical study data suggest that exon 14-mutant kinase activity is inhibited by imatinib (Corless et al. 2005).

4.7.1.3. RTK-WT GIST

For patients with metastatic GIST that lacks a *KIT*/*PDGFRA* mutation, we recommend referral to a high volume GIST treatment center. Patients with *BRAF*-mutant, *NTRK3*-translocated, or *FGFR1*-translocated mutant GIST should be considered for enrollment in a

study of an appropriate agent. Based on a single case report as well as our personal results from treating *BRAF*-mutant GIST, consideration of off label use of a BRAF inhibitor or combined BRAF and MEK inhibitor treatment could be considered.

Currently, there is no validated effective treatment for patients with *RAS*-mutant or *NF1*-mutant GIST. Theoretically, these tumors might respond to a MEK inhibitor, but there are no published data on this approach. In our experience, these patients do not respond to imatinib therapy. Potentially, KIT/VEGFR inhibitors might have better activity but this has not been proven. In these cases, use of serial surgical debulking to control disease could be considered.

Treatment of SDH-deficient GIST with imatinib results in a very low response rate (~2%) (Boikos, Pappo, et al. 2016). There is some data to suggest that these patients actually have a better response to second-line sunitinib than front-line imatinib(Janeway and Weldon 2012). This could reflect VEGFR inhibition by sunitinib, as increased HIF1α in these tumors leads to VEGF up-regulation. In the future, treatments directed at the oncometabolites and/or cellular hypermethylation may yield superior results to current therapy. In some cases, metastatic disease can behave quite indolently, therefore selected patients may benefit from observation and/or serial surgical debulking. Given the rarity of this type of GIST and the complexity of molecular classification, genetic counseling, and therapeutic decision making, referral of such patients to a high-volume GIST treatment center is recommended.

In addition, patients with SDHB-deficient tumors should undergo additional testing to determine if their tumor has loss-of-function mutations involving an SDH subunit. For patients with tumor associated *SDH* mutations that are felt to result in loss of SDH-

complex function, we recommend genetic counseling and consideration of testing for an underlying germline *SDH* subunit mutation (i.e. Carney-Stratakis). Patients with germline loss-of-function mutations of an SDH subunit should undergo additional genetic counseling to discuss screening other family members and to review recommendations for surveillance for the potential development of paraganglioma, pheochromocytoma or additional GIST (Wada, Arai, et al. 2016; Ricketts et al. 2010).

Finally, we would note that currently 1% of patients will be classified as having a "quintuple WT" GIST. As new molecular classes of GIST are described in the future, tumors from patients with metastatic disease should be re-tested to see if this would change therapeutic decision making. This recommendation also applies to patients previously classified as *KIT*/*PDGFRA* WT GIST based on limited genotyping for only *KIT* or *PDGFRA* mutations.

4.7.2. Adjuvant Therapy Following Primary GIST Resection

Approximately 99% of GISTs can now be categorized based on molecular diagnostics, informing therapeutic decisions in both the adjuvant and advanced disease settings. For example, biomarker analyses of patients treated with adjuvant imatinib after complete surgical resection of primary disease have indicated that patients with primary *KIT* exon 11 mutations, especially deletion mutations are the only proven subgroup to benefit from adjuvant imatinib. Notably, patients with GISTs harboring *KIT* exon 9 mutations, *PDGFRA* D842V mutations, or those lacking mutations in either *KIT* or *PDGFRA* have no discernible benefit with adjuvant imatinib therapy (Joensuu et al. 2016; Corless et al. 2014). Based on these results, and extrapolating from the clinical outcomes of patients with

advanced GIST treated with imatinib, we recommend that physicians who are considering a recommendation of adjuvant therapy for resected primary GIST should first determine the genotype of the patient's tumor. Patients with moderate to high-risk *KIT* exon 11-mutant GIST should be considered for treatment with three years of standard dose imatinib. In contrast, patients with *PDGFRA* D842V mutant GIST or whose tumor lacks any *KIT*/*PDGFRA* mutations should not be treated with adjuvant imatinib. In addition, *KIT* exon 9-mutant GIST patients have not been proven to benefit from the lower standard dose (400 mg daily) of imatinib therapy in the adjuvant setting. It is unknown if patients with *KIT* exon 9-mutant GIST would benefit from high dose imatinib in the adjuvant setting. Finally, we also recommend that patients with high risk GIST with imatinib-sensitive *PDGFRA* mutations (e.g. those other than D842V) be offered at least three years of adjuvant imatinib (Corless et al. 2005).

4.7.3. Primary resistance to front-line therapy

The treatment of metastatic GIST is limited by the eventual emergence of resistance to one or more TKIs. Resistance to front-line treatment with imatinib can be divided into two categories: primary and secondary. Approximately 10% of patients with GIST have primary resistance, defined as progression within the first 6 months of treatment. With proper molecular subtyping, this resistance is typically foreseeable and therapy can be adjusted in some cases. As discussed earlier, clinical responses to imatinib correlates with the primary tumor genotype, with the probability of primary resistance to imatinib for *KIT* exon 11, *KIT* exon 9, and RTK-WT GISTs being 5%, 16%, and 23%, respectively (Heinrich, Corless, Demetri, et al. 2003; Heinrich, Owzar, et al. 2008;

'Comparison of two doses of imatinib for the treatment of unresectable or metastatic gastrointestinal stromal tumors: a meta-analysis of 1,640 patients' 2010; Debiec-Rychter et al. 2004).

Primary resistance is seen at high frequency in *PDGFRA*-mutant GISTs. *In vitro*, the most common *PDGFRA* mutation in GIST, D842V, is strongly resistant to imatinib (Heinrich, Griffith, et al. 2012). This finding is mirrored by clinical results with patients with *PDGFRA* D842V-mutant GIST having low response rates and very short progression-free and overall survival during imatinib treatment.

As discussed earlier, RTK-WT GISTs have mutations downstream of KIT or affecting entirely different pathways (e.g. SDH) (Janeway et al. 2011; Agaram et al. 2008; Hostein et al. 2010). Hence, these GISTs have much lower response rates to imatinib, but may respond to alternative agents, such as KIT/VEGFR inhibitors for treatment of pediatric/*SDH*-mutant GIST, and BRAF/MEK inhibitors for *BRAF*/*RAS*-mutant GIST (Janeway et al. 2009). Some patients with RTK-WT GIST have prolonged disease-free and overall survival during front-line imatinib treatment. Whether this situation is due to their underlying indolent biology or by a subgroup of tumors with partial KIT-dependency remains unclear (Heinrich, Owzar, et al. 2008).

4.7.4. Secondary resistance to TKI therapy

After an initial benefit from imatinib, most patients eventually experience disease progression caused by secondary resistance. It is now established that acquired mutations in *KIT* or *PDGFRA* account for the vast majority of cases of secondary resistance in RTK-

mutant GIST, and that these mutations occur almost exclusively in the same allele as the primary oncogenic driver mutation (Corless, Barnett, and Heinrich 2011).

In a phase II imatinib study for advanced GIST, 67% of the patients whose tumor showed imatinib resistance had a secondary or acquired mutation in *KIT*. These mutations were common among tumors with a primary exon 11 mutation, but were not observed in RTK-WT GISTs (Heinrich et al. 2006). Indeed, secondary mutations of *KIT* have never been reported in RTK-WT GIST. Unlike primary mutations that activate KIT, which are predominantly found in exons 9 or 11, the secondary mutations associated with TKI resistance are typically concentrated in either the ATP-binding pocket (encoded by exons 13 and 14) or the kinase activation loop (encoded by exons 17 and 18)(Heinrich et al. 2006). Drug resistance has also been observed in *PDGFRA*-mutant GISTs, most commonly by acquiring a D842V mutation (activation loop) (Heinrich et al. 2006; Debiec-Rychter et al. 2005). However, there have been no reliable reports of a secondary *KIT* mutation arising in a GIST with a primary *PDGFRA* mutation, or vice versa, during treatment with imatinib.

Additional studies using more sensitive assays have identified secondary mutations in more than 80% of drug-resistant GIST lesions (Corless, Barnett, and Heinrich 2011). There can be significant heterogeneity of resistance across different metastatic lesions in a patient, and even within different areas of the same lesion (Corless, Barnett, and Heinrich 2011). For example, there are reports of up to 5 different drug resistance mutations in different portions of an individual lesion and up to 7 different secondary resistance mutations across multiple tumors in the same patient (Liegl et al. 2008). This heterogeneity of resistance significantly affects the efficacy of salvage TKI therapy after front-line imatinib, because the diversity of resistant, minority clones precludes the

systemic eradication of GIST cells by any particular TKI. Given the problems of tumor heterogeneity and the limited predictive value of lesion genotyping to predict response to changing medical therapy, biopsy of progressive lesions solely to assay for secondary resistance mutations and thereby select subsequent TKI therapy is not recommended. In the future, the use of liquid biopsy techniques to characterize secondary resistance mutations in circulating tumor DNA (ctDNA) may be clinically useful (see below).

4.8. Expert commentary on approaches to molecular diagnosis of GIST

As discussed above, all GISTs with a significant risk of recurrence should be molecularly tested. It is well established that tumor genotyping plays an important role in defining the prognosis and treatment of patients with GIST. Nevertheless, molecular diagnostic practices are currently under-utilized in the management of GIST patients (Barrios et al. 2015; Schoffski et al. 2016). Because of this, GIST patients may receive less than optimal treatment and inadequate genetic counseling. **Figure 20** presents a molecular diagnostic decision tree to genotype newly diagnosed GIST. Since SDHB-deficient GISTs are limited to the stomach, we recommend that SDHB IHC should be performed on all gastric GIST, as it prevents unnecessary sequencing for *KIT* and *PDGFRA* mutations. SDHB-deficient GISTs should be submitted for *SDHx* sequencing so that genetic counseling and follow-up screening can be offered to these patients. If treatment with imatinib is under consideration, then SDHB IHC-positive gastric and all non-gastric tumors should be sequenced for *KIT* and *PDGFRA* mutations. The remaining cases (less than 15%) are candidates for additional testing for mutations in *NF1, BRAF* and the *RAS* genes. Many labs now offer next generation sequencing panels that cover all the genes

relevant to GIST (Shi et al. 2016). However, screening for fusions involving the *NTRK* and *FGFR* gene families is only currently available from a few specialty labs. Following molecular classification, patients should be treated in the adjuvant or metastatic setting as discussed above for specific molecular subtypes of GIST.

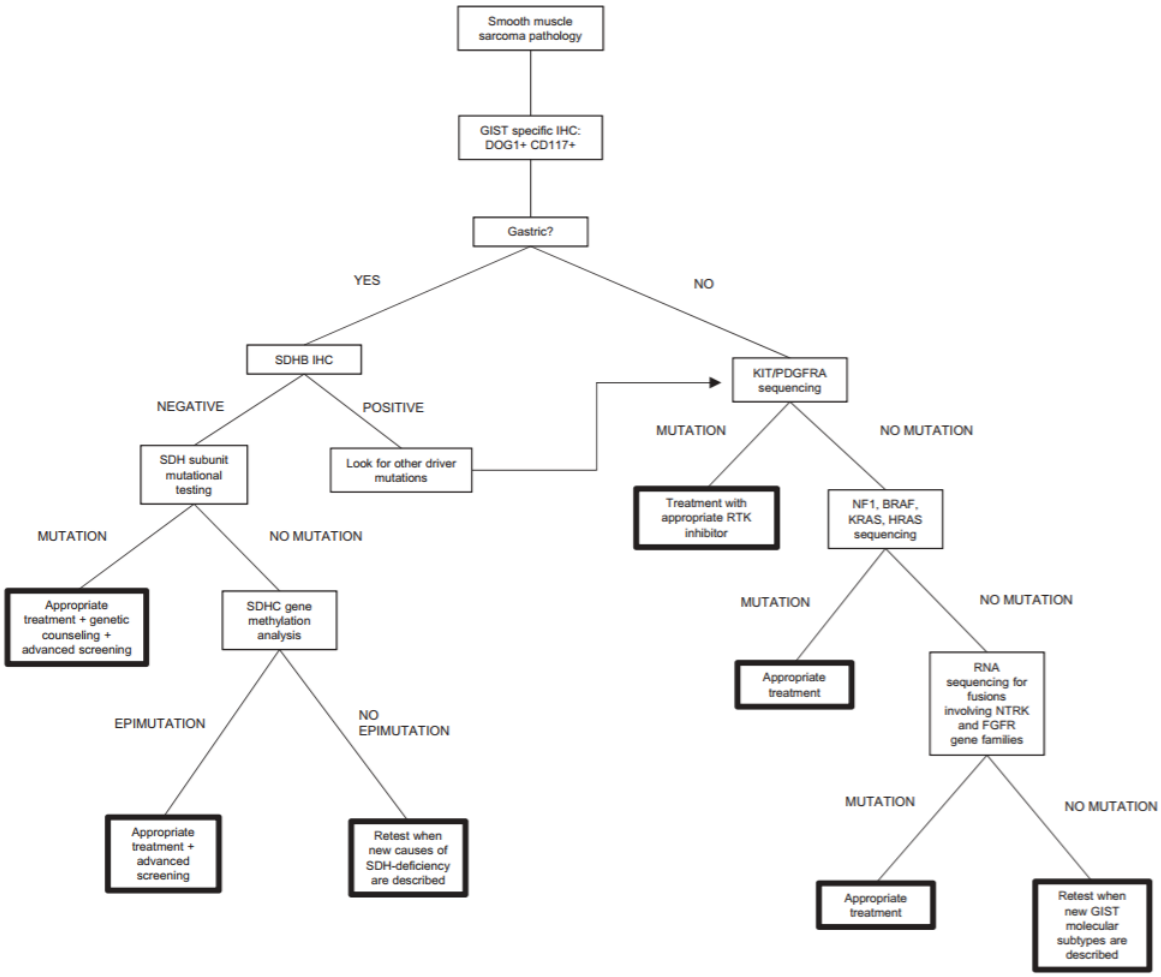

Figure 20. Decision tree for diagnosis and treatment of GIST.
The boxes show the decision nodes and recommended course of action for optimized diagnosis and treatment of GIST based on molecular classification. The end point boxes are indicated by the presence of a thick border.

4.9. Five-year view

As technology advances over the next five years, our ability to diagnosis and treat molecular subtypes of resistant GIST will also improve. Mutations that confer resistance to clinically approved TKIs used to treat GIST have emerged as the major factor limiting the survival of patients with metastatic GIST. Currently, an invasive biopsy is needed in order to identify the primary oncogenic mutation and usually is not repeated after a patient relapses solely to identify an acquired resistance mutation. Instead, each patient is treated with TKIs in the same sequence (imatinib followed by sunitinib followed by regorafenib), in accordance with standard professional and health authority guidelines. However, these currently approved inhibitors have serious potency issues against some or all activation loop mutations that are known to be associated with imatinib-resistant GIST. Thus, tumors with secondary activation loop mutations tend to become the dominant clinical problem in patients with resistance to one or more TKIs. Currently, a number of novel inhibitors with activity against KIT activation loop mutations are in phase 1 clinical studies (NCT02508532, NCT02571036). Assuming that these or other inhibitors prove to be safe and effective for treatment of TKI-resistant GIST, one could envision a clinical scenario where the choice of therapy for a given patient might be informed by having information on which particular resistance mutations exist amongst different tumors in a single patient.

Liquid biopsy, a technique to identify tumor mutations in circulating tumor DNA (ctDNA), could allow a global assessment of the various types of secondary mutations in a given patient with multi-focal TKI-resistant GIST. This diagnostic approach has been validated in several types of solid tumors (Schwaederle et al. 2016; Douillard et al. 2014;

Fribbens et al. 2016; Romanel et al. 2015; Siravegna et al. 2015). In the case of GIST, *KIT* and *PDGFRA* mutations can be detected from plasma/blood samples of GIST patients (Maier et al. 2013) including secondary *KIT* mutations in patients undergoing imatinib therapy (Wada, Kurokawa, et al. 2016). There is an ongoing clinical trial to determine if there is an association between changes in circulating tumor DNA with GIST disease progression, as measured by conventional methods (NCT02443948). Clinical decision making based on this technology has not yet been validated. Ultimately, some form of clinical study comparing standard treatment vs. ctDNA guided treatment will be needed to prove that genotype guided therapy is superior to current treatment guidelines. In addition to guiding management of advanced disease, this technology could also be used to monitor for recurrence after curative intent surgical resection. Monitoring for the primary *KIT* mutation associated with a resected tumor could be used to supplement or replace conventional imaging, assuming that ctDNA detection of recurrence has a sensitivity that is similar or superior to imaging studies.

4.10. Key issues

- IHC can distinguish GIST from other tumor types with similar histology but different clinical behavior. Molecular classification based on mutation testing is crucial for the optimal treatment of GIST.
- Some GIST, particularly SDH-deficient tumors, can be caused by a germline mutation. Identification of individuals with an inherited susceptibility to GIST allows for appropriate genetic counseling, screening of other family member,

and surveillance strategies for early detection of other tumors that can independently arise later in life.

- Known oncogenic drivers in GIST include mutations in *KIT, PDGFRA, SDHA/B/C/D, BRAF, RAS, NF1*, and translocations involving RTKs other than KIT/PDGFRA (e.g. NTRK3).

- Oncogenic driver mutations confer unique clinical features requiring different treatment strategies .

- The majority of GISTs have mutations in *KIT* or *PDGFRA* and can be successfully treated with tyrosine kinase inhibitors.

- In the future, precision medicine treatment of GISTs with molecular abnormalities other than *KIT*/*PDGFRA* mutations may become clinically available.

- ctDNA offers a potential strategy for detecting and characterizing secondary mutations in patients treated with TKIs. Future clinical studies are required to define the sensitivity and clinical utility of this testing in the management of patients with GIST.

5. CHAPTER FIVE: Conclusions and Future Directions

5.1. Conclusions

The goal of my dissertation work is to turn bench-side experiments into tangible results that help optimize clinical management for patients with GIST.

Chapter 1 reviews my protein complex of interest, SDH. To understand the biochemical, molecular, and clinical implications of genetic variants in SDH, it was important to first understand the basic biology of the SDH complex and its role in human disease. Due to SDH's dual role in aerobic metabolism, this complex is highly conserved, as a result decades of research across multiple species has provided us with a firm understanding of the assembly of the complex, the structure, and the catalytic function. I used all of this information, as well as the established yeast model to understand functional effects of *SDHA* variants in **Chapter 2**. **Chapter 1** also discusses the role of SDH in disease, emphasizing the importance of a deeper understanding of the pathogenic, loss-of-function variants in SDH and how understanding more about these variants can change clinical practice.

In **Chapter 2** SDHA variants of unknown significance are categorized based on how they affect SDH complex function, and whether or not they predispose patients to SDH-deficient cancer. In this study, we combined data from clinical observations, a functional yeast model, and a computational model to determine the pathogenicity of 22 *SDHA* VUS. We gathered *SDHA* VUS from two primary sources: The OHSU Knight Diagnostics Laboratory and the literature. We used a yeast model to identify the functional effect of a VUS on mitochondrial function with a variety of biochemical assays. The computational

model was used to visualize variants' effect on protein structure. We were able to conclude functional effects of variants using our three-prong approach to understanding VUS. We determined that 16 (73%) of the alterations are pathogenic, causing loss of SDH function, and six (27%) had no effect on SDH function. Based on these results, we reclassified the majority of the VUS tested as pathogenic, thus highlighting the need for more thorough functional assessment of inherited SDH variants. In addition to classifying variants, this chapter also underscored the importance of clinical SDHB IHC to identify SDH-deficient cancers. In our yeast model, Sdh1 protein expression was retained in some loss-of-function *Sdh1* variants. However, Sdh2 protein was consistently decreased in all loss-of-function *Sdh1* variants. This challenges the clinical role of SDHA IHC to identify pathogenic SDHA mutations.

Based on our work in **Chapter 2**, 27% of variants had no effect on SDH function despite negative SDHB IHC. These tumors remain unclassified but must have some molecular mechanism to cause SDH-deficiency. In order to identify novel causes of SDH-deficiency in GIST samples we designed a custom NGS AmpliSeq panel of SDH-related genes (*SDHA, SDHB, SDHC, SDHD, SDHAF1, SDHAF2, SDHAF3, SDHAF4, NDUFAB1, DARS2*, *FH, IDH1, IDH2)*, validated the panel with normal spleen samples, and tested nine GIST samples with no known molecular drivers (see **Chapter 3).** We hypothesized that there are novel causes of SDH-deficiency potentially including hypermethylation of SDH-related gene promoters, genomic mutations in SDH-related gene promoters that result in decrease SDHx protein expression, or genomic mutations in recently identified SDH assembly factors. Unfortunately, we found no new mutations in any of the SDH-related

genes or their promoters. However, there are many future directions associated with this panel that have high potential to impact the field (see **Section 5.2**).

The previous chapters have focused on the role of SDH loss-of-function variants in GIST pathogenesis, however SDH-deficient GIST comprise only a small subset of GIST. Historically, GIST has a been used as a model system for the use of molecular diagnosis to guide the selection of appropriate therapy. Multiple principal driver genes have been identified, dividing GISTs into molecularly distinct groups that require different therapies, and in some cases different dosing. **Chapter 4** focuses on the evolution of our understanding of the molecular basis of GIST and how modern molecular diagnostics should be used to optimize the therapeutic approach. I hope that the SDH-field will advance to the level of the KIT-mutant GIST-field so we can identify specific treatments and/or screening recommendations for each type of SDH mutation.

5.2. Future directions

In **Chapter 3** we discuss a NGS SDH-related gene panel that was created to identify novel causes of SDH-deficiency in GIST. Unfortunately, we were unable to clearly identify any mutations in these tumors that would be solely responsible for SDH-deficiency. We did uncover one, previously unrecognized heterozygous SDHA mutation, G184R. We were unable to make a conclusion about whether or not it affects function using our *in silico* analysis tools, so an obvious next step is to use our functional tests in our yeast model (**Chapter 2**).

Interestingly, this heterozygous variant (if indeed loss-of-function) continues a theme of SDH-deficient tumors with SDHA heterozygosity for pathogenic variants. Based on the current model of tumorigenesis, the *SDHx* genes are tumor suppressors, meaning that

there must be two hits (inactivating both alleles) to cause SDH-deficiency and therefore cancer. However in our results from **Chapter 2,** we notice 4 of the 26 tumors are heterozygous for a pathogenic, loss-of-function SDHA mutation but the second hit was not detected. We concluded that there must be some other cause of SDH-deficiency (such as hypermethylation, large genomic deletion) that would cause loss of heterozygosity that was not identified. The Killian group also saw SDH-deficient tumors that were heterozygotes for loss-of-function SDHA mutations. After assessing *SDHx* promoter hypermethylation and genomic deletions by copy number and genotyping microarray, they still found 8 cases of SDH-deficient GIST without a second hit. In all 8 cases, the first hit was a point mutation in SDHA (Killian et al. 2014). *We hypothesize this group of tumors, containing a heterozygous pathogenic SDHA mutation, represents a novel cause of SDH-deficiency.*

Many questions still surround this hypothesis since there are patients born with germline, pathogenic *SDHA* variants that do not ever develop GIST (see **Section 1.7.3** on penetrance). Because of the inconsistent penetrance, there must be a second downstream event that causes these cells to become tumorigenic. Having a better understanding of the mechanism of tumorigenesis would help to tease apart what this second downstream event could be. Potential experiments include measuring succinate levels in loss-of-function heterozygote tumors vs. homozygous tumors to establish the physiological levels of succinate in these tumors.

It will be difficult to show that heterozygous SDHA mutations indeed cause these tumors because of the many potential causes of SDH-deficiency that have not yet been discovered. For this reason, it is important we continue to rule out all other possible

causes of SDH-deficiency. Therefore, other future directions include further validation and expansion of our current panel to identify novel causes of SDH-deficiency. This additional work would include promoter mutation/epimutation analysis and testing for large genome deletions of SDHx and assembly factors, using microarrays.

As we perform additional tumor specimen testing, our panel may still identify novel mutations in SDHx promoters or the new assembly factors. Only a very small sample size (nine GIST samples), were run on the panel. Increasing the number of samples and the type of SDH-deficient tumor, for example also including paragangliomas and pheochromocytomas, will increase our chances of finding novel causes of SDH-deficiency.

An additional benefit from the use of our panel may be to identify new variants that might influence prevalence for families with known loss-of-function germline mutations in SDHx. As a reminder, clinically we observe inconsistent phenotypes and penetrance with patients that are born with known pathogenic, germline *SDHx* variants suggesting that other environmental, genetic or epigenetic factors influence the clinical phenotype. Current studies evaluate penetrance by identifying one family member that presented with the disease and then monitoring the other family members with the same germline mutation to see if they do or do not present with the same phenotype (Bausch et al. 2017). These are biased cohorts since there could be other passenger mutations that are affecting the penetrance of these loss-of-function mutations. In late July 2017, evidence validating our hypothesis that the new assembly factors are involved in SDH-deficient cancers was published. A *SDHAF3* variant was associated with increased prevalence in familial and sporadic PC/PGL (Dwight et al. 2017). The germline variant, SDHAF3 Phe53Leu, was found in patients that also have loss-of-function *SDHB* germline variants. Functional studies

using a yeast model showed SDHAF3 Phe53Leu had a significant reduction in SDH activity compared to WT controls. Upon further analysis, this germline variant was present in the normal population but had an increased prevalence in disease-affected individuals compared to disease-free individuals. Although this is not a direct correlation to SDH-deficiency like the other SDHAFs, mutations in *SDHAF3* seem to play some role in human disease.

Ideally, we would screen all patients with germline *SDHx* variants to try to uncover a mutation in a second SDH-related gene and then over time (or retrospectively) correlate the genotype with cancer phenotype. Additionally, since a disruption in epigenetics, hypermethylation of DNA and histones, is thought to play a role in tumorigenesis we could also measure the methylome of each one of these patients and provide epi-genotype/phenotype correlations. Based on this we could stratify patients and their families into high and low risk categories which could better guide screening recommendations including when to start screening, how frequently it should be done, and what specific tumors to be looking for. Additionally, this might further our understanding of the mechanism of tumorigenesis in SDH-deficient cells and could potentially help inform our clinical decisions about targeted therapeutic strategies.

Our last future direction stems from a collaboration with Foundation Medicine. Foundation Medicine performs clinical genome testing for the diagnosis and treatment of cancer. They provide a commercially-available, clinically-validated, large sequencing panel to identify genetic mutations to help clinicians match patients with appropriate targeted therapies, immunotherapies and clinical trials. Their sequencing panel includes 315 cancer-related genes, including the four SDH subunits. Foundation Medicine has agreed

to share with the Heinrich lab all the genomic data for any patient sample that was found to have an SDHx mutation. Through this collaboration, we will have unprecedented access to results from clinical sequencing of a large library of solid tumor samples. We hope that the analysis of this dataset will broaden the scope of tumors currently associated with SDHx mutation.

Continuing the theme of this dissertation, these future directions focus on identifying genetic mechanisms linked to cancer. Specifically, the future directions attempt to classify GISTs with unknown driver mutations, understand new genetic risk factors for SDH-deficient GIST, and identify SDH mutations in cancers not currently associated with SDH-deficiency. With a better understanding of which mutations are responsible for tumorigenesis, we will be able to translate genetic data into actionable clinical practices.

6. APPENDIX A: LMTK3 is essential for oncogenic signaling in *KIT*-mutant GIST and melanoma

Lillian R. Klug, **Amber E. Bannon**, Nathalie Javidi-Sharifi, Ajia Town, William H. Fleming, Jonathan A. Fletcher, Jeffrey W. Tyner, Michael C. Heinrich

6.1. Preface

Inhibiting KIT has been very successful in most KIT-mutant GIST. However, a large number of patients will eventually progress on these therapies through various resistance mechanisms, mostly internal KIT mutations that allow them to be constitutively active. Ideally, we could target a protein upstream of KIT that is important for KIT-dependent tumor cells but not important for normal, KIT-independent cells. This chapter details the elegant work of Lillian Klug in finding Lemur Tyrosine Kinase 3 (LMTK3) as an essential regulator of KIT. As second author, my contributions were mostly technical. During my attempt to establish an SDH-deficient xenograft model, I developed the methodology and performed the mouse experiments that demonstrated a decrease in KIT-dependent tumor growth after treatment of GIST cells with LMTK3 siRNA. A huge thank you to Dr. William H. Fleming and his lab for training in the basic skills needed for performing mouse work. I also assisted in the conception and design, development of methodology, analysis and interpretation of data and editing of the manuscript which is currently under review at *Cancer Research*.

6.2. Abstract

Certain cancers, including gastrointestinal stromal tumor (GIST) and subsets of melanoma, are caused by somatic *KIT* mutations that result in constitutive KIT receptor tyrosine kinase activity to drive proliferation. The treatment of these *KIT*-mutant cancers has been revolutionized with the advent of KIT-directed cancer therapies. KIT tyrosine kinase inhibitors (TKI) are superior to conventional chemotherapy in their ability to control advanced *KIT*-mutant disease. However, these therapies have a limited duration of activity due to drug-resistant secondary *KIT* mutations that arise (or that are selected for) during KIT TKI treatment. To overcome the problem of KIT TKI resistance, we sought to identify novel therapeutic targets in *KIT*-mutant GIST and melanoma cells using a human tyrosine kinome silencing RNA (siRNA) screen. From this screen, we identified lemur tyrosine kinase 3 (*LMTK3*) and herein describe its essential role in *KIT*-mutant GIST and melanoma cells. *LMTK3* silencing in *KIT*-mutant cells decreased KIT activity and downstream signaling, resulting in reduced proliferation and increased cell death. Furthermore, targeting of *LMTK3* delayed GIST growth in an *in vivo* xenograft model. We found this effect to be specific to *KIT*-mutant cells that depend upon KIT signaling, as viability of KIT-independent GIST or melanoma cells was not affected by *LMTK3* silencing. Notably, *LMTK3* silencing reduced viability of all *KIT*-mutant cell lines we tested, even those with drug-resistant secondary *KIT* mutations. These data suggest the potential for targeting of *LMTK3* as a treatment for patients with *KIT*-mutant cancer, particularly after failure of KIT TKI.

6.3. Introduction

The type III receptor tyrosine kinase KIT and its cognate ligand, stem cell factor (SCF), play important roles during development, as well as in adult stem cell maintenance (Witte 1990). Normal KIT activity is induced upon SCF binding and signals to numerous downstream pathways, including PI3K/AKT and MEK/ERK, to drive proliferation and survival of cells (Lev, Givol, and Yarden 1991; Lev, Yarden, and Givol 1992). Gain-of-function mutations in KIT causing ligand-independent kinase activation are known to drive neoplastic growth in multiple tissues (Furitsu et al. 1993).

KIT-mutant tumors include the majority of gastrointestinal stromal tumors (GIST) and mastocytosis, as well as subsets of melanoma, acute myeloid leukemia, and seminoma (Beadling et al. 2008; Larizza, Magnani, and Beghini 2005; Nagata et al. 1995; Tian et al. 1999; Kemmer et al. 2004). Somatic activating *KIT* mutations driving neoplasia are fairly rare overall, but within certain tumor types or subtypes, the frequency can be quite high. Of the 5,000 new cases of GIST that are diagnosed each year in the U.S., over 70% of these cases are caused by *KIT* mutations (Corless, Barnett, and Heinrich 2011). In melanoma, *KIT* mutations make up the majority of oncogenic driver mutations in acral and mucosal subtypes, as well as melanomas arising from chronically sun-damaged skin (Beadling et al. 2008; Hodi et al. 2013). Both GIST and these melanoma subtypes have poor response to conventional cytotoxic therapies and radiation (Dematteo et al. 2002; Spencer and Mehnert 2016). However, KIT TKI therapies have improved treatment outcomes for these patients. The median overall survival of patients with advanced GIST is now estimated to be 7-8 years, and a subset of patients live more than 10 years (Blanke, Demetri, et al. 2008; Blanke, Rankin, et al. 2008; Verweij et al. 2004); this is in contrast to an overall survival of

12-18 months with conventional chemotherapies (Edmonson et al. 2002). Although no KIT-targeted treatments are yet approved for *KIT*-mutant melanoma, early clinical trials have shown promise(Carvajal et al. 2015; Hodi et al. 2008; Guo et al. 2011; Hodi et al. 2013).

While KIT TKI treatments, such as imatinib, can provide significant clinical benefit, they are rarely curative. The majority of GIST patients will develop drug resistance over the course of KIT TKI treatment; the median time to tumor progression on first-line imatinib therapy is 20-24 months (Demetri et al. 2002). Resistance to KIT TKIs in GIST is almost exclusively caused by secondary *KIT* mutations, most commonly affecting the ATP binding pocket (V654A, T670I) or the activation loop (codons 816, 820, 822, 823 or 829 with multiple amino acid substitutions reported for most of these codons) (Weisberg and Griffin 2003; Antonescu et al. 2005; Roberts et al. 2007; Liegl et al. 2008). Primary mutations that affect these domains can also confer drug resistance. Drug-resistant tumors remain KIT-dependent, but these secondary mutations can interfere with KIT TKI binding. Disease management is complicated in the advanced setting with the existence of inter- and intra-lesional heterogeneity of *KIT* mutations (Liegl et al. 2008). Patients can have various secondary mutations between and within lesions, and each mutation can have different sensitivity profiles to individual KIT TKIs (Liegl et al. 2008; Gramza, Corless, and Heinrich 2009).

In the face of heterogeneous *KIT* mutations in these tumors, KIT TKIs have limited ability to control *KIT*-mutant disease once clinical resistance develops, leaving patients with few treatment options. Because of this, we sought to identify novel targets in *KIT*-mutant cancer cells using a previously described siRNA screen methodology called RNAi Assisted Protein Identification (RAPID), which targets all predicted members of the

human tyrosine kinome (Tyner et al. 2009). Using this approach, we identified the protein kinase lemur tyrosine kinase 3 (*LMTK3*) as an essential gene in *KIT*-mutant GIST and melanoma cells. Despite its name, LMTK3 is, in fact, a serine/threonine kinase with few identified substrates or functions (Wang and Brautigan 2002; Tomomura et al. 2007). LMTK3 has been implicated in promoting cancer growth and the roles of LMTK3 have been described in breast cancer, although mechanisms are not fully understood in other tumor types (Giamas et al. 2011; Stebbing et al. 2013; Xu et al. 2014; Xu et al. 2015).

This study describes our findings of the essential role for LMTK3 in promoting the viability of all *KIT*-mutant GIST and melanoma cells that we have studied to date, including those with mutations conferring KIT TKI resistance. We show that silencing of *LMTK3* decreased KIT phosphorylation and downstream signaling and that this loss of KIT activity is responsible for the decreased viability. Finally, we show that *LMTK3* silencing reduced the growth of GIST xenografts *in vivo*. These data suggest that LMTK3 is a regulator of oncogenic KIT activity, and because of its essential role in *KIT*-mutant cells regardless of the nature of their *KIT* mutation, LMTK3 has potential as a therapeutic target in KIT TKI-resistant *KIT*-mutant human cancers.

6.4. Materials and methods

Cell lines. The GIST-T1 cell line, which was derived from a KIT exon 11 mutant patient tumor (Taguchi et al. 2002), and secondary KIT-mutant GIST-T1 cell lines were generously provided by Dr. Sebastian Bauer in 2012 (West German Cancer Center, Essen, Germany). The GIST-T1 cell lines containing secondary KIT mutations were produced by long-term imatinib exposure of GIST-T1 cells. GIST430 (ex 11) represents a clonal cell line from the

patient-derived GIST430 cell line (Bauer et al. 2006). GIST430 (ex 11) contains a homozygous KIT exon 11 deletion, but has spontaneously lost the heterozygous secondary V654A mutation, which is present in the original line. The GIST54 line came from a patient-derived KIT-mutant cell line that spontaneously lost KIT expression while in culture. MaMel (144aI) cells were generously provided by Dr. Dirk Schadendorf in 2012 (West German Cancer Center, Essen, Germany); this cell line was derived from a primary melanoma and contains a KIT exon 9 mutation (S476I) (Ma and Rubin 2014). Cell lines containing KIT mutations were authenticated by KIT gene sequencing and KIT TKI sensitivity experiments. GIST430 (ex 11) and GIST-T1 cell lines are grown in IMDM with 15% FBS, 1% L-glutamine, and 1% penicillin/streptomycin. GIST cell lines with secondary mutations were maintained in imatinib at the doses shown in **Table 12**. GIST54 were grown in above medium, but with 5% FBS. MaMel were grown in RPMI with 10% FBS, 1% L-glutamine, and 1% penicillin/streptomycin. GIST882 and GIST48 were grown in above RPMI medium with 15% FBS. Upon receipt, GIST and MaMel cell lines were tested for mycoplasma contamination by Venor™ GeM Mycoplasma Detection Kit (Sigma, MP0025) and were found to be negative. HEK293, HT1080 (ATCC® CCL-121™) and SKMEL2 (ATCC® HTB-68™) were purchased from ATCC within 6 months of performing described experiments. The stable LMTK3$^{myc\text{-}DDK}$ expressing GIST430 (ex11) cell line was derived by transduction with virus produced using pLENTI-LMTK3$^{myc\text{-}DDK}$, then selected and maintained in G418 antibiotic (Sigma). Cell lines were maintained in culture for the minimum necessary time to perform experiments, generally not exceeding one month from thaw.

Cell line	Tumor origin	*KIT* mutation	IC_{50}: imatinib [nM]	Maintenance KIT TKI
GIST430 (ex 11)*	GIST	Exon 11 del (codons 560-576)	15	none
GIST430+V654A	GIST	Exon 11 del + V654A	1000	100nM imatinib
GIST-T1	GIST	Exon 11 deletion (codons 560-578)	20	none
GIST-T1 + T670I	GIST	Exon 11 deletion + T670I	5000	200nM imatinib
GIST-T1 + D816E	GIST	Exon 11 deletion + D816E	2000	200nM imatinib
GIST-T1 + D820A	GIST	Exon 11 deletion + D820A	2000	200nM imatinib
GIST-T1 + A829P	GIST	Exon 11 deletion + A829P	2500	100nM imatinib
GIST48	GIST	Exon 11 deletion + D820A	2000	none
GIST882	GIST	K642E	500	none
GIST54	GIST	Ex 11 del (codons 551-557) + Y823D**	n/a	none
MaMel (MaMel-144I)	Melanoma	S476I	700	none

Table 12. Human *KIT*-mutant cell lines used in this study

*GIST430 (ex 11) cells only have a deletion within *KIT* exon 11 and are derived from previously described GIST430 cell line that have an exon 11 deletion and a secondary V654A mutation in *KIT*

**GIST54 cells have *KIT* mutations, but lack KIT protein expression, making them KIT-independent

RAPID siRNA screen and siRNA transfection. Human tyrosine kinase siRNA screen (RAPID) (Tyner et al. 2009) was performed in triplicate for each cell line. The tyrosine kinase library used in this study contains 4 siRNA targeting constructs per well (purchased from Dharmacon), and we manually added single and pooled nonspecific siRNA as well as siRNA pools (4 constructs per target) against ephrin type-A receptor 5 (*EPHA5*), *EPHA6*, src-related kinase lacking C-terminal regulatory tyrosine and N-terminal myristylation (*SRMS*), apoptosis-associated tyrosine kinase (*AATK*), lemur tyrosine kinase 3 (*LMTK3*),

N-RAS, K-RAS (all from Dharmacon). These were added separately because they are not included in the standard tyrosine kinase library. Cells were plated in 96-well plates and transfected with siRNA pools using oligofectamine (Invitrogen). After 96 hour incubation at 37°C, viability was assayed using MTS reagent. Data from each screen experiment were corrected for row or column plating bias and triplicate experiments were averaged. The median effect and standard deviation of the data from each screen experiment were calculated. Genes exceeding one standard deviation from the median of each screen were considered for comparison between the three cell lines. We tested three individual *KIT*-mutant cell lines to avoid the possibility of identifying targets idiosyncratic to one particular cell line.

For other siRNA experiments, siGENOME siRNA pools were purchased from Dharmacon/GE: *LMTK3*: M-005338-03-0005, *KIT*: M-003150-02-0005, NT: D-001206-13-05, *PLK1*: M-003290-01-0005, custom *LMTK3* 3'UTR: 5'CAGAAGAGGGGUUGAGAAUUU-3'.

Reagents. Imatinib mesylate (STI571, Novartis), cycloheximide (Sigma), and G418 (Sigma) were dissolved in sterile water or PBS for cell culture. The expression plasmid pCMV6-LMTK3$^{myc\text{-}DDK}$ (RC223140) was obtained from Origene and used for construction of pLENTI-LMTK3$^{myc\text{-}DDK}$ (using pLENTI-C-$^{myc\text{-}DDK}$-IRES-Neo, PS100081).

Quantitative RT-PCR. Total RNA was extracted (RNeasy, Qiagen), cDNA was synthesized using 1ug of total RNA (MultiScribe RT, Applied Biosystems), and quantitative RT-PCR was performed on a LightCycler 480 (Roche) using Probes Master Mix (Roche). FAM Taqman primers for *LMTK3* (Hs01090726_g1) and *KIT* (Hs00174029_m1) were purchased from Life Technologies. Custom primers and hydrolysis probe (IDT) were used to detect a 66-bp *GAPDH* amplicon: GAPDH forward CACTAGGCGCTCACTGTTCT, GAPDH reverse

GCGAACTCCCCGTTG, GAPDH probe 5′TexRd-XN/TGGGGAAGGTGAAGGTCGGA/3′IAbRQSp.

Viability and caspase activity assays. Cells were plated, treated/transfected, and incubated in opaque 96-well plates (Corning). Viability was measured using the Cell Titer Glo reagent (Promega) after 15-minute incubation according to manufacturer's instructions. Activity of caspases 3 and 7 was measured using Caspase 3/7 Glo (Promega) after 60-minute incubation. The results of both assays were measured on the GloMax luminometer (Promega).

Protein harvest and Western blotting. Cells were scraped from flasks for lysis with HGNT lysis buffer (HEPES, NaCl, EDTA, Triton X-100, Glycerol) with 1X protease and phosphatase inhibitor cocktail (Cell signaling). Western blotting was performed by standard SDS-PAGE protocol using the Criterion electrophoresis system (Biorad), Transblot Turbo transfer system (Biorad), and imaged using the Chemidoc imaging system (Biorad).

Antibodies. Total KIT antibody was purchased from Genway (GWB-92B1FC). Phospho-KIT (Y703) (44-492) antibody was purchased from Biosource. Pan-phospho-tyrosine antibody was from BD (610000). Cell signaling supplied phospho-KIT (Y719) (#3391), phospho-AKT (S473) (#9271), total AKT (#9272), phospho-ERK1/2 (T202/Y204) (#9101), total ERK1/2 (#9102), β-tubulin (#2146), and Myc-Tag-HRP (#2040). c-KIT (C-19) conjugated beads (Santa Cruz, sc-168 AC) were used for KIT immunoprecipitations.

Cycloheximide time course. Cycloheximide (Sigma) was applied to cells for the indicated times at 20μg/mL in growth medium. KIT protein was quantified from 20ug total protein

lysate using PathScan Total c-KIT ELISA (Cell Signaling, #7197C), following standard protocol.

GIST xenograft. One million viable GIST430 (ex 11) cells were implanted subcutaneously in the flank of male NOD.Cg-*Rag1*^{tm1Mom} *Il2rg*$^{tm1Wjl/SzJ}$ (NRG) mice (Jackson Laboratories, n=8) 24 hours post transfection with non-targeting or *LMTK3*-targeting siRNA. Each mouse bore one non-targeting tumor and one *LMTK3*-targeted tumor on opposing flanks. Cells were suspended in 50% matrigel (Corning) for implantation. Tumors were palpated every three days; once a palpable mass was detected, tumors were measured using calipers every three days until sacrifice. Animals were humanely euthanized before total tumor burden reached 2 cm^3, as dictated by our IACUC protocol.

Statistics. All experiments were performed with at least 3 biological replicates. One-way ANOVA or t tests were calculated using PRISM (Graph Pad) software. All error bars represent standard error unless otherwise indicated.

6.5. Results

6.5.1. *LMTK3* identified as essential for viability of mutant KIT-dependent cells

To identify novel targets in KIT-mutant cancers, we performed a siRNA screen using viability as a read-out. The siRNA library encompassed all known and predicted human tyrosine kinases, as well as NRAS and KRAS (93 genes total)(Tyner 2011; Tyner et al. 2009). We measured viability 96 hours after transfecting cells with siRNA pools against

each target in three KIT-mutant cell lines: two GIST and one melanoma. (**Figure 21, Table 13**).

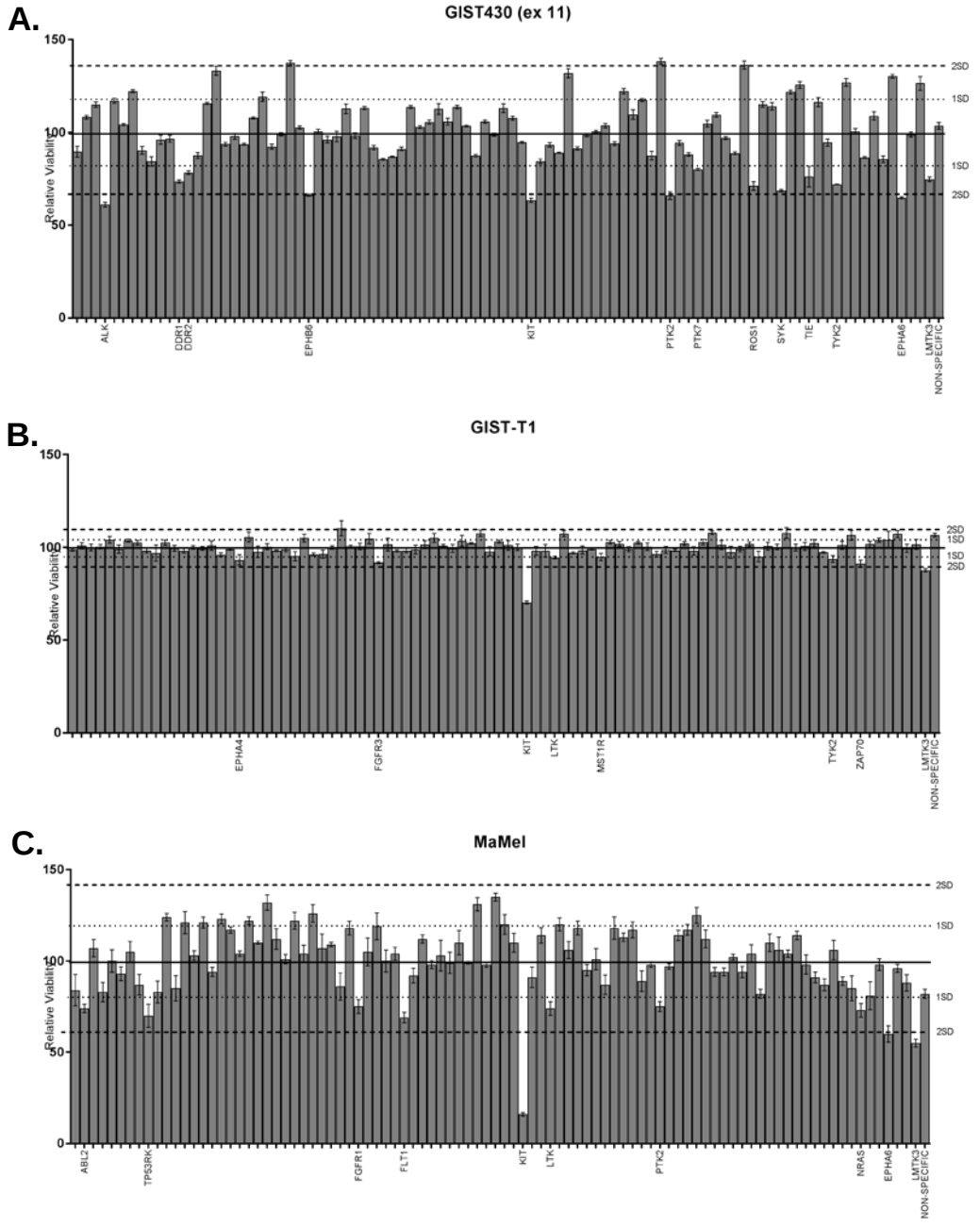

Figure 21. Human tyrosine kinase RAPID siRNA screen data from *KIT*-mutant cell lines.
Average viability of triplicate experiments relative to the plate median for GIST430 (ex 11) (A), GIST-T1 (B), and MaMel (C) cell lines. Error bars represent standard error from the plate median within triplicate

experiments. Plate median is represented by a solid line. One and two standard deviations of all the data from the plate median are represented with dotted lines.

GIST430 (ex11)			GIST-T1			MaMel		
Gene	**Average**	**SE**	**Gene**	**Average**	**SE**	**Gene**	**Average**	**SE**
ABL1	89.63	2.91	ABL1	98.75	0.63	ABL1	83.96	8.59
ABL2	108.16	0.99	ABL2	100.90	1.70	ABL2	73.81	2.37
TNK2	114.99	1.37	TNK2	99.96	1.75	TNK2	107.24	4.75
ALK	61.04	1.24	ALK	100.33	1.11	ALK	82.92	5.30
AXL	117.03	1.29	AXL	104.04	1.88	AXL	100.48	6.13
BLK	104.21	0.56	BLK	99.00	2.20	BLK	93.41	3.77
BMX	122.29	0.87	BMX	103.68	0.81	BMX	105.21	5.71
BTK	90.35	2.09	BTK	102.52	1.29	BTK	87.10	5.59
TP53RK	84.41	2.54	TP53RK	98.33	1.38	TP53RK	69.60	6.36
CSF1R	96.07	2.45	CSF1R	96.90	4.32	CSF1R	83.19	5.93
CSK	96.53	1.85	CSK	102.55	1.44	CSK	123.73	2.07
DDR1	73.60	0.82	DDR1	99.51	1.51	DDR1	85.34	6.92
DDR2	78.37	0.96	DDR2	98.19	1.28	DDR2	120.70	6.03
STYK1	87.55	1.61	STYK1	99.95	0.90	STYK1	102.57	2.58
EGFR	115.63	0.53	EGFR	99.45	0.99	EGFR	120.84	3.02
EPHA1	133.29	2.50	EPHA1	101.00	2.53	EPHA1	93.72	2.41
EPHA2	93.68	1.04	EPHA2	96.00	1.01	EPHA2	122.75	2.70
EPHA3	97.95	1.59	EPHA3	99.11	0.59	EPHA3	117.44	1.75
EPHA4	93.63	0.47	EPHA4	93.20	2.84	EPHA4	104.07	1.52
EPHA7	107.83	0.58	EPHA7	105.60	2.68	EPHA7	122.04	2.10
EPHA8	119.18	2.47	EPHA8	97.63	3.07	EPHA8	110.14	0.84
EPHB1	92.35	1.33	EPHB1	100.37	1.55	EPHB1	132.24	4.24
EPHB2	99.00	0.89	EPHB2	98.23	0.43	EPHB2	111.94	5.61
EPHB3	137.49	1.26	EPHB3	98.86	1.13	EPHB3	101.30	2.53
EPHB4	102.62	0.78	EPHB4	95.25	2.45	EPHB4	121.62	4.65
EPHB6	66.10	0.51	EPHB6	104.99	2.08	EPHB6	104.07	4.67
ERBB2	100.46	1.16	ERBB2	96.16	0.72	ERBB2	125.56	4.85
ERBB3	96.15	1.80	ERBB3	96.42	2.18	ERBB3	107.37	7.78
ERBB4	97.80	2.82	ERBB4	99.93	0.86	ERBB4	108.62	1.16
FER	112.70	2.58	FER	110.33	4.10	FER	86.20	7.47
FES	98.30	1.56	FES	100.47	0.65	FES	118.20	3.80
FGFR1	113.20	0.91	FGFR1	100.51	1.69	FGFR1	75.26	3.84
FGFR2	91.85	1.05	FGFR2	104.74	2.82	FGFR2	105.35	7.61
FGFR3	85.52	0.53	FGFR3	91.76	0.57	FGFR3	119.14	7.38
FGFR4	86.95	0.32	FGFR4	101.57	3.36	FGFR4	100.02	5.97
FGR	91.10	0.99	FGR	98.08	0.61	FGR	104.45	3.57
FLT1	113.65	0.85	FLT1	98.23	1.18	FLT1	68.79	2.83
FLT3	102.91	0.69	FLT3	98.82	2.36	FLT3	92.48	3.95
FLT4	105.59	1.01	FLT4	101.45	2.13	FLT4	111.55	2.27
FRK	112.61	2.86	FRK	105.14	2.38	FRK	97.78	2.20
FYN	105.80	1.84	FYN	100.83	0.72	FYN	102.85	8.42
HCK	113.65	1.00	HCK	99.41	2.09	HCK	98.78	5.84

IGF1R	103.45	0.49	IGF1R	103.53	2.91	IGF1R	110.17	6.64
INSR	87.50	0.61	INSR	102.21	0.46	INSR	99.04	0.59
ITK	105.82	0.77	ITK	107.61	1.71	ITK	130.80	3.63
JAK1	98.82	0.89	JAK1	97.86	2.48	JAK1	98.23	1.47
JAK2	113.05	2.38	JAK2	103.12	0.88	JAK2	135.22	2.13
JAK3	107.67	1.10	JAK3	101.11	2.59	JAK3	119.57	5.40
KDR	94.64	0.53	KDR	100.06	1.68	KDR	110.19	5.16
KIT	**63.38**	**1.21**	**KIT**	**70.35**	**0.83**	**KIT**	**16.09**	**1.03**
LMTK2	84.39	1.26	LMTK2	98.11	2.37	LMTK2	91.14	5.61
LCK	93.31	1.19	LCK	98.15	3.30	LCK	114.09	4.22
LTK	88.99	0.27	LTK	94.57	0.69	LTK	73.57	3.73
LYN	131.91	2.45	LYN	107.45	1.69	LYN	120.38	3.53
MATK	91.35	0.81	MATK	97.05	0.55	MATK	106.32	4.70
MERTK	98.56	0.95	MERTK	98.53	2.13	MERTK	117.75	3.84
MET	100.54	0.54	MET	99.15	0.47	MET	94.68	3.10
MST1R	103.60	1.24	MST1R	94.85	1.89	MST1R	101.33	5.79
MUSK	94.00	1.11	MUSK	102.81	1.00	MUSK	87.33	5.29
NTRK1	122.25	1.46	NTRK1	101.82	1.39	NTRK1	117.94	6.10
NTRK2	109.61	2.54	NTRK2	98.98	1.31	NTRK2	112.62	2.32
NTRK3	117.43	0.85	NTRK3	102.50	0.68	NTRK3	116.67	4.37
PDGFRA	87.48	2.26	PDGFRA	100.39	1.99	PDGFRA	88.65	5.65
PDGFRB	138.28	1.55	PDGFRB	96.37	1.52	PDGFRB	97.54	1.50
PTK2	65.94	2.05	PTK2	98.63	1.86	PTK2	74.92	2.81
PTK2B	94.34	1.37	PTK2B	98.49	0.61	PTK2B	96.54	1.53
PTK6	88.11	0.86	PTK6	102.09	1.07	PTK6	113.59	2.74
PTK7	80.09	0.50	PTK7	98.08	2.23	PTK7	116.59	2.96
PTK9	104.73	1.81	PTK9	102.90	1.51	PTK9	125.39	4.37
PTK9L	109.42	1.26	PTK9L	107.90	0.90	PTK9L	111.86	4.88
RET	97.02	0.78	RET	101.32	2.45	RET	93.68	2.37
ROR1	88.75	0.67	ROR1	97.31	3.23	ROR1	93.92	2.14
ROR2	136.31	2.16	ROR2	99.04	1.47	ROR2	102.21	1.57
ROS1	71.17	2.32	ROS1	101.71	1.19	ROS1	94.25	3.08
RYK	115.11	1.52	RYK	95.06	2.86	RYK	103.77	4.91
SRC	114.03	2.00	SRC	100.70	2.12	SRC	81.82	2.47
SYK	68.67	0.63	SYK	100.22	1.39	SYK	110.46	4.80
TEC	121.73	1.04	TEC	107.75	2.89	TEC	106.46	7.02
TEK	125.64	1.80	TEK	99.97	1.78	TEK	104.45	2.00
TIE	76.18	5.60	TIE	100.61	2.16	TIE	114.30	2.25
TNK1	116.37	2.42	TNK1	102.21	2.00	TNK1	98.10	5.29
TXK	94.51	1.94	TXK	97.30	0.45	TXK	90.92	3.01
TYK2	71.97	0.25	TYK2	93.73	1.85	TYK2	87.20	3.25
TYRO3	126.96	2.04	TYRO3	101.17	2.23	TYRO3	105.80	5.32
YES1	100.53	1.50	YES1	106.57	2.66	YES1	89.15	2.35
ZAP70	86.52	0.46	ZAP70	91.19	1.95	ZAP70	85.12	6.82
NRAS	108.90	2.16	NRAS	101.69	1.67	NRAS	72.53	3.77
KRAS	85.54	1.78	KRAS	103.89	1.12	KRAS	80.50	7.67
EPHA5	130.31	1.03	EPHA5	104.19	4.51	EPHA5	98.25	3.21
EPHA6	64.75	0.51	EPHA6	107.25	1.88	EPHA6	60.33	4.51
SRMS	98.84	1.40	SRMS	99.47	2.15	SRMS	96.19	2.18
AATK	126.44	3.61	AATK	101.62	2.67	AATK	88.42	4.44
LMTK3	74.72	1.20	**LMTK3**	87.66	0.88	**LMTK3**	55.24	2.06

NON-SPECIFIC	103.54	1.83	NON-SPECIFIC	106.64	1.05	NON-SPECIFIC	82.29	2.45

Average of Means	STDEV of Means	2*STDEV	Average of Means	STDEV of Means	2*STDEV	Average of Means	STDEV of Means	2*STDEV
100.06	17.68	35.37	99.83	4.97	9.90	99.40	19.34	38.67

Table 13. RAPID screen data.
Human tyrosine kinase siRNA RAPID screen results from three *KIT*-mutant cell lines. Average viability and standard error (SE) are shown as a percentage of median viability across entire screen (shown at bottom).

Candidates that negatively affected viability were determined for each cell line by calculating the median and standard deviation across each entire screen experiment; candidates for further comparison were those that reduced viability greater than one standard deviation from the median (Javidi-Sharifi et al. 2015; Tyner 2011; Tyner et al. 2009). All candidates within this cut off were found to have a statistically significant effect on viability (**Figure 22**).

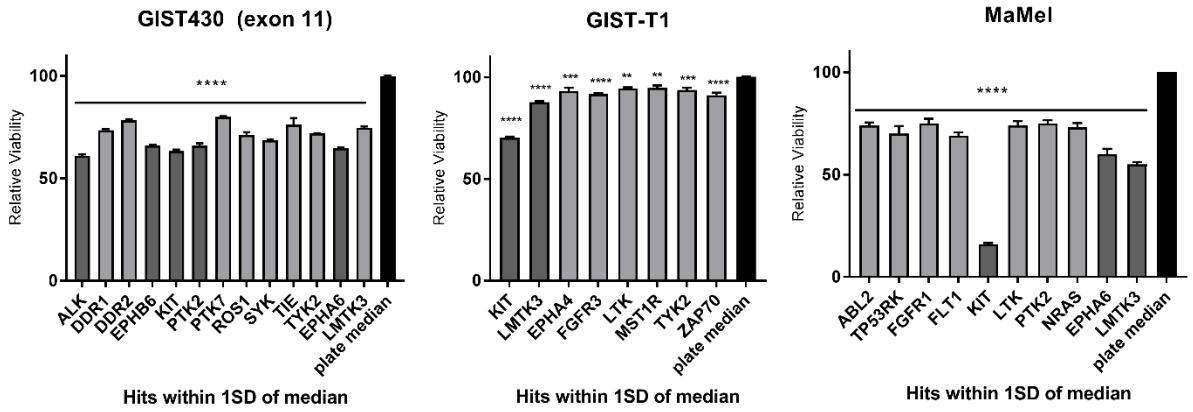

Figure 22. Statistical analysis of hits from KIT-mutant cell RAPID screens.
Viability relative to plate median of hits within 1 standard deviation from tyrosine kinase RAPID screens. Plate median shown in black, dark gray bars show hits that reached 2 standard deviations from the median, and light gray bars are hits found within 1 standard deviation from the median. A. GIST430 (exon 11). B. GIST-T1. C. MaMel. Statistics show results of One-way ANOVA with multiple comparisons to plate median. The p values are indicated by asterisks: ****, p<0.0001; ***, p<0.0005; **, p<0.005.

These genes were then compared across the three cell lines to identify common candidates (**Figure 23A**). The majority of genes were hits in only one cell line. Those few

targets that were shared between lines were validated in independent siRNA experiments (**Figure 23B**). For validation experiments, silencing of the essential cell cycle gene PLK1 served as a positive control across all cell lines and gave indication of success of transfection within a cell line. KIT siRNA served as an additional positive control in mutant KIT-dependent cell lines, and was, as expected, an identified candidate from the screens in each of the KIT-mutant cell lines. The only target besides KIT that was shared by all three cell lines was the protein kinase LMTK3 (**Figure 23A**). KIT silencing showed significant negative effect on viability in GIST-T1, GIST430 (ex11), and MaMel, in most cases comparable to PLK1 silencing; the silencing of LMTK3 decreased viability nearly to this level in all three cell lines (**Figure 23B**). Moreover, to corroborate these data, we found that multiple individual siRNAs against LMTK3 decreased viability in KIT-mutant GIST and melanoma cell lines and were able to knock down LMTK3 protein (**Figure 24**). Because we were unable to measure endogenous LMTK3 protein due to lack of a suitable antibody, we used epitope-tagged exogenous LMTK3myc to measure the effect of pooled and individual siRNAs.

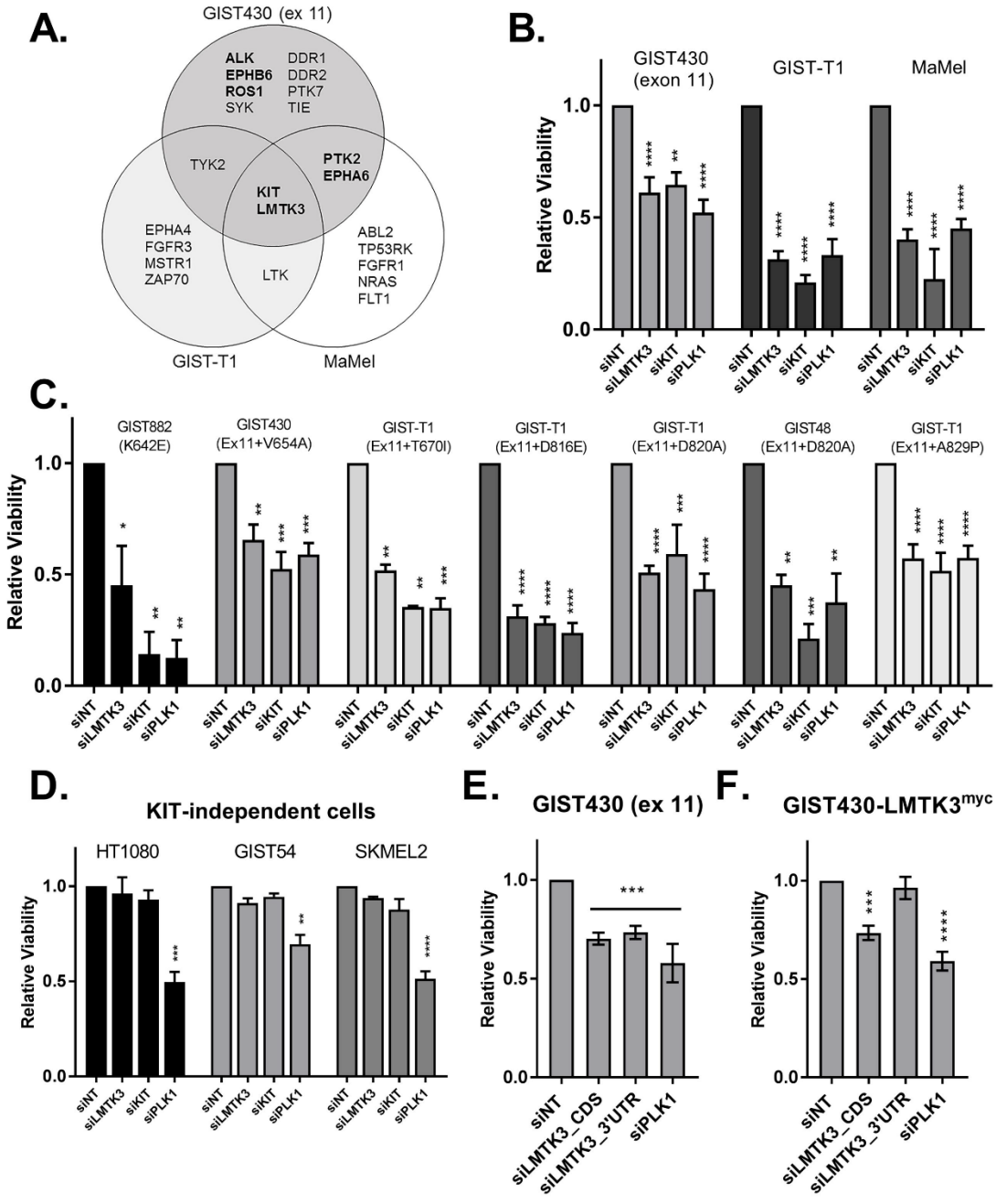

Figure 23. Silencing of the protein kinase LMTK3 specifically reduces viability of mutant KIT-dependent GIST and melanoma cells.

A. Venn diagram of hits from RAPID tyrosine kinase siRNA screens performed in KIT-mutant GIST430 (ex11), GIST-T1, and MaMel cell lines. Significance threshold of 2 SD (bold text) or 1 SD (regular text). B. Viability 96 hours post-transfection with non-targeting (NT), LMTK3, and KIT siRNA. C. Viability of KIT-mutant GIST cell lines was measured 96 hours post-transfection with indicated siRNAs. D. Viability of KIT-independent GIST

and melanoma cells measured 96 hours post-transfection with indicated siRNA. E-F. Viability of GIST430 (ex11) and GIST430-LMTK3myc cells 96 hours post-transfection with shown siRNA. The p values of one-way ANOVA for each cell line with multiple comparisons to NT siRNA are indicated by asterisks: *, p<0.05;**, p<0.005; ***, p<0.001; ****, p<0.0001.

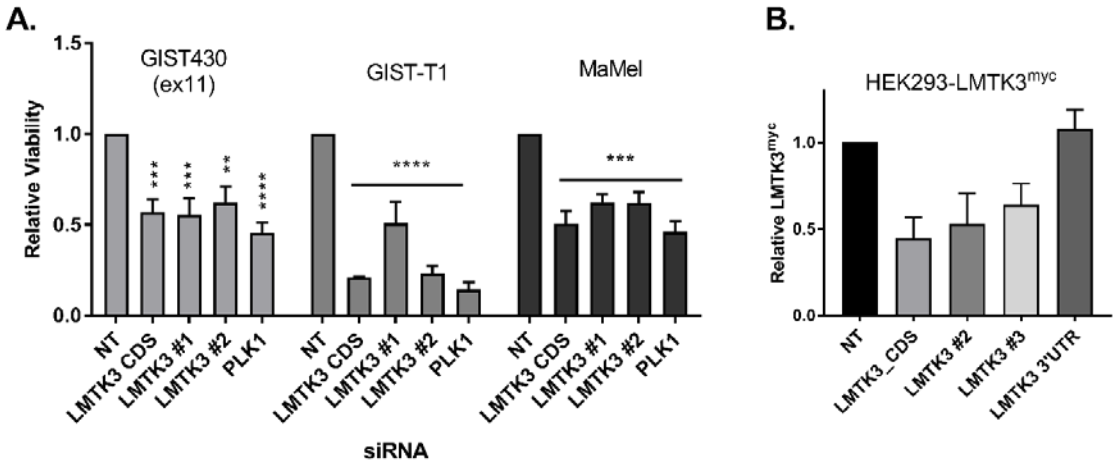

Figure 24. Individual siRNAs targeting *LMTK3* decreased viability of *KIT*-mutant cells.
A. Cell viability relative to non-targeting (NT) siRNA 96 hours post-transfection of GIST430 (ex11), GIST-T1, and MaMel cells. B. Knockdown of LMTK3^{myc} in stable HEK293 cells 72 hours post-transfection. Immunoblot and quantification of LMTK3^{myc} protein normalized to β-tubulin. LMTK3 protein detected using anti-myc^{Tag} antibody. The p values for t tests compared to NT siRNA are indicated by asterisks: ****, p<0.0001; **, p<0.005; *, p<0.05.

To determine the breadth of the effect of LMTK3 silencing in KIT-mutant cells, we expanded experiments to include a library of GIST and melanoma cell lines. These included GIST cell lines derived from those used in our initial screens (GIST430 [ex 11] and GIST-T1) and other GIST cell lines that have secondary KIT mutations conferring resistance to KIT TKIs (**Table 12**). LMTK3 silencing in all mutant KIT-dependent cell lines, including those with KIT TKI-resistance mutations, decreased cell viability relative to non-targeting control siRNA (**Figure 23C**). In contrast, KIT independent fibrosarcoma (HT1080), GIST (GIST54), and melanoma (SKMEL2) cell lines showed no significant

change in viability after LMTK3 silencing when compared to the non-targeting siRNA (**Figure 23D**).

To further determine the specificity of the effects of LMTK3 silencing on KIT-mutant cells, we created a stable GIST430 (ex 11) cell line expressing a c-myc epitope-tagged LMTK3 by lentiviral transduction (GIST430-LMTK3myc). This construct contained the coding DNA sequence (CDS) of LMTK3, but lacked the 5' and 3' UTRs. Experiments were then performed in these, as well as control GIST430 (ex 11) cells, using siRNAs targeting the LMTK3 CDS (siLMTK3_CDS) or the LMTK3 3'UTR (siLMTK3_3'UTR). LMTK3 knockdown with either the CDS-targeting or 3'UTR-targeting siRNAs significantly decreased cell viability in GIST430 (ex 11) cells, which only express endogenous LMTK3 (**Figure 23E**). However, only siRNA targeting the LMTK3 CDS, but not the 3'UTR, was able to decrease cell viability in the GIST430-LMTK3myc cells (**Figure 23E**), suggesting the

impact of *LMTK3* silencing is due to on-target effects on endogenous LMTK3. To clarify the mechanism by which *LMTK3* silencing was decreasing viability in mutant KIT-dependent cells, we investigated the role of apoptosis. We measured the activity of caspases 3 and 7 in *KIT*-mutant cell lines 96 hours post-siRNA transfection. We observed a significant increase in caspase 3/7 activity after *LMTK3* silencing, as well as a concordant increase in the cleavage of PARP by immunoblotting (**Figure 25A-B**). Further, we measured caspase induction in GIST430 (ex11) vs GIST430-LMTK3myc cells treated with LMTK3 CDS siRNA or LMTK3 3'UTR siRNA to determine the specificity of LMTK3 knockdown for this phenotype. We observed that exogenous LMTK3 expression

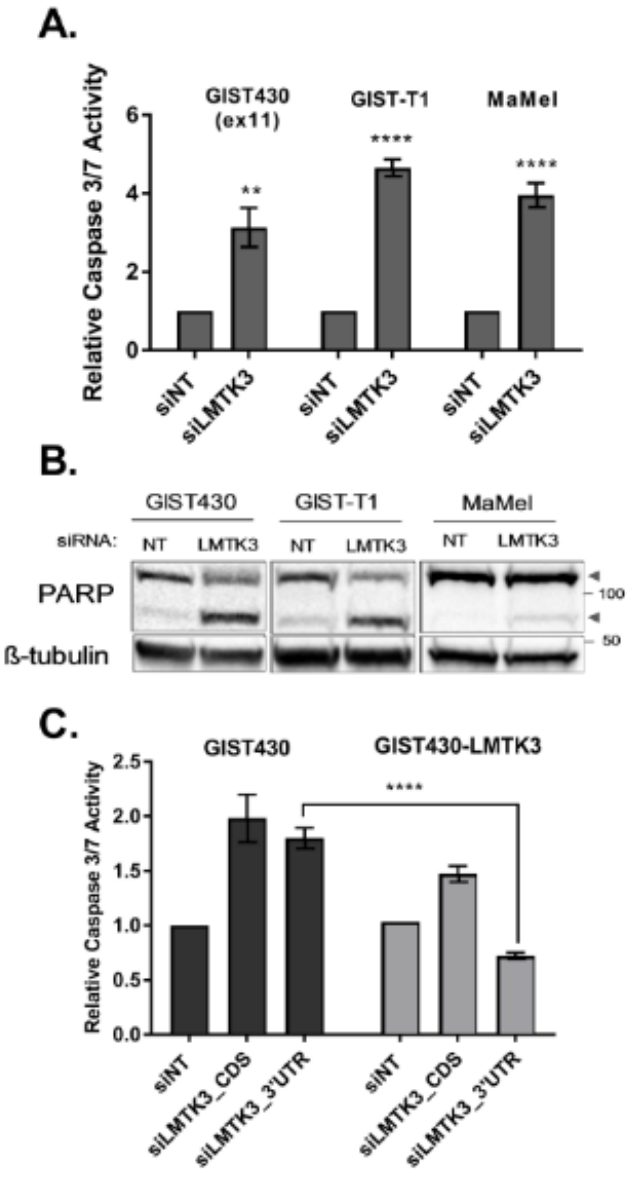

Figure 25. Viability decrease after LMTK3 silencing is due to induction of apoptosis.
A. Activity of caspases 3 and 7 96 hours post-transfection with NT or LMTK3 siRNA in KIT-mutant cells. B. Immunoblot showing cleavage (lower arrowhead, 90kDa) of full-length PARP (upper arrowhead, 110kDa), 72 hours post-siRNA transfection. C. Activity of caspases 3 and 7 96 hours post-transfection with NT, LMTK3 CDS or 3'UTR siRNA in GIST430 (ex11) or GIST430-LMTK3myc cells. The p values of t test for each cell line are indicated by asterisks: **, $p<0.005$; ***, $p<0.001$; ****, $p<0.0001$.

was able to prevent the induction of apoptosis seen when LMTK3 is knocked down, further indicating that LMTK3 silencing specifically induces apoptosis to reduce viability in mutant KIT-dependent cells (**Figure 25C**).

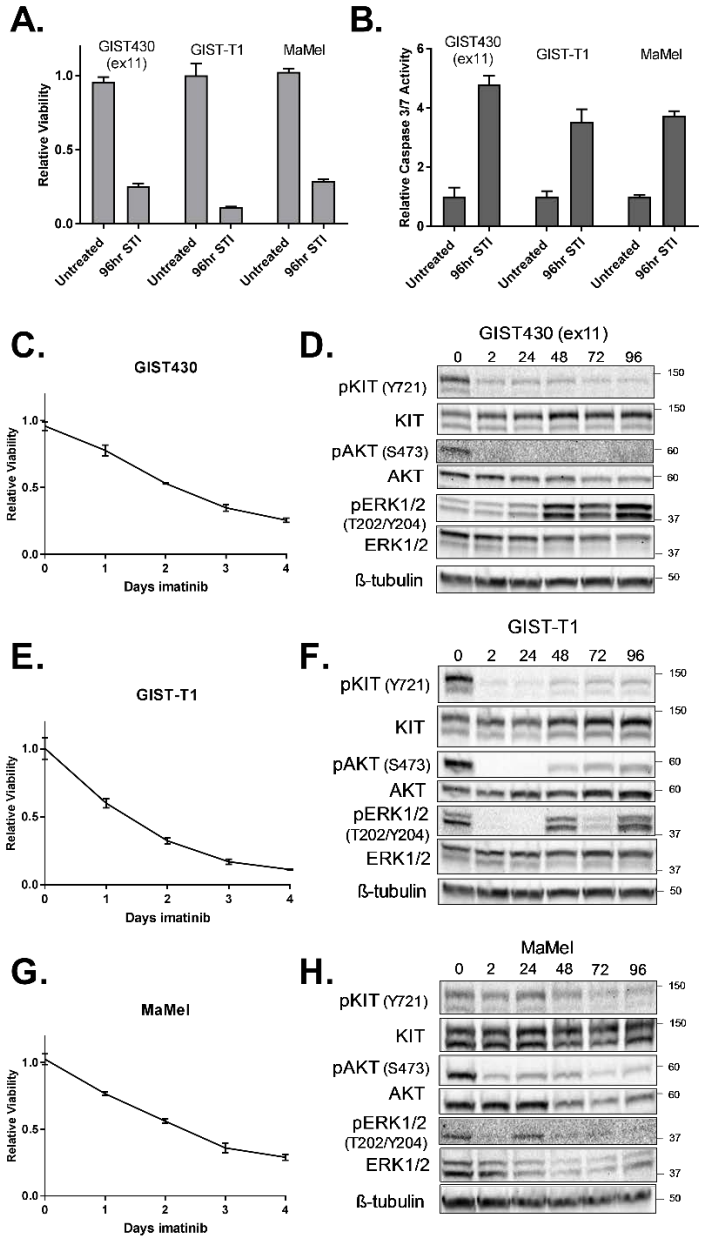

Figure 26. KIT TK inhibition results in phenotypes similar to those observed with *LMTK3* silencing in KIT-dependent cells. Treatment of GIST430 (ex11) and GIST-T1 with 100nM imatinib. MaMel treated with 250nM imatinib. Viability (A) and caspase 3/7 activity (B) of *KIT*-mutant GIST and melanoma cell lines after 96 hours of imatinib treatment. Bars represent average of triplicate experiments with standard deviation shown. C, E, G. Viability of indicated cell lines treated with 100nM or 250nM imatinib over 4 days. Average of triplicate experiments with standard deviation shown. D, F, H. Corresponding immunoblots of indicated cell lines treated with 100nM or 250nM imatinib over 4 days (time shown in

6.5.2. LMTK3 affects KIT activity and downstream signaling

The phenotype of LMTK3 silencing in mutant KIT-dependent cells was akin to that observed when KIT activity was inhibited (**Figure 26**). The similarity between the effect of LMTK3 knockdown on viability and apoptosis with KIT inhibition, and the fact that *LMTK3* silencing decreased the viability of KIT-

dependent but not KIT-independent cells, suggested that loss of LMTK3 may be affecting KIT signaling.

To test this hypothesis, we determined the activity of KIT after siRNA transfection by measuring phosphorylation of KIT protein at tyrosine 721 (Y721), an autophosphorylation site indicative of kinase activity. *LMTK3* silencing significantly decreased phosphorylation of KIT at tyrosine 721 (Y721) in both *KIT*-mutant GIST and melanoma cells (**Figure 28A, Figure 28C**). Congruent with this observation, phosphorylation at other activation sites in KIT, including tyrosine 703 (Y703), as well as total KIT tyrosine phosphorylation, decreased after *LMTK3* silencing (**Figure 27**). These data suggest that KIT activity is reduced after *LMTK3* silencing. We observed a similar decrease in phosphorylated KIT in TKI-resistant *KIT*-mutant GIST cells (**Figure 28B-C**). Notably, total KIT protein expression also significantly decreased after *LMTK3* silencing in all *KIT*-mutant cells in our study (**Figure 28D**).

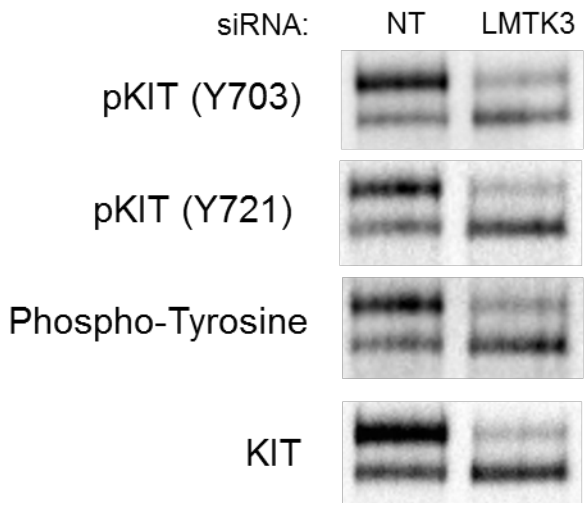

Figure 27. Phosphorylation of KIT decreased with *LMTK3* silencing.
Immunoblot of KIT immunoprecipitation from GIST430 (ex11) 72 hours post-transfection with indicated siRNAs.

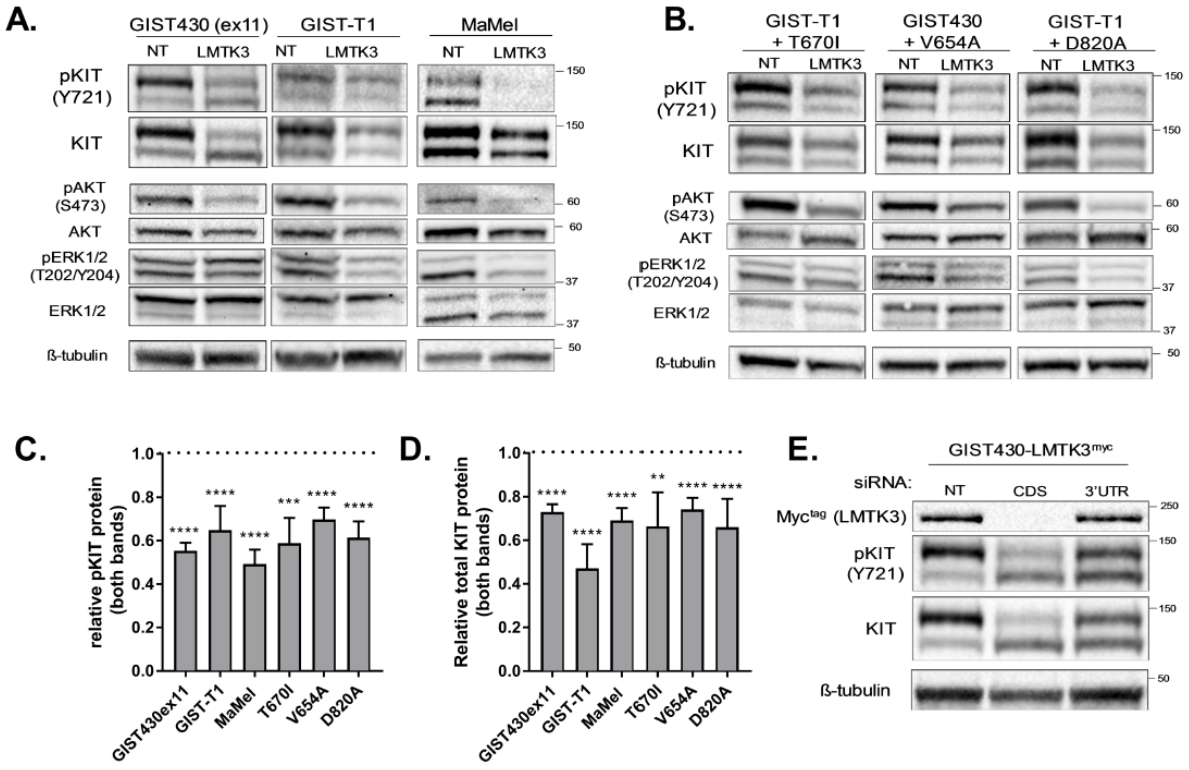

Figure 28. Silencing of LMTK3 in KIT-mutant GIST and melanoma cells reduces KIT activity. Immunoblotting of imatinib-sensitive GIST and melanoma cell lines (A) or imatinib-resistant GIST cell lines (B) 72 hours post-transfection with non-targeting (NT) or LMTK3 siRNA. C-D. Quantification of phospho-KIT (Y721) or total KIT protein from immunoblots, normalized to β-tubulin. E. Immunoblot of whole cell extracts from GIST430-LMTK3myc stable cells 72 hours post-transfection with NT, LMTK3 CDS, or LMTK3 3'UTR siRNA. Bars show average protein relative to NT siRNA of experiments performed > triplicate. The p values of t tests for each cell line compared to NT indicated by asterisks: **, p<0.005; ***, p<0.001; ****, p<0.0001.

Because loss of KIT activity can result in cell death in mutant KIT-dependent cells, we tested the ability of exogenous LMTK3^{myc} to affect this phenotype by targeting GIST430-LMTK3^{myc} cells with *LMTK3* CDS siRNA or *LMTK3* 3'UTR siRNA. We found that maintenance of LMTK3 expression was able to partially restore the loss of phospho-KIT in GIST430-LMTK3^{myc} cells (**Figure 28E**). This result is in agreement with our data showing a restoration of viability and lack of apoptosis induction under the same conditions. These

data suggest that *LMTK3* silencing kills mutant KIT-dependent cells by affecting KIT activity.

Upon observing the effect of loss of LMTK3 on KIT activity, we investigated how KIT phosphorylation is affected by LMTK3 overexpression. We measured auto-phosphorylated KIT (Y721) in GIST430-LMTK3^{myc} clones with variable levels LMTK3^{myc} expression. We found that LMTK3^{myc} protein abundance was highly correlated with KIT activity (**Figure 29,** R^2= 0.9459).

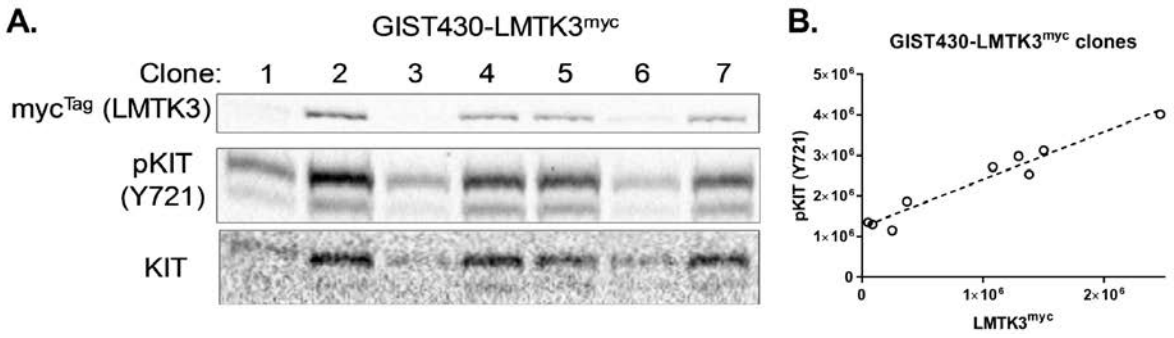

Figure 29. LMTK3 expression in GIST430 positively correlates with auto-phosphorylated KIT.
A. Immunoblot of whole cell lysates from GIST430 (ex11)-LMTK3myc clones. B. Correlation of LMTK3myc protein and phospho-KIT protein in GIST430 (ex11)-LMTK3myc clones. Protein abundance quantified by densitometry. Dotted line represents linear best fit (R2=0.9459).

These cells, however, do not show a change in imatinib sensitivity or abundance of *KIT* transcript (**Figure 30**).

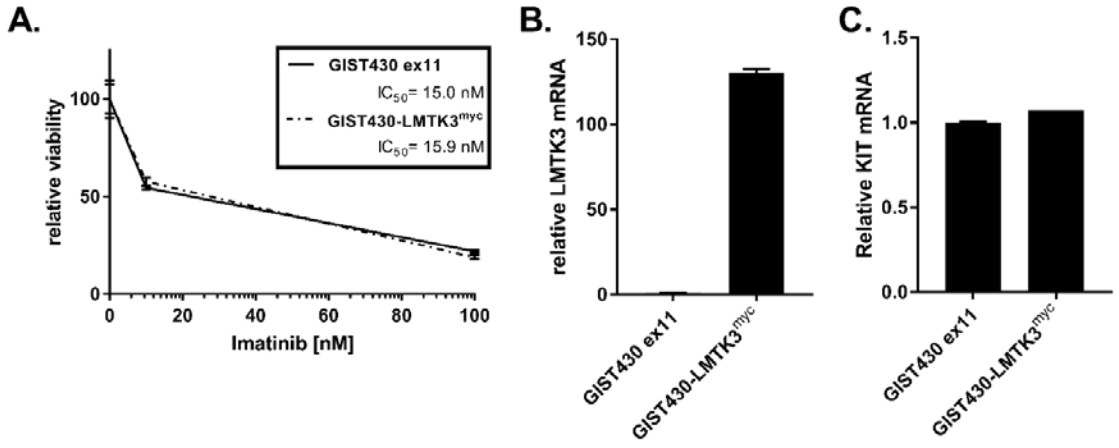

Figure 30. GIST430-LMTK3^{myc} stable cells have similar sensitivity to KIT TKI and *KIT* transcript abundance as parental GIST430 (ex11) cells.
A. Dose curve of viability of GIST430 (ex11) and GIST430-LMTK3^{myc} 96 hours post-imatinib treatment at the indicated doses. IC_{50} calculated by non-linear regression. B-C. *LMTK3* (B) and *KIT* (C) transcript abundance of GIST430-LMTK3^{myc} relative to GIST430 (ex11) parental cells.

To further investigate the effect of *LMTK3* silencing on KIT signaling pathways, we probed immunoblots for signaling components that are known to support proliferation and survival. In both KIT-dependent GIST and melanoma cell lines, *LMTK3* silencing reduced levels of activated AKT (phospho-S473) and activated ERK1 and ERK2 (phospho-T202/Y204, **Figure 28A)**. One exception to this, was GIST430 (ex 11) cells, which only showed a decrease in phospho-AKT, but not phospho-ERK. However, this pattern was identical to what is seen in GIST430 (ex 11) after KIT TKI treatment, which results in cell death, suggesting this pathway is insufficient for viability maintenance (**Figure 26C-D**). Importantly, activity of AKT and ERK pathway components is also decreased in GIST cell

lines that harbor drug-resistant *KIT* mutations (**Figure 28B**). Moreover, no effect is seen on these pathways in KIT-independent cell lines after *LMTK3* silencing (**Figure 31**).

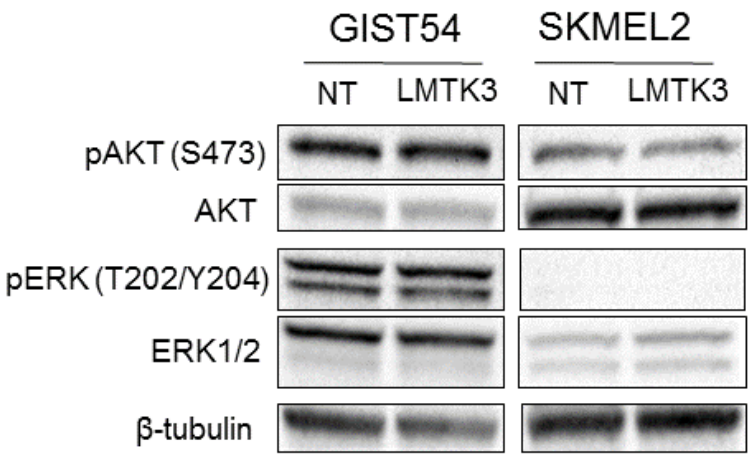

Figure 31. *LMTK3* silencing does not affect AKT or ERK1/2 activity in KIT-independent GIST and melanoma cells.
Immunoblots of GIST54 and SKMEL2 cell lines 72 hours post-siRNA transfection with NT or *LMTK3* siRNA. Immunoblotting for phospho-KIT (Y721) and total KIT showed no signal.

Collectively, these data suggest that LMTK3 regulates KIT activity in a way that is similar to the effect of KIT inhibitor treatment. However, these data differ from KIT kinase inhibitor treatment in that *LMTK3* silencing kills mutant KIT-dependent cells regardless of *KIT* mutation. One explanation for this could be due to the effect on total KIT protein, which could be responsible for the decrease observed in KIT activity and downstream signaling. To investigate possible mechanisms by which total KIT protein may be affected after LMTK3 knockdown, we first measured *KIT* transcript levels. We found that *LMTK3* siRNA did not significantly change *KIT* transcript abundance, despite a significant decrease in *LMTK3* mRNA in KIT-dependent GIST and melanoma cell lines (**Figure 32A-C**).

We then measured the stability of KIT protein to discern if *LMTK3* silencing had any effect on KIT protein turnover. We transfected cells with non-targeting or *LMTK3* siRNA and treated with the translation inhibitor Cycloheximide (CHX) at least 48 hours post-transfection. We collected protein at 0, 4, 8, and 24 hours after application of

cycloheximide and measured total KIT protein in whole cell lysates by KIT ELISA. Knockdown of LMTK3 did not shorten KIT protein half-life; in fact, in GIST430 (ex 11) cells, KIT protein half-life is slightly longer than when *LMTK3* is silenced, despite the cells having 30% less KIT protein at time 0 relative to the addition of cycloheximide (**Figure 32D**). In MaMel and GIST-T1 cell lines, KIT protein half-life was the same in cells treated with non-targeting or *LMTK3* siRNA (**Figure 32E-F**).

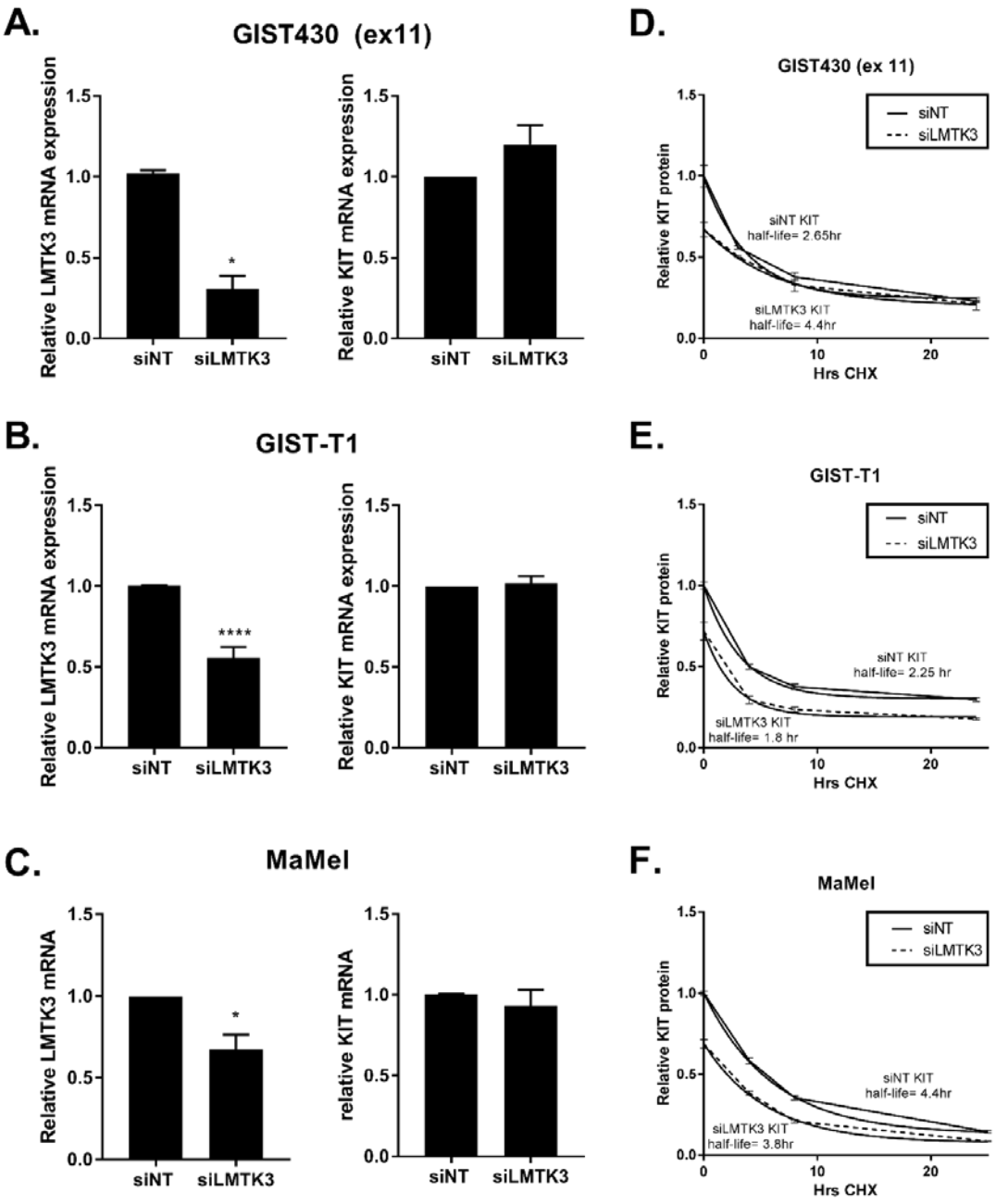

Figure 32. *LMTK3* silencing does not affect *KIT* transcript abundance or change KIT protein half-life. A-C. *LMTK3* and *KIT* transcript abundance relative to NT siRNA at 72 hours post-transfection with *LMTK3* 3'UTR siRNA in indicated cell lines. D-F. KIT protein abundance after inhibition of translation with cycloheximide in indicated cell lines. Cycloheximide was applied after siRNA transfection at time point determined to have LMTK3 knockdown and <25% reduction in KIT protein (GIST430 ex11: 48hr, GIST-T1: 48hr, MaMel: 72hr). Protein half-life calculated by one-phase decay, shown by smooth lines tracing data

6.5.3. Silencing *LMTK3* in *KIT*-mutant GIST cells reduces tumor growth *in vivo*

To understand the role of LMTK3 in regulating the *in vivo* growth of *KIT*-mutant GIST cells, we injected 1 x 10^6 GIST430 (ex 11) cells subcutaneously into male NRG mice. GIST430 (ex 11) cells were transfected with non-targeting or *LMTK3* siRNA 24 hours prior to injection. *LMTK3* silencing or non-targeting siRNA-treated control tumor cells were implanted separately into the right or left flank, respectively, of each recipient mouse (n=8). Non-targeted tumors were palpable within 3 weeks of injection and tumor size was measured via calipers three times weekly. All animals were euthanized 6 weeks post-implantation. Non-targeted tumors grew at a rapid rate after becoming palpable at 3 weeks, reaching an average volume of 1 cm^3 at the time of euthanasia. In contrast, tumors in which *LMTK3* had been silenced were not palpable until at least 4 weeks. These tumors grew much slower and were significantly smaller at the time of sacrifice (0.1 cm^3 average volume, $p < 0.005$, **Figure 33**). Taken together these data suggest that GIST cells in which *LMTK3* has been silenced have reduced viability in both *in vitro* and *in vivo* experiments.

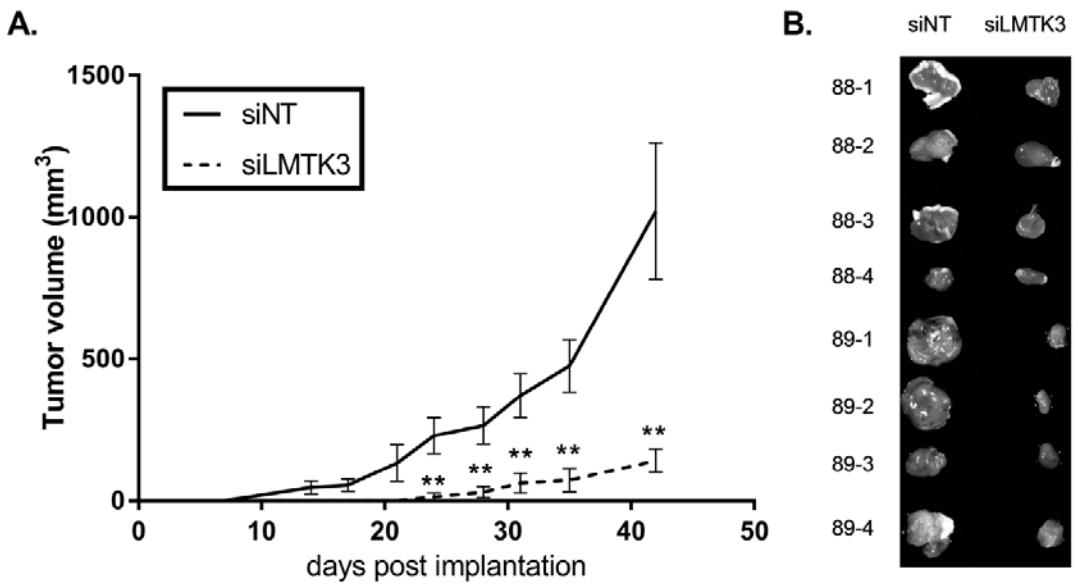

Figure 33. LMTK3 silencing prevents GIST xenograft growth in vivo.
A. Subcutaneous tumor volume growth after implantation of GIST430 (ex11) cells treated with the indicated siRNAs into each flank of an NRG mouse, (n=8) B. Tumors dissected from each flank after sacrifice at day 42 of each animal (identification numbers shown on left). The p values for t tests between NT and LMTK3 siRNA averages on each day are indicated by asterisks: **, p<0.005.

6.6. Discussion

Despite the therapeutic success of KIT tyrosine kinase inhibitors for treating *KIT*-mutant cancers, drug resistance presents a significant clinical barrier. With this in mind, we used a siRNA screen targeting human tyrosine kinases to identify novel therapeutic candidates in *KIT*-mutant GIST and melanoma. In this report, we describe a novel target, *LMTK3*, which was identified using three individual mutant KIT-dependent cell lines, two GIST and one melanoma. We found that silencing *LMTK3* reduced viability in KIT-dependent cells bearing various *KIT* mutations *in vitro*, and severely slowed GIST growth *in vivo*. The effect of LMTK3 loss in *KIT*-mutant cells reproduces phenotypes we observe with KIT inhibition, including loss of viability specifically in KIT-dependent, but not KIT-independent cells, and the induction of apoptosis. These similar phenotypes led us to

examine KIT activity after *LMTK3* silencing; we found phosphorylation of tyrosine 721, an autophosphorylation site, was reduced after loss of LMTK3. There was also a concomitant reduction of signaling through AKT and ERK pathways, which are known to drive proliferation and survival of *KIT*-mutant cells. In agreement with these knockdown data, we show that exogenous LMTK3 expression is sufficient to increase KIT phosphorylation.

Most significantly KIT activity and downstream signaling was decreased in both KIT TKI-sensitive and -resistant cell lines after *LMTK3* silencing. Secondary *KIT* point mutations such as T670I, V654A, and D820A confer resistance to imatinib and have variable sensitivity to second and third line KIT inhibitors (sunitinib and regorafenib)(Gramza, Corless, and Heinrich 2009; Garner et al. 2014). Insufficient inhibition of KIT activity allows for maintained KIT signaling through AKT and ERK to prevent cell death. Targeting LMTK3, however, can affect pro-proliferative/ pro-survival signaling in all KIT-dependent cells, regardless of *KIT* mutation(s). Furthermore, GIST treatments targeting proteins other than KIT have been proposed previously, but few have specificity for *KIT*-mutant cells. Targets without cancer cell specificity typically can have off-target effects that can narrow the therapeutic window when given systemically. *LMTK3* silencing, however, seems to specifically impair *KIT*-mutant cells. These aspects suggest that LMTK3 has promise as a therapeutic target for TKI-resistant KIT-dependent tumors.

LMTK3 has been implicated in other cancer types by supporting driver mutations, such as ERα in breast cancer (Giamas et al. 2011). While LMTK3 appears to play a direct role in regulating *ESR1* transcription and ERα protein stability in breast cancer, these mechanisms appear dissimilar to those in mutant KIT-dependent cells. Silencing of *LMTK3* in mutant KIT-dependent GIST and melanoma decreases KIT phosphorylation and

downstream proliferative signaling; it also has an effect on total KIT protein, but does not affect *KIT* transcription or total KIT stability. However, our data do not rule out effects on KIT translation or intracellular trafficking/ compartmentalization that would impair signaling. It is not clear if the effect on total KIT protein is the cause or the result of decreased KIT activity, but this effect is most significant since these cells rely on mutant KIT activity.

The specific functions of LMTK3 that promote cancer remain to be elucidated, but will be essential for developing strategies to inhibit KIT in *KIT*-mutant cancer patients. Members of the LMTK family have both kinase-dependent and kinase-independent functions. LMTK3 kinase activity has been described *in vitro*, but few substrates are known. Our data suggest that LMTK3 plays a role in regulation of KIT activity in *KIT*-mutant cells, but it remains to be determined if LMTK3 kinase activity is required. However, as a we learn more about this kinase, there may be the potential for enzymatic inhibition of LMTK3 with a small molecule and, thus the possibility of a treatment for patients with KIT TKI-resistant disease.

6.7. Acknowledgements

Thank you to Dr. Sebastian Bauer (West German Cancer Center, Essen, Germany) for generously providing *KIT*-mutant GIST cell lines. Thank you to Dr. Dirk Schadendorf (West German Cancer Center, Essen, Germany) for generously providing the MaMel (144aI) cell line. Deepest thanks to Arin McKinley, Diana Griffith, and Ashley Young for their technical and administrative support during the course of this study.

7. References

Acín-Pérez, Rebeca, Isabel Carrascoso, Francesc Baixauli, Marta Roche-Molina, Ana Latorre-Pellicer, Patricio Fernández-Silva, María Mittelbrunn, Francisco Sanchez-Madrid, Acisclo Pérez-Martos, Clifford A. Lowell, Giovanni Manfredi, and José Antonio Enríquez. 2014. 'ROS-Triggered Phosphorylation of Complex II by Fgr Kinase Regulates Cellular Adaptation to Fuel Use', *Cell metabolism*, 19: 1020-33.

Adam, J., M. Yang, T. Soga, and P. J. Pollard. 2014. 'Rare insights into cancer biology', *Oncogene*, 33: 2547-56.

Adzhubei, I. A., S. Schmidt, L. Peshkin, V. E. Ramensky, A. Gerasimova, P. Bork, A. S. Kondrashov, and S. R. Sunyaev. 2010. 'A method and server for predicting damaging missense mutations', *Nat Methods*, 7: 248-9.

Agaram, N. P., G. C. Wong, T. Guo, R. G. Maki, S. Singer, R. P. Dematteo, P. Besmer, and C. R. Antonescu. 2008. 'Novel V600E BRAF mutations in imatinib-naive and imatinib-resistant gastrointestinal stromal tumors', *Genes Chromosomes Cancer*, 47: 853-9.

Alston, C. L., C. Ceccatelli Berti, E. L. Blakely, M. Olahova, L. He, C. J. McMahon, S. E. Olpin, I. P. Hargreaves, C. Nolli, R. McFarland, P. Goffrini, M. J. O'Sullivan, and R. W. Taylor. 2015. 'A recessive homozygous p.Asp92Gly SDHD mutation causes prenatal cardiomyopathy and a severe mitochondrial complex II deficiency', *Hum Genet*, 134: 869-79.

Alston, C. L., J. E. Davison, F. Meloni, F. H. van der Westhuizen, L. He, H. T. Hornig-Do, A. C. Peet, P. Gissen, P. Goffrini, I. Ferrero, E. Wassmer, R. McFarland, and R. W. Taylor. 2012. 'Recessive germline SDHA and SDHB mutations causing leukodystrophy and isolated mitochondrial complex II deficiency', *J Med Genet*, 49: 569-77.

Andersson, J., H. Sihto, J. M. Meis-Kindblom, H. Joensuu, N. Nupponen, and L. G. Kindblom. 2005. 'NF1-associated gastrointestinal stromal tumors have unique clinical, phenotypic, and genotypic characteristics', *Am J Surg Pathol*, 29: 1170-6.

Antonescu, C. R., P. Besmer, T. Guo, K. Arkun, G. Hom, B. Koryotowski, M. A. Leversha, P. D. Jeffrey, D. Desantis, S. Singer, M. F. Brennan, R. G. Maki, and R. P. DeMatteo. 2005. 'Acquired resistance to imatinib in gastrointestinal stromal tumor occurs through secondary gene mutation', *Clin Cancer Res*, 11: 4182-90.

Ardissone, Anna, Federica Invernizzi, Alessia Nasca, Isabella Moroni, Laura Farina, and Daniele Ghezzi. 2015. 'Mitochondrial leukoencephalopathy and complex II deficiency associated with a recessive SDHB mutation with reduced penetrance', *Molecular Genetics and Metabolism Reports*, 5: 51-54.

Arpaci, T., F. Tokat, R. B. Arpaci, T. Akbas, G. Ugurluer, and S. Yavuz. 2015. 'Primary pericardial extragastrointestinal stromal tumor: A case report and literature review', *Oncol Lett*, 9: 2726-28.

Astuti, D., F. Latif, A. Dallol, P. L. Dahia, F. Douglas, E. George, F. Skoldberg, E. S. Husebye, C. Eng, and E. R. Maher. 2001. 'Gene mutations in the succinate dehydrogenase subunit SDHB cause susceptibility to familial pheochromocytoma and to familial paraganglioma', *Am J Hum Genet*, 69: 49-54.

Bafunno, V., T. A. Giancaspero, C. Brizio, D. Bufano, S. Passarella, E. Boles, and M. Barile. 2004. 'Riboflavin uptake and FAD synthesis in Saccharomyces cerevisiae mitochondria: involvement of the Flx1p carrier in FAD export', *J Biol Chem*, 279: 95-102.

Bannon, A. E., J. D. Kent, I. Forquer, A. Town, L. R. Klug, K. E. McCann, C. Beadling, O. Harismendy, J. K. Sicklick, C. L. Corless, U. Shinde, and M. C. Heinrich. 2017. 'Biochemical, Molecular, and Clinical Characterization of Succinate Dehydrogenase Subunit A Variants of Unknown Significance', *Clin Cancer Res*.

Bannon, A. E., L. R. Klug, C. L. Corless, and M. C. Heinrich. 2017. 'Using molecular diagnostic testing to personalize the treatment of patients with gastrointestinal stromal tumors', *Expert Rev Mol Diagn*.

Barrios, C. H., M. E. Blackstein, J. Y. Blay, P. G. Casali, M. Chacon, J. Gu, Y. K. Kang, T. Nishida, D. Purkayastha, R. C. Woodman, and P. Reichardt. 2015. 'The GOLD ReGISTry: a Global, Prospective, Observational Registry Collecting Longitudinal Data on Patients with Advanced and Localised Gastrointestinal Stromal Tumours', *Eur J Cancer*, 51: 2423-33.

Bauer, S., L. K. Yu, G. D. Demetri, and J. A. Fletcher. 2006. 'Heat shock protein 90 inhibition in imatinib-resistant gastrointestinal stromal tumor', *Cancer Res*, 66: 9153-61.

Bausch, B., F. Schiavi, Y. Ni, J. Welander, A. Patocs, J. Ngeow, U. Wellner, A. Malinoc, E. Taschin, G. Barbon, V. Lanza, P. Soderkvist, A. Stenman, C. Larsson, F. Svahn, J. L. Chen, J. Marquard, M. Fraenkel, M. A. Walter, M. Peczkowska, A. Prejbisz, B. Jarzab, K. Hasse-Lazar, S. Petersenn, L. C. Moeller, A. Meyer, N. Reisch, A. Trupka, C. Brase, M. Galiano, S. F. Preuss, P. Kwok, N. Lendvai, G. Berisha, O. Makay, C. C. Boedeker, G. Weryha, K. Racz, A. Januszewicz, M. K. Walz, O. Gimm, G. Opocher, C. Eng, and H. P. Neumann. 2017. 'Clinical Characterization of the Pheochromocytoma and Paraganglioma Susceptibility Genes SDHA, TMEM127, MAX, and SDHAF2 for Gene-Informed Prevention', *JAMA Oncol*.

Baysal, B. E. 2004. 'Genomic imprinting and environment in hereditary paraganglioma', *Am J Med Genet C Semin Med Genet*, 129c: 85-90.

———. 2007. 'A recurrent stop-codon mutation in succinate dehydrogenase subunit B gene in normal peripheral blood and childhood T-cell acute leukemia', *PLoS ONE*, 2: e436.

Baysal, B. E., R. E. Ferrell, J. E. Willett-Brozick, E. C. Lawrence, D. Myssiorek, A. Bosch, A. van der Mey, P. E. Taschner, W. S. Rubinstein, E. N. Myers, C. W. Richard, 3rd, C. J. Cornelisse, P. Devilee, and B. Devlin. 2000. 'Mutations in SDHD, a mitochondrial complex II gene, in hereditary paraganglioma', *Science*, 287: 848-51.

Baysal, B. E., E. C. Lawrence, and R. E. Ferrell. 2007. 'Sequence variation in human succinate dehydrogenase genes: evidence for long-term balancing selection on SDHA', *BMC Biol*, 5: 12.

Beadling, C., E. Jacobson-Dunlop, F. S. Hodi, C. Le, A. Warrick, J. Patterson, A. Town, A. Harlow, F. Cruz, 3rd, S. Azar, B. P. Rubin, S. Muller, R. West, M. C. Heinrich, and C. L. Corless. 2008. 'KIT gene mutations and copy number in melanoma subtypes', *Clin Cancer Res*, 14: 6821-8.

Beadling, C., T. L. Neff, M. C. Heinrich, K. Rhodes, M. Thornton, J. Leamon, M. Andersen, and C. L. Corless. 2013. 'Combining highly multiplexed PCR with semiconductor-based sequencing for rapid cancer genotyping', *J Mol Diagn*, 15: 171-6.

Beamer, L. C. 2014. 'Cowden syndrome: what oncology nurses need to know about increased risk of developing certain cancers', *Oncol Nurs Forum*, 41: 555-7.

Belinsky, M. G., K. Q. Cai, Y. Zhou, B. Luo, J. Pei, L. Rink, and M. von Mehren. 2017. 'Succinate dehydrogenase deficiency in a PDGFRA mutated GIST', *BMC Cancer*, 17: 512.

Belinsky, M. G., L. Rink, D. B. Flieder, M. S. Jahromi, J. D. Schiffman, A. K. Godwin, and Mv Mehren. 2013. 'Overexpression of insulin-like growth factor 1 receptor and frequent mutational inactivation of SDHA in wild-type SDHB-negative gastrointestinal stromal tumors', *Genes Chromosomes Cancer*, 52: 214-24.

Bezawork-Geleta, A., L. Dong, J. Rohlena, and J. Neuzil. 2016. 'The Assembly Factor SDHAF2 Is Dispensable for Flavination of the Catalytic Subunit of Mitochondrial Complex II in Breast Cancer Cells', *J Biol Chem*, 291: 21414-20.

Bezawork-Geleta, A., J. Rohlena, L. Dong, K. Pacak, and J. Neuzil. 2017. 'Mitochondrial Complex II: At the Crossroads', *Trends Biochem Sci*.

Birch-Machin, M. A., R. W. Taylor, B. Cochran, B. A. Ackrell, and D. M. Turnbull. 2000. 'Late-onset optic atrophy, ataxia, and myopathy associated with a mutation of a complex II gene', *Ann Neurol*, 48: 330-5.

Blanke, C. D., G. D. Demetri, M. von Mehren, M. C. Heinrich, B. Eisenberg, J. A. Fletcher, C. L. Corless, C. D. Fletcher, P. J. Roberts, D. Heinz, E. Wehre, Z. Nikolova, and H. Joensuu. 2008. 'Long-term results from a randomized phase II trial of standard- versus higher-dose imatinib mesylate for patients with unresectable or metastatic gastrointestinal stromal tumors expressing KIT', *J Clin Oncol*, 26: 620-5.

Blanke, C. D., C. Rankin, G. D. Demetri, C. W. Ryan, M. von Mehren, R. S. Benjamin, A. K. Raymond, V. H. Bramwell, L. H. Baker, R. G. Maki, M. Tanaka, J. R. Hecht, M. C. Heinrich, C. D. Fletcher, J. J. Crowley, and E. C. Borden. 2008. 'Phase III randomized, intergroup trial assessing imatinib mesylate at two dose levels in patients with unresectable or metastatic gastrointestinal stromal tumors expressing the kit receptor tyrosine kinase: S0033', *J Clin Oncol*, 26: 626-32.

Boikos, S. A., A. S. Pappo, J. K. Killian, M. P. LaQuaglia, C. B. Weldon, S. George, J. C. Trent, M. von Mehren, J. A. Wright, J. D. Schiffman, M. Raygada, K. Pacak, P. S. Meltzer, M. M. Miettinen, C. Stratakis, K. A. Janeway, and L. J. Helman. 2016. 'Molecular Subtypes of KIT/PDGFRA Wild-Type Gastrointestinal Stromal Tumors: A Report From the National Institutes of Health Gastrointestinal Stromal Tumor Clinic', *JAMA Oncol*, 2: 922-8.

Boikos, S. A., P. Xekouki, E. Fumagalli, F. R. Faucz, M. Raygada, E. Szarek, E. Ball, S. Y. Kim, M. Miettinen, L. J. Helman, J. A. Carney, K. Pacak, and C. A. Stratakis. 2016. 'Carney triad can be (rarely) associated with germline succinate dehydrogenase defects', *Eur J Hum Genet*, 24: 569-73.

Bourgeron, T., P. Rustin, D. Chretien, M. Birch-Machin, M. Bourgeois, E. Viegas-Pequignot, A. Munnich, and A. Rotig. 1995. 'Mutation of a nuclear succinate dehydrogenase gene results in mitochondrial respiratory chain deficiency', *Nat Genet*, 11: 144-9.

Braymer, J. J., and R. Lill. 2017. 'Iron-Sulfur Cluster Biogenesis and Trafficking in Mitochondria', *J Biol Chem*.

Brenca, M., S. Rossi, M. Polano, D. Gasparotto, L. Zanatta, D. Racanelli, L. Valori, S. Lamon, A. P. Dei Tos, and R. Maestro. 2016. 'Transcriptome sequencing identifies ETV6-NTRK3 as a gene fusion involved in GIST', *J Pathol*, 238: 543-9.

Buffet, A., A. Venisse, V. Nau, I. Roncellin, V. Boccio, N. Le Pottier, M. Boussion, C. Travers, C. Simian, N. Burnichon, N. Abermil, J. Favier, X. Jeunemaitre, and A. P. Gimenez-Roqueplo. 2012. 'A decade (2001-2010) of genetic testing for pheochromocytoma and paraganglioma', *Horm Metab Res*, 44: 359-66.

Bugiani, M., E. Lamantea, F. Invernizzi, I. Moroni, A. Bizzi, M. Zeviani, and G. Uziel. 2006. 'Effects of riboflavin in children with complex II deficiency', *Brain Dev*, 28: 576-81.

Burnichon, N., N. Abermil, A. Buffet, J. Favier, and A. P. Gimenez-Roqueplo. 2012. 'The genetics of paragangliomas', *Eur Ann Otorhinolaryngol Head Neck Dis*, 129: 315-8.

Burnichon, N., J. J. Briere, R. Libe, L. Vescovo, J. Riviere, F. Tissier, E. Jouanno, X. Jeunemaitre, P. Benit, A. Tzagoloff, P. Rustin, J. Bertherat, J. Favier, and A. P. Gimenez-Roqueplo. 2010. 'SDHA is a tumor suppressor gene causing paraganglioma', *Hum Mol Genet*, 19: 3011-20.

Burnichon, N., V. Rohmer, L. Amar, P. Herman, S. Leboulleux, V. Darrouzet, P. Niccoli, D. Gaillard, G. Chabrier, F. Chabolle, I. Coupier, P. Thieblot, P. Lecomte, J. Bertherat, N. Wion-Barbot, A. Murat, A. Venisse, P. F. Plouin, X. Jeunemaitre, and A. P. Gimenez-Roqueplo. 2009. 'The succinate dehydrogenase genetic testing in a large prospective series of patients with paragangliomas', *J Clin Endocrinol Metab*, 94: 2817-27.

Carney, J. A., S. G. Sheps, V. L. Go, and H. Gordon. 1977. 'The triad of gastric leiomyosarcoma, functioning extra-adrenal paraganglioma and pulmonary chondroma', *N Engl J Med*, 296: 1517-8.

Carney, J. A., and C. A. Stratakis. 2002. 'Familial paraganglioma and gastric stromal sarcoma: a new syndrome distinct from the Carney triad', *Am J Med Genet*, 108: 132-9.

Carvajal, R. D., D. P. Lawrence, J. S. Weber, T. F. Gajewski, R. Gonzalez, J. Lutzky, S. J. O'Day, O. Hamid, J. D. Wolchok, P. B. Chapman, R. J. Sullivan, J. B. Teitcher, N. Ramaiya, A. Giobbie-Hurder, C. R. Antonescu, M. C. Heinrich, B. C. Bastian, C. L. Corless, J. A. Fletcher, and F. S. Hodi. 2015. 'Phase II Study of Nilotinib in Melanoma Harboring KIT Alterations Following Progression to Prior KIT Inhibition', *Clin Cancer Res*, 21: 2289-96.

Cecchini, G., I. Schroder, R. P. Gunsalus, and E. Maklashina. 2002. 'Succinate dehydrogenase and fumarate reductase from Escherichia coli', *Biochim Biophys Acta*, 1553: 140-57.

Celestino, R., J. Lima, A. Faustino, J. Vinagre, V. Maximo, A. Gouveia, P. Soares, and J. M. Lopes. 2013. 'Molecular alterations and expression of succinate dehydrogenase complex

in wild-type KIT/PDGFRA/BRAF gastrointestinal stromal tumors', *Eur J Hum Genet*, 21: 503-10.
Chapman, K. B., S. D. Solomon, and J. D. Boeke. 1992. 'SDH1, the gene encoding the succinate dehydrogenase flavoprotein subunit from Saccharomyces cerevisiae', *Gene*, 118: 131-6.
Chen, H., S. Hirota, K. Isozaki, H. Sun, A. Ohashi, K. Kinoshita, P. O'Brien, L. Kapusta, I. Dardick, T. Obayashi, T. Okazaki, Y. Shinomura, Y. Matsuzawa, and Y. Kitamura. 2002. 'Polyclonal nature of diffuse proliferation of interstitial cells of Cajal in patients with familial and multiple gastrointestinal stromal tumours', *Gut*, 51: 793-6.
Cimen, H., M. J. Han, Y. Yang, Q. Tong, H. Koc, and E. C. Koc. 2010. 'Regulation of succinate dehydrogenase activity by SIRT3 in mammalian mitochondria', *Biochemistry*, 49: 304-11.
'Comparison of two doses of imatinib for the treatment of unresectable or metastatic gastrointestinal stromal tumors: a meta-analysis of 1,640 patients'. 2010. *J Clin Oncol*, 28: 1247-53.
Corless, C. L., K. V. Ballman, C. R. Antonescu, V. Kolesnikova, R. G. Maki, P. W. Pisters, M. E. Blackstein, C. D. Blanke, G. D. Demetri, M. C. Heinrich, M. von Mehren, S. Patel, M. D. McCarter, K. Owzar, and R. P. DeMatteo. 2014. 'Pathologic and molecular features correlate with long-term outcome after adjuvant therapy of resected primary GI stromal tumor: the ACOSOG Z9001 trial', *J Clin Oncol*, 32: 1563-70.
Corless, C. L., C. M. Barnett, and M. C. Heinrich. 2011. 'Gastrointestinal stromal tumours: origin and molecular oncology', *Nat Rev Cancer*, 11: 865-78.
Corless, C. L., A. Schroeder, D. Griffith, A. Town, L. McGreevey, P. Harrell, S. Shiraga, T. Bainbridge, J. Morich, and M. C. Heinrich. 2005. 'PDGFRA mutations in gastrointestinal stromal tumors: frequency, spectrum and in vitro sensitivity to imatinib', *J Clin Oncol*, 23: 5357-64.
Daniels, M., I. Lurkin, R. Pauli, E. Erbstosser, U. Hildebrandt, K. Hellwig, U. Zschille, P. Luders, G. Kruger, J. Knolle, B. Stengel, F. Prall, K. Hertel, H. Lobeck, B. Popp, F. Theissig, P. Wunsch, E. Zwarthoff, A. Agaimy, and R. Schneider-Stock. 2011. 'Spectrum of KIT/PDGFRA/BRAF mutations and Phosphatidylinositol-3-Kinase pathway gene alterations in gastrointestinal stromal tumors (GIST)', *Cancer Lett*, 312: 43-54.
Davili, Z., S. Johar, C. Hughes, D. Kveselis, and J. Hoo. 2007. 'Succinate dehydrogenase deficiency associated with dilated cardiomyopathy and ventricular noncompaction', *Eur J Pediatr*, 166: 867-70.
de Raedt, T., J. Cools, M. Debiec-Rychter, H. Brems, N. Mentens, R. Sciot, J. Himpens, I. de Wever, P. Schoffski, P. Marynen, and E. Legius. 2006. 'Intestinal neurofibromatosis is a subtype of familial GIST and results from a dominant activating mutation in PDGFRA', *Gastroenterology*, 131: 1907-12.
Debiec-Rychter, M., J. Cools, H. Dumez, R. Sciot, M. Stul, N. Mentens, H. Vranckx, B. Wasag, H. Prenen, J. Roesel, A. Hagemeijer, A. Van Oosterom, and P. Marynen. 2005. 'Mechanisms of resistance to imatinib mesylate in gastrointestinal stromal tumors and activity of the PKC412 inhibitor against imatinib-resistant mutants', *Gastroenterology*, 128: 270-9.
Debiec-Rychter, M., B. Wasag, M. Stul, I. De Wever, A. Van Oosterom, A. Hagemeijer, and R. Sciot. 2004. 'Gastrointestinal stromal tumours (GISTs) negative for KIT (CD117 antigen) immunoreactivity', *J Pathol*, 202: 430-8.
Dematteo, R. P., M. C. Heinrich, W. M. El-Rifai, and G. Demetri. 2002. 'Clinical management of gastrointestinal stromal tumors: before and after STI-571', *Hum Pathol*, 33: 466-77.
Demetri, G. D., M. von Mehren, C. R. Antonescu, R. P. DeMatteo, K. N. Ganjoo, R. G. Maki, P. W. Pisters, C. P. Raut, R. F. Riedel, S. Schuetze, H. M. Sundar, J. C. Trent, and J. D. Wayne. 2010. 'NCCN Task Force report: update on the management of patients with gastrointestinal stromal tumors', *J Natl Compr Canc Netw*, 8 Suppl 2: S1-41; quiz S42-4.
Demetri, G. D., M. von Mehren, C. D. Blanke, A. D. Van den Abbeele, B. Eisenberg, P. J. Roberts, M. C. Heinrich, D. A. Tuveson, S. Singer, M. Janicek, J. A. Fletcher, S. G. Silverman, S. L. Silberman, R. Capdeville, B. Kiese, B. Peng, S. Dimitrijevic, B. J. Druker, C. Corless, C. D. Fletcher, and H. Joensuu. 2002. 'Efficacy and safety of imatinib mesylate in advanced gastrointestinal stromal tumors', *N Engl J Med*, 347: 472-80.

Dibb, N. J., S. M. Dilworth, and C. D. Mol. 2004. 'Switching on kinases: oncogenic activation of BRAF and the PDGFR family', *Nat Rev Cancer*, 4: 718-27.
Douillard, J. Y., G. Ostoros, M. Cobo, T. Ciuleanu, R. McCormack, A. Webster, and T. Milenkova. 2014. 'First-line gefitinib in Caucasian EGFR mutation-positive NSCLC patients: a phase-IV, open-label, single-arm study', *Br J Cancer*, 110: 55-62.
Doyle, L. A., D. Nelson, M. C. Heinrich, C. L. Corless, and J. L. Hornick. 2012. 'Loss of succinate dehydrogenase subunit B (SDHB) expression is limited to a distinctive subset of gastric wild-type gastrointestinal stromal tumours: a comprehensive genotype-phenotype correlation study', *Histopathology*, 61: 801-9.
Dudek, J., P. Rehling, and M. van der Laan. 2013. 'Mitochondrial protein import: common principles and physiological networks', *Biochim Biophys Acta*, 1833: 274-85.
Dwight, T., D. E. Benn, A. Clarkson, R. Vilain, L. Lipton, B. G. Robinson, R. J. Clifton-Bligh, and A. J. Gill. 2013. 'Loss of SDHA expression identifies SDHA mutations in succinate dehydrogenase-deficient gastrointestinal stromal tumors', *Am J Surg Pathol*, 37: 226-33.
Dwight, Trisha, Un Na, Edward Kim, Ying Zhu, Anne Louise Richardson, Bruce G. Robinson, Katherine M. Tucker, Anthony J. Gill, Diana E. Benn, Roderick J. Clifton-Bligh, and Dennis R. Winge. 2017. 'Analysis of SDHAF3 in familial and sporadic pheochromocytoma and paraganglioma', *BMC Cancer*, 17: 497.
Edmonson, J. H., R. S. Marks, J. C. Buckner, and M. R. Mahoney. 2002. 'Contrast of response to dacarbazine, mitomycin, doxorubicin, and cisplatin (DMAP) plus GM-CSF between patients with advanced malignant gastrointestinal stromal tumors and patients with other advanced leiomyosarcomas', *Cancer Invest*, 20: 605-12.
Emile, J. F., S. Brahimi, J. M. Coindre, P. P. Bringuier, G. Monges, P. Samb, L. Doucet, I. Hostein, B. Landi, M. P. Buisine, A. Neuville, O. Bouche, P. Cervera, J. L. Pretet, J. Tisserand, A. Gauthier, A. Le Cesne, J. C. Sabourin, J. Y. Scoazec, S. Bonvalot, C. L. Corless, M. C. Heinrich, J. Y. Blay, and P. Aegerter. 2012. 'Frequencies of KIT and PDGFRA mutations in the MolecGIST prospective population-based study differ from those of advanced GISTs', *Med Oncol*, 29: 1765-72.
Evenepoel, L., T. G. Papathomas, N. Krol, E. Korpershoek, R. R. de Krijger, A. Persu, and W. N. Dinjens. 2015. 'Toward an improved definition of the genetic and tumor spectrum associated with SDH germ-line mutations', *Genet Med*, 17: 610-20.
Finley, Lydia W. S., Wilhelm Haas, Valérie Desquiret-Dumas, Douglas C. Wallace, Vincent Procaccio, Steven P. Gygi, and Marcia C. Haigis. 2011. 'Succinate Dehydrogenase Is a Direct Target of Sirtuin 3 Deacetylase Activity', *PLoS ONE*, 6: e23295.
Fischer, F., A. Hamann, and H. D. Osiewacz. 2012. 'Mitochondrial quality control: an integrated network of pathways', *Trends Biochem Sci*, 37: 284-92.
Fokkema, I. F., P. E. Taschner, G. C. Schaafsma, J. Celli, J. F. Laros, and J. T. den Dunnen. 2011. 'LOVD v.2.0: the next generation in gene variant databases', *Hum Mutat*, 32: 557-63.
Fontanesi, F., F. Diaz, and A. Barrientos. 2009. 'Evaluation of the mitochondrial respiratory chain and oxidative phosphorylation system using yeast models of OXPHOS deficiencies', *Curr Protoc Hum Genet*, Chapter 19: Unit19.5.
Fontanesi, F., I. C. Soto, D. Horn, and A. Barrientos. 2006. 'Assembly of mitochondrial cytochrome c-oxidase, a complicated and highly regulated cellular process', *Am J Physiol Cell Physiol*, 291: C1129-47.
Fribbens, C., B. O'Leary, L. Kilburn, S. Hrebien, I. Garcia-Murillas, M. Beaney, M. Cristofanilli, F. Andre, S. Loi, S. Loibl, J. Jiang, C. H. Bartlett, M. Koehler, M. Dowsett, J. M. Bliss, S. R. Johnston, and N. C. Turner. 2016. 'Plasma ESR1 Mutations and the Treatment of Estrogen Receptor-Positive Advanced Breast Cancer', *J Clin Oncol*, 34: 2961-8.
Furitsu, T., T. Tsujimura, T. Tono, H. Ikeda, H. Kitayama, U. Koshimizu, H. Sugahara, J. H. Butterfield, L. K. Ashman, Y. Kanayama, and et al. 1993. 'Identification of mutations in the coding sequence of the proto-oncogene c-kit in a human mast cell leukemia cell line causing ligand-independent activation of c-kit product', *J Clin Invest*, 92: 1736-44.
Gaal, J., C. A. Stratakis, J. A. Carney, E. R. Ball, E. Korpershoek, M. B. Lodish, I. Levy, P. Xekouki, F. H. van Nederveen, M. A. den Bakker, M. O'Sullivan, W. N. Dinjens, and R. R.

de Krijger. 2011. 'SDHB immunohistochemistry: a useful tool in the diagnosis of Carney-Stratakis and Carney triad gastrointestinal stromal tumors', *Mod Pathol*, 24: 147-51.
Garner, A. P., J. M. Gozgit, R. Anjum, S. Vodala, A. Schrock, T. Zhou, C. Serrano, G. Eilers, M. Zhu, J. Ketzer, S. Wardwell, Y. Ning, Y. Song, A. Kohlmann, F. Wang, T. Clackson, M. C. Heinrich, J. A. Fletcher, S. Bauer, and V. M. Rivera. 2014. 'Ponatinib inhibits polyclonal drug-resistant KIT oncoproteins and shows therapeutic potential in heavily pretreated gastrointestinal stromal tumor (GIST) patients', *Clin Cancer Res*, 20: 5745-55.
Ghezzi, D., P. Goffrini, G. Uziel, R. Horvath, T. Klopstock, H. Lochmuller, P. D'Adamo, P. Gasparini, T. M. Strom, H. Prokisch, F. Invernizzi, I. Ferrero, and M. Zeviani. 2009. 'SDHAF1, encoding a LYR complex-II specific assembly factor, is mutated in SDH-defective infantile leukoencephalopathy', *Nat Genet*, 41: 654-6.
Giamas, G., A. Filipovic, J. Jacob, W. Messier, H. Zhang, D. Yang, W. Zhang, B. A. Shifa, A. Photiou, C. Tralau-Stewart, L. Castellano, A. R. Green, R. C. Coombes, I. O. Ellis, S. Ali, H. J. Lenz, and J. Stebbing. 2011. 'Kinome screening for regulators of the estrogen receptor identifies LMTK3 as a new therapeutic target in breast cancer', *Nat Med*, 17: 715-9.
Gill, A. J., D. E. Benn, A. Chou, A. Clarkson, A. Muljono, G. Y. Meyer-Rochow, A. L. Richardson, S. B. Sidhu, B. G. Robinson, and R. J. Clifton-Bligh. 2010. 'Immunohistochemistry for SDHB triages genetic testing of SDHB, SDHC, and SDHD in paraganglioma-pheochromocytoma syndromes', *Hum Pathol*, 41: 805-14.
Gill, A. J., A. Chou, R. E. Vilain, and R. J. Clifton-Bligh. 2011. '"Pediatric-type" gastrointestinal stromal tumors are SDHB negative ("type 2") GISTs', *Am J Surg Pathol*, 35: 1245-7; author reply 47-8.
Goffrini, P., T. Ercolino, E. Panizza, V. Giache, L. Cavone, A. Chiarugi, V. Dima, I. Ferrero, and M. Mannelli. 2009. 'Functional study in a yeast model of a novel succinate dehydrogenase subunit B gene germline missense mutation (C191Y) diagnosed in a patient affected by a glomus tumor', *Hum Mol Genet*, 18: 1860-8.
Gramza, A. W., C. L. Corless, and M. C. Heinrich. 2009. 'Resistance to Tyrosine Kinase Inhibitors in Gastrointestinal Stromal Tumors', *Clin Cancer Res*, 15: 7510-18.
Guo, J., L. Si, Y. Kong, K. T. Flaherty, X. Xu, Y. Zhu, C. L. Corless, L. Li, H. Li, X. Sheng, C. Cui, Z. Chi, S. Li, M. Han, L. Mao, X. Lin, N. Du, X. Zhang, J. Li, B. Wang, and S. Qin. 2011. 'Phase II, open-label, single-arm trial of imatinib mesylate in patients with metastatic melanoma harboring c-Kit mutation or amplification', *J Clin Oncol*, 29: 2904-9.
Guzy, R. D., B. Sharma, E. Bell, N. S. Chandel, and P. T. Schumacker. 2008. 'Loss of the SdhB, but Not the SdhA, subunit of complex II triggers reactive oxygen species-dependent hypoxia-inducible factor activation and tumorigenesis', *Mol Cell Biol*, 28: 718-31.
Hagerhall, C., and L. Hederstedt. 1996. 'A structural model for the membrane-integral domain of succinate: quinone oxidoreductases', *FEBS Lett*, 389: 25-31.
Haller, F., E. A. Moskalev, F. R. Faucz, S. Barthelmess, S. Wiemann, M. Bieg, G. Assie, J. Bertherat, I. M. Schaefer, C. Otto, E. Rattenberry, E. R. Maher, P. Strobel, M. Werner, J. A. Carney, A. Hartmann, C. A. Stratakis, and A. Agaimy. 2014. 'Aberrant DNA hypermethylation of SDHC: a novel mechanism of tumor development in Carney triad', *Endocr Relat Cancer*, 21: 567-77.
Hao, H. X., O. Khalimonchuk, M. Schraders, N. Dephoure, J. P. Bayley, H. Kunst, P. Devilee, C. W. Cremers, J. D. Schiffman, B. G. Bentz, S. P. Gygi, D. R. Winge, H. Kremer, and J. Rutter. 2009. 'SDH5, a gene required for flavination of succinate dehydrogenase, is mutated in paraganglioma', *Science*, 325: 1139-42.
Heinrich, M. C., C. L. Corless, C. D. Blanke, G. D. Demetri, H. Joensuu, P. J. Roberts, B. L. Eisenberg, M. von Mehren, C. D. Fletcher, K. Sandau, K. McDougall, W. B. Ou, C. J. Chen, and J. A. Fletcher. 2006. 'Molecular correlates of imatinib resistance in gastrointestinal stromal tumors', *J Clin Oncol*, 24: 4764-74.
Heinrich, M. C., C. L. Corless, G. D. Demetri, C. D. Blanke, M. von Mehren, H. Joensuu, L. S. McGreevey, C. J. Chen, A. D. Van den Abbeele, B. J. Druker, B. Kiese, B. Eisenberg, P. J. Roberts, S. Singer, C. D. Fletcher, S. Silberman, S. Dimitrijevic, and J. A. Fletcher.

2003. 'Kinase mutations and imatinib response in patients with metastatic gastrointestinal stromal tumor', *J Clin Oncol*, 21: 4342-9.
Heinrich, M. C., C. L. Corless, A. Duensing, L. McGreevey, C. J. Chen, N. Joseph, S. Singer, D. J. Griffith, A. Haley, A. Town, G. D. Demetri, C. D. Fletcher, and J. A. Fletcher. 2003. 'PDGFRA activating mutations in gastrointestinal stromal tumors', *Science*, 299: 708-10.
Heinrich, M. C., D. J. Griffith, B. J. Druker, C. L. Wait, K. A. Ott, and A. J. Zigler. 2000. 'Inhibition of c-kit receptor tyrosine kinase activity by STI 571, a selective tyrosine kinase inhibitor', *Blood*, 96: 925-32.
Heinrich, M. C., D. Griffith, A. McKinley, J. Patterson, A. Presnell, A. Ramachandran, and M. Debiec-Rychter. 2012. 'Crenolanib inhibits the drug-resistant PDGFRA D842V mutation associated with imatinib-resistant gastrointestinal stromal tumors', *Clin Cancer Res*, 18: 4375-84.
Heinrich, M. C., R. G. Maki, C. L. Corless, C. R. Antonescu, A. Harlow, D. Griffith, A. Town, A. McKinley, W. B. Ou, J. A. Fletcher, C. D. Fletcher, X. Huang, D. P. Cohen, C. M. Baum, and G. D. Demetri. 2008. 'Primary and secondary kinase genotypes correlate with the biological and clinical activity of sunitinib in imatinib-resistant gastrointestinal stromal tumor', *J Clin Oncol*, 26: 5352-9.
Heinrich, M. C., A. Marino-Enriquez, A. Presnell, R. S. Donsky, D. J. Griffith, A. McKinley, J. Patterson, T. Taguchi, C. W. Liang, and J. A. Fletcher. 2012. 'Sorafenib inhibits many kinase mutations associated with drug-resistant gastrointestinal stromal tumors', *Mol Cancer Ther*, 11: 1770-80.
Heinrich, M. C., K. Owzar, C. L. Corless, D. Hollis, E. C. Borden, C. D. Fletcher, C. W. Ryan, M. von Mehren, C. D. Blanke, C. Rankin, R. S. Benjamin, V. H. Bramwell, G. D. Demetri, M. M. Bertagnolli, and J. A. Fletcher. 2008. 'Correlation of kinase genotype and clinical outcome in the North American Intergroup Phase III Trial of imatinib mesylate for treatment of advanced gastrointestinal stromal tumor: CALGB 150105 Study by Cancer and Leukemia Group B and Southwest Oncology Group', *J Clin Oncol*, 26: 5360-7.
Heinrich, M., R. Jones, P. Schoffski, S. Bauer, M. von Mehren, F. Eskens, P. Cassier, O. MIr, H. Shi, T. Alvarez-Diez, M.E. Healy, B. Wolf, and S. George. 2016. "Preliminary safety and activity in a first-in-human phase 1 study of BLU-285, a potent, highly-selective inhibitor of KIT and PDGFRα activation loop mutants in advanced gastrointestinal stromal tumor (GIST)." In *EORTC-NCI-AACR*. Germany.
Heinrich, M., C. Rankin, C. D. Blanke, G. D. Demetri, E. C. Borden, C. W. Ryan, M. von Mehren, M. E. Blackstein, D. A. Priebat, W. D. Tap, R. G. Maki, C. L. Corless, J. A. Fletcher, K. Owzar, J. J. Crowley, R. S. Benjamin, and L. H. Baker. 2017. 'Correlation of Long-term Results of Imatinib in Advanced Gastrointestinal Stromal Tumors With Next-Generation Sequencing Results: Analysis of Phase 3 SWOG Intergroup Trial S0033', *JAMA Oncol*.
Hirota, S., K. Isozaki, Y. Moriyama, K. Hashimoto, T. Nishida, S. Ishiguro, K. Kawano, M. Hanada, A. Kurata, M. Takeda, G. Muhammad Tunio, Y. Matsuzawa, Y. Kanakura, Y. Shinomura, and Y. Kitamura. 1998. 'Gain-of-function mutations of c-kit in human gastrointestinal stromal tumors', *Science*, 279: 577-80.
Hirota, S., A. Ohashi, T. Nishida, K. Isozaki, K. Kinoshita, Y. Shinomura, and Y. Kitamura. 2003. 'Gain-of-function mutations of platelet-derived growth factor receptor alpha gene in gastrointestinal stromal tumors', *Gastroenterology*, 125: 660-7.
Hobert, J. A., J. L. Mester, J. Moline, and C. Eng. 2012. 'Elevated plasma succinate in PTEN, SDHB, and SDHD mutation-positive individuals', *Genet Med*, 14: 616-9.
Hodi, F. S., C. L. Corless, A. Giobbie-Hurder, J. A. Fletcher, M. Zhu, A. Marino-Enriquez, P. Friedlander, R. Gonzalez, J. S. Weber, T. F. Gajewski, S. J. O'Day, K. B. Kim, D. Lawrence, K. T. Flaherty, J. J. Luke, F. A. Collichio, M. S. Ernstoff, M. C. Heinrich, C. Beadling, K. A. Zukotynski, J. T. Yap, A. D. Van den Abbeele, G. D. Demetri, and D. E. Fisher. 2013. 'Imatinib for melanomas harboring mutationally activated or amplified KIT arising on mucosal, acral, and chronically sun-damaged skin', *J Clin Oncol*, 31: 3182-90.
Hodi, F. S., P. Friedlander, C. L. Corless, M. C. Heinrich, S. Mac Rae, A. Kruse, J. Jagannathan, A. D. Van den Abbeele, E. F. Velazquez, G. D. Demetri, and D. E. Fisher. 2008. 'Major response to imatinib mesylate in KIT-mutated melanoma', *J Clin Oncol*, 26: 2046-51.

Horvath, R., A. Abicht, E. Holinski-Feder, A. Laner, K. Gempel, H. Prokisch, H. Lochmuller, T. Klopstock, and M. Jaksch. 2006. 'Leigh syndrome caused by mutations in the flavoprotein (Fp) subunit of succinate dehydrogenase (SDHA)', *J Neurol Neurosurg Psychiatry*, 77: 74-6.

Hostein, I., N. Faur, C. Primois, F. Boury, J. Denard, J. F. Emile, P. P. Bringuier, J. Y. Scoazec, and J. M. Coindre. 2010. 'BRAF mutation status in gastrointestinal stromal tumors', *Am J Clin Pathol*, 133: 141-8.

Huang, S., N. L. Taylor, E. Stroher, R. Fenske, and A. H. Millar. 2013. 'Succinate dehydrogenase assembly factor 2 is needed for assembly and activity of mitochondrial complex II and for normal root elongation in Arabidopsis', *Plant J*, 73: 429-41.

Isozaki, K., S. Hirota, A. Nakama, J. Miyagawa, Y. Shinomura, Z. Xu, S. Nomura, and Y. Kitamura. 1995. 'Disturbed intestinal movement, bile reflux to the stomach, and deficiency of c-kit-expressing cells in Ws/Ws mutant rats', *Gastroenterology*, 109: 456-64.

Italiano, A., C. L. Chen, Y. S. Sung, S. Singer, R. P. DeMatteo, M. P. LaQuaglia, P. Besmer, N. Socci, and C. R. Antonescu. 2012. 'SDHA loss of function mutations in a subset of young adult wild-type gastrointestinal stromal tumors', *BMC Cancer*, 12: 408.

Ito, T., M. Yamamura, T. Hirai, T. Ishikawa, T. Kanda, T. Nakai, M. Ohkouchi, Y. Hashikura, K. Isozaki, and S. Hirota. 2014. 'Gastrointestinal stromal tumors with exon 8 c-kit gene mutation might occur at extragastric sites and have metastasis-prone nature', *Int J Clin Exp Pathol*, 7: 8024-31.

Iverson, T. M. 2013. 'Catalytic mechanisms of complex II enzymes: a structural perspective', *Biochim Biophys Acta*, 1827: 648-57.

Jackson, C. B., J. M. Nuoffer, D. Hahn, H. Prokisch, B. Haberberger, M. Gautschi, A. Haberli, S. Gallati, and A. Schaller. 2014. 'Mutations in SDHD lead to autosomal recessive encephalomyopathy and isolated mitochondrial complex II deficiency', *J Med Genet*, 51: 170-5.

Jain-Ghai, S., J. M. Cameron, A. Al Maawali, S. Blaser, N. MacKay, B. Robinson, and J. Raiman. 2013. 'Complex II deficiency--a case report and review of the literature', *Am J Med Genet A*, 161a: 285-94.

Janeway, K. A., K. H. Albritton, A. D. Van Den Abbeele, G. Z. D'Amato, P. Pedrazzoli, S. Siena, J. Picus, J. E. Butrynski, M. Schlemmer, M. C. Heinrich, and G. D. Demetri. 2009. 'Sunitinib treatment in pediatric patients with advanced GIST following failure of imatinib', *Pediatr Blood Cancer*, 52: 767-71.

Janeway, K. A., S. Y. Kim, M. Lodish, V. Nose, P. Rustin, J. Gaal, P. L. Dahia, B. Liegl, E. R. Ball, M. Raygada, A. H. Lai, L. Kelly, J. L. Hornick, M. O'Sullivan, R. R. de Krijger, W. N. Dinjens, G. D. Demetri, C. R. Antonescu, J. A. Fletcher, L. Helman, and C. A. Stratakis. 2011. 'Defects in succinate dehydrogenase in gastrointestinal stromal tumors lacking KIT and PDGFRA mutations', *Proc Natl Acad Sci U S A*, 108: 314-8.

Janeway, K. A., and C. B. Weldon. 2012. 'Pediatric gastrointestinal stromal tumor', *Semin Pediatr Surg*, 21: 31-43.

Javidi-Sharifi, N., E. Traer, J. Martinez, A. Gupta, T. Taguchi, J. Dunlap, M. C. Heinrich, C. L. Corless, B. P. Rubin, B. J. Druker, and J. W. Tyner. 2015. 'Crosstalk between KIT and FGFR3 Promotes Gastrointestinal Stromal Tumor Cell Growth and Drug Resistance', *Cancer Res*, 75: 880-91.

Joensuu, H., M. Eriksson, K. Sundby Hall, A. Reichardt, J. T. Hartmann, D. Pink, G. Ramadori, P. Hohenberger, S. E. Al-Batran, M. Schlemmer, S. Bauer, E. Wardelmann, B. Nilsson, H. Sihto, P. Bono, R. Kallio, J. Junnila, T. Alvegard, and P. Reichardt. 2016. 'Adjuvant Imatinib for High-Risk GI Stromal Tumor: Analysis of a Randomized Trial', *J Clin Oncol*, 34: 244-50.

Kemmer, K., C. L. Corless, J. A. Fletcher, L. McGreevey, A. Haley, D. Griffith, O. W. Cummings, C. Wait, A. Town, and M. C. Heinrich. 2004. 'KIT mutations are common in testicular seminomas', *Am J Pathol*, 164: 305-13.

Killian, J. K., S. Y. Kim, M. Miettinen, C. Smith, M. Merino, M. Tsokos, M. Quezado, W. I. Smith, Jr., M. S. Jahromi, P. Xekouki, E. Szarek, R. L. Walker, J. Lasota, M. Raffeld, B. Klotzle, Z. Wang, L. Jones, Y. Zhu, Y. Wang, J. J. Waterfall, M. J. O'Sullivan, M. Bibikova, K.

Pacak, C. Stratakis, K. A. Janeway, J. D. Schiffman, J. B. Fan, L. Helman, and P. S. Meltzer. 2013. 'Succinate dehydrogenase mutation underlies global epigenomic divergence in gastrointestinal stromal tumor', *Cancer Discov*, 3: 648-57.

Killian, J. K., M. Miettinen, R. L. Walker, Y. Wang, Y. J. Zhu, J. J. Waterfall, N. Noyes, P. Retnakumar, Z. Yang, W. I. Smith, Jr., M. S. Killian, C. C. Lau, M. Pineda, J. Walling, H. Stevenson, C. Smith, Z. Wang, J. Lasota, S. Y. Kim, S. A. Boikos, L. J. Helman, and P. S. Meltzer. 2014. 'Recurrent epimutation of SDHC in gastrointestinal stromal tumors', *Sci Transl Med*, 6: 268ra177.

Kim, H. J., M. Y. Jeong, U. Na, and D. R. Winge. 2012. 'Flavinylation and assembly of succinate dehydrogenase are dependent on the C-terminal tail of the flavoprotein subunit', *J Biol Chem*, 287: 40670-9.

Kindblom, L. G., H. E. Remotti, F. Aldenborg, and J. M. Meis-Kindblom. 1998. 'Gastrointestinal pacemaker cell tumor (GIPACT): gastrointestinal stromal tumors show phenotypic characteristics of the interstitial cells of Cajal', *Am J Pathol*, 152: 1259-69.

King, A., M. A. Selak, and E. Gottlieb. 2006. 'Succinate dehydrogenase and fumarate hydratase: linking mitochondrial dysfunction and cancer', *Oncogene*, 25: 4675-82.

King, Kathryn S., Tamara Prodanov, Vitaly Kantorovich, Tito Fojo, Jacqueline K. Hewitt, Margaret Zacharin, Robert Wesley, Maya Lodish, Margarita Raygada, Anne-Paule Gimenez-Roqueplo, Shana McCormack, Graeme Eisenhofer, Dragana Milosevic, Electron Kebebew, Constantine A. Stratakis, and Karel Pacak. 2011. 'Metastatic Pheochromocytoma/Paraganglioma Related to Primary Tumor Development in Childhood or Adolescence: Significant Link to SDHB Mutations', *Journal of Clinical Oncology*, 29: 4137-42.

Kinoshita, K., S. Hirota, K. Isozaki, A. Ohashi, T. Nishida, Y. Kitamura, Y. Shinomura, and Y. Matsuzawa. 2004. 'Absence of c-kit gene mutations in gastrointestinal stromal tumours from neurofibromatosis type 1 patients', *J Pathol*, 202: 80-5.

Kitanovic, A., F. Bonowski, F. Heigwer, P. Ruoff, I. Kitanovic, C. Ungewiss, and S. Wolfl. 2012. 'Acetic acid treatment in S. cerevisiae creates significant energy deficiency and nutrient starvation that is dependent on the activity of the mitochondrial transcriptional complex Hap2-3-4-5', *Front Oncol*, 2: 118.

Korpershoek, E., J. Favier, J. Gaal, N. Burnichon, B. van Gessel, L. Oudijk, C. Badoual, N. Gadessaud, A. Venisse, J. P. Bayley, M. F. van Dooren, W. W. de Herder, F. Tissier, P. F. Plouin, F. H. van Nederveen, W. N. Dinjens, A. P. Gimenez-Roqueplo, and R. R. de Krijger. 2011. 'SDHA immunohistochemistry detects germline SDHA gene mutations in apparently sporadic paragangliomas and pheochromocytomas', *J Clin Endocrinol Metab*, 96: E1472-6.

Kounosu, A. 2014. 'Analysis of covalent flavinylation using thermostable succinate dehydrogenase from Thermus thermophilus and Sulfolobus tokodaii lacking SdhE homologs', *FEBS Lett*, 588: 1058-63.

Landrum, M. J., J. M. Lee, M. Benson, G. Brown, C. Chao, S. Chitipiralla, B. Gu, J. Hart, D. Hoffman, J. Hoover, W. Jang, K. Katz, M. Ovetsky, G. Riley, A. Sethi, R. Tully, R. Villamarin-Salomon, W. Rubinstein, and D. R. Maglott. 2016. 'ClinVar: public archive of interpretations of clinically relevant variants', *Nucleic Acids Res*, 44: D862-8.

Larizza, L., I. Magnani, and A. Beghini. 2005. 'The Kasumi-1 cell line: a t(8;21)-kit mutant model for acute myeloid leukemia', *Leuk Lymphoma*, 46: 247-55.

Lasota, J., C. L. Corless, M. C. Heinrich, M. Debiec-Rychter, R. Sciot, E. Wardelmann, S. Merkelbach-Bruse, H. U. Schildhaus, S. E. Steigen, J. Stachura, A. Wozniak, C. Antonescu, O. Daum, J. Martin, J. G. Del Muro, and M. Miettinen. 2008. 'Clinicopathologic profile of gastrointestinal stromal tumors (GISTs) with primary KIT exon 13 or exon 17 mutations: a multicenter study on 54 cases', *Mod Pathol*, 21: 476-84.

Lasota, J., J. Stachura, and M. Miettinen. 2006. 'GISTs with PDGFRA exon 14 mutations represent subset of clinically favorable gastric tumors with epithelioid morphology', *Lab Invest*, 86: 94-100.

Lasserre, Jean-Paul, Alain Dautant, Raeka S. Aiyar, Roza Kucharczyk, Annie Glatigny, Déborah Tribouillard-Tanvier, Joanna Rytka, Marc Blondel, Natalia Skoczen, Pascal Reynier,

Laras Pitayu, Agnès Rötig, Agnès Delahodde, Lars M. Steinmetz, Geneviève Dujardin, Vincent Procaccio, and Jean-Paul di Rago. 2015. 'Yeast as a system for modeling mitochondrial disease mechanisms and discovering therapies', *Disease Models & Mechanisms*, 8: 509-26.

Lek, M., K. J. Karczewski, E. V. Minikel, K. E. Samocha, E. Banks, T. Fennell, A. H. O'Donnell-Luria, J. S. Ware, A. J. Hill, B. B. Cummings, T. Tukiainen, D. P. Birnbaum, J. A. Kosmicki, L. E. Duncan, K. Estrada, F. Zhao, J. Zou, E. Pierce-Hoffman, J. Berghout, D. N. Cooper, N. Deflaux, M. DePristo, R. Do, J. Flannick, M. Fromer, L. Gauthier, J. Goldstein, N. Gupta, D. Howrigan, A. Kiezun, M. I. Kurki, A. L. Moonshine, P. Natarajan, L. Orozco, G. M. Peloso, R. Poplin, M. A. Rivas, V. Ruano-Rubio, S. A. Rose, D. M. Ruderfer, K. Shakir, P. D. Stenson, C. Stevens, B. P. Thomas, G. Tiao, M. T. Tusie-Luna, B. Weisburd, H. H. Won, D. Yu, D. M. Altshuler, D. Ardissino, M. Boehnke, J. Danesh, S. Donnelly, R. Elosua, J. C. Florez, S. B. Gabriel, G. Getz, S. J. Glatt, C. M. Hultman, S. Kathiresan, M. Laakso, S. McCarroll, M. I. McCarthy, D. McGovern, R. McPherson, B. M. Neale, A. Palotie, S. M. Purcell, D. Saleheen, J. M. Scharf, P. Sklar, P. F. Sullivan, J. Tuomilehto, M. T. Tsuang, H. C. Watkins, J. G. Wilson, M. J. Daly, and D. G. MacArthur. 2016. 'Analysis of protein-coding genetic variation in 60,706 humans', *Nature*, 536: 285-91.

Lenders, J. W., Q. Y. Duh, G. Eisenhofer, A. P. Gimenez-Roqueplo, S. K. Grebe, M. H. Murad, M. Naruse, K. Pacak, and W. F. Young, Jr. 2014. 'Pheochromocytoma and paraganglioma: an endocrine society clinical practice guideline', *J Clin Endocrinol Metab*, 99: 1915-42.

Lendvai, Nikoletta, Robert Pawlosky, Petra Bullova, Graeme Eisenhofer, Attila Patocs, Richard L. Veech, and Karel Pacak. 2014. 'Succinate-to-Fumarate Ratio as a New Metabolic Marker to Detect the Presence of SDHB/D-related Paraganglioma: Initial Experimental and Ex Vivo Findings', *Endocrinology*, 155: 27-32.

Letouze, E., C. Martinelli, C. Loriot, N. Burnichon, N. Abermil, C. Ottolenghi, M. Janin, M. Menara, A. T. Nguyen, P. Benit, A. Buffet, C. Marcaillou, J. Bertherat, L. Amar, P. Rustin, A. De Reynies, A. P. Gimenez-Roqueplo, and J. Favier. 2013. 'SDH mutations establish a hypermethylator phenotype in paraganglioma', *Cancer Cell*, 23: 739-52.

Lev, S., D. Givol, and Y. Yarden. 1991. 'A specific combination of substrates is involved in signal transduction by the kit-encoded receptor', *Embo j*, 10: 647-54.

Lev, S., Y. Yarden, and D. Givol. 1992. 'Dimerization and activation of the kit receptor by monovalent and bivalent binding of the stem cell factor', *J Biol Chem*, 267: 15970-7.

Levitas, A., E. Muhammad, G. Harel, A. Saada, V. C. Caspi, E. Manor, J. C. Beck, V. Sheffield, and R. Parvari. 2010. 'Familial neonatal isolated cardiomyopathy caused by a mutation in the flavoprotein subunit of succinate dehydrogenase', *Eur J Hum Genet*, 18: 1160-5.

Liegl, B., J. L. Hornick, C. L. Corless, and C. D. Fletcher. 2009. 'Monoclonal antibody DOG1.1 shows higher sensitivity than KIT in the diagnosis of gastrointestinal stromal tumors, including unusual subtypes', *Am J Surg Pathol*, 33: 437-46.

Liegl, B., I. Kepten, C. Le, M. Zhu, G. D. Demetri, M. C. Heinrich, C. D. Fletcher, C. L. Corless, and J. A. Fletcher. 2008. 'Heterogeneity of kinase inhibitor resistance mechanisms in GIST', *J Pathol*, 216: 64-74.

Lill, R., B. Hoffmann, S. Molik, A. J. Pierik, N. Rietzschel, O. Stehling, M. A. Uzarska, H. Webert, C. Wilbrecht, and U. Muhlenhoff. 2012. 'The role of mitochondria in cellular iron-sulfur protein biogenesis and iron metabolism', *Biochim Biophys Acta*, 1823: 1491-508.

Long, K. B., J. E. Butrynski, S. D. Blank, K. S. Ebrahim, D. M. Dressel, M. C. Heinrich, C. L. Corless, and J. L. Hornick. 2010. 'Primary extragastrointestinal stromal tumor of the pleura: report of a unique case with genetic confirmation', *Am J Surg Pathol*, 34: 907-12.

Lux, M. L., B. P. Rubin, T. L. Biase, C. J. Chen, T. Maclure, G. Demetri, S. Xiao, S. Singer, C. D. Fletcher, and J. A. Fletcher. 2000. 'KIT extracellular and kinase domain mutations in gastrointestinal stromal tumors', *Am J Pathol*, 156: 791-5.

Ma, Shuang, and Brian P. Rubin. 2014. 'Apoptosis-associated tyrosine kinase 1 inhibits growth and migration and promotes apoptosis in melanoma', *Lab Invest*, 94: 430-38.

Ma, Y. Y., T. F. Wu, Y. P. Liu, Q. Wang, X. Y. Li, Y. Ding, J. Q. Song, X. Y. Shi, W. N. Zhang, M. Zhao, L. Y. Hu, J. Ju, Z. L. Wang, Y. L. Yang, and L. P. Zou. 2014. 'Two compound

frame-shift mutations in succinate dehydrogenase gene of a Chinese boy with encephalopathy', *Brain Dev*, 36: 394-8.
MacKenzie, E. D., M. A. Selak, D. A. Tennant, L. J. Payne, S. Crosby, C. M. Frederiksen, D. G. Watson, and E. Gottlieb. 2007. 'Cell-permeating alpha-ketoglutarate derivatives alleviate pseudohypoxia in succinate dehydrogenase-deficient cells', *Mol Cell Biol*, 27: 3282-9.
Maier, J., T. Lange, I. Kerle, K. Specht, M. Bruegel, C. Wickenhauser, P. Jost, D. Niederwieser, C. Peschel, J. Duyster, and N. von Bubnoff. 2013. 'Detection of mutant free circulating tumor DNA in the plasma of patients with gastrointestinal stromal tumor harboring activating mutations of CKIT or PDGFRA', *Clin Cancer Res*, 19: 4854-67.
Maio, N., D. Ghezzi, D. Verrigni, T. Rizza, E. Bertini, D. Martinelli, M. Zeviani, A. Singh, R. Carrozzo, and T. A. Rouault. 2016. 'Disease-Causing SDHAF1 Mutations Impair Transfer of Fe-S Clusters to SDHB', *Cell Metab*, 23: 292-302.
Maio, N., A. Singh, H. Uhrigshardt, N. Saxena, W. H. Tong, and T. A. Rouault. 2014. 'Cochaperone binding to LYR motifs confers specificity of iron sulfur cluster delivery', *Cell Metab*, 19: 445-57.
Martin, J., A. Poveda, A. Llombart-Bosch, R. Ramos, J. A. Lopez-Guerrero, J. Garcia del Muro, J. Maurel, S. Calabuig, A. Gutierrez, J. L. Gonzalez de Sande, J. Martinez, A. De Juan, N. Lainez, F. Losa, V. Alija, P. Escudero, A. Casado, P. Garcia, R. Blanco, and J. M. Buesa. 2005. 'Deletions affecting codons 557-558 of the c-KIT gene indicate a poor prognosis in patients with completely resected gastrointestinal stromal tumors: a study by the Spanish Group for Sarcoma Research (GEIS)', *J Clin Oncol*, 23: 6190-8.
Mazur, M. T., and H. B. Clark. 1983. 'Gastric stromal tumors. Reappraisal of histogenesis', *Am J Surg Pathol*, 7: 507-19.
Miettinen, M., J. K. Killian, Z. F. Wang, J. Lasota, C. Lau, L. Jones, R. Walker, M. Pineda, Y. J. Zhu, S. Y. Kim, L. Helman, and P. Meltzer. 2013. 'Immunohistochemical loss of succinate dehydrogenase subunit A (SDHA) in gastrointestinal stromal tumors (GISTs) signals SDHA germline mutation', *Am J Surg Pathol*, 37: 234-40.
Miettinen, M., Z. F. Wang, M. Sarlomo-Rikala, C. Osuch, P. Rutkowski, and J. Lasota. 2011. 'Succinate dehydrogenase-deficient GISTs: a clinicopathologic, immunohistochemical, and molecular genetic study of 66 gastric GISTs with predilection to young age', *Am J Surg Pathol*, 35: 1712-21.
Miranda, C., M. Nucifora, F. Molinari, E. Conca, M. C. Anania, A. Bordoni, P. Saletti, L. Mazzucchelli, S. Pilotti, M. A. Pierotti, E. Tamborini, A. Greco, and M. Frattini. 2012. 'KRAS and BRAF mutations predict primary resistance to imatinib in gastrointestinal stromal tumors', *Clin Cancer Res*, 18: 1769-76.
Mol, C. D., D. R. Dougan, T. R. Schneider, R. J. Skene, M. L. Kraus, D. N. Scheibe, G. P. Snell, H. Zou, B. C. Sang, and K. P. Wilson. 2004. 'Structural basis for the autoinhibition and STI-571 inhibition of c-Kit tyrosine kinase', *J Biol Chem*, 279: 31655-63.
Muller, F., A. R. Crofts, and D. M. Kramer. 2002. 'Multiple Q-cycle bypass reactions at the Qo site of the cytochrome bc1 complex', *Biochemistry*, 41: 7866-74.
Na, U., W. Yu, J. Cox, D. K. Bricker, K. Brockmann, J. Rutter, C. S. Thummel, and D. R. Winge. 2014. 'The LYR factors SDHAF1 and SDHAF3 mediate maturation of the iron-sulfur subunit of succinate dehydrogenase', *Cell Metab*, 20: 253-66.
Nagata, H., A. S. Worobec, C. K. Oh, B. A. Chowdhury, S. Tannenbaum, Y. Suzuki, and D. D. Metcalfe. 1995. 'Identification of a point mutation in the catalytic domain of the protooncogene c-kit in peripheral blood mononuclear cells of patients who have mastocytosis with an associated hematologic disorder', *Proc Natl Acad Sci U S A*, 92: 10560-4.
Neumann, H. P., C. Pawlu, M. Peczkowska, B. Bausch, S. R. McWhinney, M. Muresan, M. Buchta, G. Franke, J. Klisch, T. A. Bley, S. Hoegerle, C. C. Boedeker, G. Opocher, J. Schipper, A. Januszewicz, and C. Eng. 2004. 'Distinct clinical features of paraganglioma syndromes associated with SDHB and SDHD gene mutations', *Jama*, 292: 943-51.
Ni, Ying, Kevin M. Zbuk, Tammy Sadler, Attila Patocs, Glenn Lobo, Emily Edelman, Petra Platzer, Mohammed S. Orloff, Kristin A. Waite, and Charis Eng. 2008. 'Germline Mutations and

Variants in the Succinate Dehydrogenase Genes in Cowden and Cowden-like Syndromes', *Am J Hum Genet*, 83: 261-68.
Niemann, S., U. Muller, D. Engelhardt, and P. Lohse. 2003. 'Autosomal dominant malignant and catecholamine-producing paraganglioma caused by a splice donor site mutation in SDHC', *Hum Genet*, 113: 92-4.
Niemeijer, N. D., T. G. Papathomas, E. Korpershoek, R. R. de Krijger, L. Oudijk, H. Morreau, J. P. Bayley, F. J. Hes, J. C. Jansen, W. N. Dinjens, and E. P. Corssmit. 2015. 'Succinate Dehydrogenase (SDH)-Deficient Pancreatic Neuroendocrine Tumor Expands the SDH-Related Tumor Spectrum', *J Clin Endocrinol Metab*, 100: E1386-93.
O'Riain, C., C. L. Corless, M. C. Heinrich, D. Keegan, M. Vioreanu, D. Maguire, and K. Sheahan. 2005. 'Gastrointestinal stromal tumors: insights from a new familial GIST kindred with unusual genetic and pathologic features', *Am J Surg Pathol*, 29: 1680-3.
Ohlenbusch, Andreas, Simon Edvardson, Johannes Skorpen, Alf Bjornstad, Ann Saada, Orly Elpeleg, Jutta Gärtner, and Knut Brockmann. 2012. 'Leukoencephalopathy with accumulated succinate is indicative of SDHAF1 related complex II deficiency', *Orphanet Journal of Rare Diseases*, 7: 69-69.
Oudijk, L., J. Gaal, E. Korpershoek, F. H. van Nederveen, L. Kelly, G. Schiavon, J. Verweij, R. H. Mathijssen, M. A. den Bakker, R. A. Oldenburg, R. L. van Loon, M. J. O'Sullivan, R. R. de Krijger, and W. N. Dinjens. 2013. 'SDHA mutations in adult and pediatric wild-type gastrointestinal stromal tumors', *Mod Pathol*, 26: 456-63.
Oyedotun, K. S., and B. D. Lemire. 2004. 'The quaternary structure of the Saccharomyces cerevisiae succinate dehydrogenase. Homology modeling, cofactor docking, and molecular dynamics simulation studies', *J Biol Chem*, 279: 9424-31.
Oyedotun, K. S., C. S. Sit, and B. D. Lemire. 2007. 'The Saccharomyces cerevisiae succinate dehydrogenase does not require heme for ubiquinone reduction', *Biochim Biophys Acta*, 1767: 1436-45.
Pagnamenta, A. T., I. P. Hargreaves, A. J. Duncan, J. W. Taanman, S. J. Heales, J. M. Land, M. Bitner-Glindzicz, J. V. Leonard, and S. Rahman. 2006. 'Phenotypic variability of mitochondrial disease caused by a nuclear mutation in complex II', *Mol Genet Metab*, 89: 214-21.
Panizza, E., T. Ercolino, L. Mori, E. Rapizzi, M. Castellano, G. Opocher, I. Ferrero, H. P. Neumann, M. Mannelli, and P. Goffrini. 2013. 'Yeast model for evaluating the pathogenic significance of SDHB, SDHC and SDHD mutations in PHEO-PGL syndrome', *Hum Mol Genet*, 22: 804-15.
Pantaleo, M. A., A. Astolfi, M. Urbini, M. Nannini, P. Paterini, V. Indio, M. Saponara, S. Formica, C. Ceccarelli, R. Casadio, G. Rossi, F. Bertolini, D. Santini, M. G. Pirini, M. Fiorentino, U. Basso, and G. Biasco. 2014. 'Analysis of all subunits, SDHA, SDHB, SDHC, SDHD, of the succinate dehydrogenase complex in KIT/PDGFRA wild-type GIST', *Eur J Hum Genet*, 22: 32-9.
Pantaleo, M. A., M. Nannini, A. Astolfi, and G. Biasco. 2011. 'A distinct pediatric-type gastrointestinal stromal tumor in adults: potential role of succinate dehydrogenase subunit A mutations', *Am J Surg Pathol*, 35: 1750-2.
Pantaleo, M. A., M. Nannini, C. L. Corless, and M. C. Heinrich. 2015. 'Quadruple wild-type (WT) GIST: defining the subset of GIST that lacks abnormalities of KIT, PDGFRA, SDH, or RAS signaling pathways', *Cancer Med*, 4: 101-3.
Parfait, B., D. Chretien, A. Rotig, C. Marsac, A. Munnich, and P. Rustin. 2000. 'Compound heterozygous mutations in the flavoprotein gene of the respiratory chain complex II in a patient with Leigh syndrome', *Hum Genet*, 106: 236-43.
Pasini, B., S. R. McWhinney, T. Bei, L. Matyakhina, S. Stergiopoulos, M. Muchow, S. A. Boikos, B. Ferrando, K. Pacak, G. Assie, E. Baudin, A. Chompret, J. W. Ellison, J. J. Briere, P. Rustin, A. P. Gimenez-Roqueplo, C. Eng, J. A. Carney, and C. A. Stratakis. 2008. 'Clinical and molecular genetics of patients with the Carney-Stratakis syndrome and germline mutations of the genes coding for the succinate dehydrogenase subunits SDHB, SDHC, and SDHD', *Eur J Hum Genet*, 16: 79-88.

Pasini, B., and C. A. Stratakis. 2009. 'SDH mutations in tumorigenesis and inherited endocrine tumours: lesson from the phaeochromocytoma-paraganglioma syndromes', *J Intern Med*, 266: 19-42.

Petropoulos, A. E., C. M. Luetje, P. J. Camarata, C. K. Whittaker, G. Lee, and B. E. Baysal. 2000. 'Genetic analysis in the diagnosis of familial paragangliomas', *Laryngoscope*, 110: 1225-9.

Pollard, P. J., J. J. Briere, N. A. Alam, J. Barwell, E. Barclay, N. C. Wortham, T. Hunt, M. Mitchell, S. Olpin, S. J. Moat, I. P. Hargreaves, S. J. Heales, Y. L. Chung, J. R. Griffiths, A. Dalgleish, J. A. McGrath, M. J. Gleeson, S. V. Hodgson, R. Poulsom, P. Rustin, and I. P. Tomlinson. 2005. 'Accumulation of Krebs cycle intermediates and over-expression of HIF1alpha in tumours which result from germline FH and SDH mutations', *Hum Mol Genet*, 14: 2231-9.

Pollard, P. J., M. El-Bahrawy, R. Poulsom, G. Elia, P. Killick, G. Kelly, T. Hunt, R. Jeffery, P. Seedhar, J. Barwell, F. Latif, M. J. Gleeson, S. V. Hodgson, G. W. Stamp, I. P. Tomlinson, and E. R. Maher. 2006. 'Expression of HIF-1alpha, HIF-2alpha (EPAS1), and their target genes in paraganglioma and pheochromocytoma with VHL and SDH mutations', *J Clin Endocrinol Metab*, 91: 4593-8.

Prodanov, Tamara, Bas Havekes, Katherine L. Nathanson, Karen T. Adams, and Karel Pacak. 2009. 'Malignant paraganglioma associated with succinate dehydrogenase subunit B in an 8-year-old child: the age of first screening?', *Pediatric nephrology (Berlin, Germany)*, 24: 1239-42.

Raygada, Margarita, Kathryn S. King, Karen T. Adams, Constantine A. Stratakis, and Karel Pacak. 2014. 'Counseling patients with succinate dehydrogenase subunit defects: genetics, preventive guidelines, and dealing with uncertainty', *Journal of pediatric endocrinology & metabolism : JPEM*, 27: 837-44.

Reva, B., Y. Antipin, and C. Sander. 2011. 'Predicting the functional impact of protein mutations: application to cancer genomics', *Nucleic Acids Res*, 39: e118.

Ricketts, C. J., J. R. Forman, E. Rattenberry, N. Bradshaw, F. Lalloo, L. Izatt, T. R. Cole, R. Armstrong, V. K. Kumar, P. J. Morrison, A. B. Atkinson, F. Douglas, S. G. Ball, J. Cook, U. Srirangalingam, P. Killick, G. Kirby, S. Aylwin, E. R. Woodward, D. G. Evans, S. V. Hodgson, V. Murday, S. L. Chew, J. M. Connell, T. L. Blundell, F. Macdonald, and E. R. Maher. 2010. 'Tumor risks and genotype-phenotype-proteotype analysis in 358 patients with germline mutations in SDHB and SDHD', *Hum Mutat*, 31: 41-51.

Roberts, K. G., A. F. Odell, E. M. Byrnes, R. M. Baleato, R. Griffith, A. B. Lyons, and L. K. Ashman. 2007. 'Resistance to c-KIT kinase inhibitors conferred by V654A mutation', *Mol Cancer Ther*, 6: 1159-66.

Robinson, K. M., R. A. Rothery, J. H. Weiner, and B. D. Lemire. 1994. 'The covalent attachment of FAD to the flavoprotein of Saccharomyces cerevisiae succinate dehydrogenase is not necessary for import and assembly into mitochondria', *Eur J Biochem*, 222: 983-90.

Romanel, A., D. Gasi Tandefelt, V. Conteduca, A. Jayaram, N. Casiraghi, D. Wetterskog, S. Salvi, D. Amadori, Z. Zafeiriou, P. Rescigno, D. Bianchini, G. Gurioli, V. Casadio, S. Carreira, J. Goodall, A. Wingate, R. Ferraldeschi, N. Tunariu, P. Flohr, U. De Giorgi, J. S. de Bono, F. Demichelis, and G. Attard. 2015. 'Plasma AR and abiraterone-resistant prostate cancer', *Sci Transl Med*, 7: 312re10.

Rubin, B. P., C. R. Antonescu, J. P. Scott-Browne, M. L. Comstock, Y. Gu, M. R. Tanas, C. B. Ware, and J. Woodell. 2005. 'A knock-in mouse model of gastrointestinal stromal tumor harboring kit K641E', *Cancer Res*, 65: 6631-9.

Rubin, B. P., S. Singer, C. Tsao, A. Duensing, M. L. Lux, R. Ruiz, M. K. Hibbard, C. J. Chen, S. Xiao, D. A. Tuveson, G. D. Demetri, C. D. Fletcher, and J. A. Fletcher. 2001. 'KIT activation is a ubiquitous feature of gastrointestinal stromal tumors', *Cancer Res*, 61: 8118-21.

Schoffski, P., A. Wozniak, O. Schoffski, L. van Eycken, and M. Debiec-Rychter. 2016. 'Overcoming Cost Implications of Mutational Analysis in Patients with Gastrointestinal Stromal Tumors: A Pragmatic Approach', *Oncol Res Treat*, 39: 811-16.

Scholz, Simone L., Susanne Horn, Rajmohan Murali, Inga Möller, Antje Sucker, Wiebke Sondermann, Mathias Stiller, Bastian Schilling, Elisabeth Livingstone, Lisa Zimmer, Henning Reis, Claudia H. Metz, Michael Zeschnigk, Annette Paschen, Klaus-Peter Steuhl, Dirk Schadendorf, Henrike Westekemper, and Klaus G. Griewank. 2015. 'Analysis of SDHD promoter mutations in various types of melanoma', *Oncotarget*, 6: 25868-82.

Schwaederle, M., H. Husain, P. T. Fanta, D. E. Piccioni, S. Kesari, R. B. Schwab, S. P. Patel, O. Harismendy, M. Ikeda, B. A. Parker, and R. Kurzrock. 2016. 'Use of Liquid Biopsies in Clinical Oncology: Pilot Experience in 168 Patients', *Clin Cancer Res*.

Schymkowitz, J., J. Borg, F. Stricher, R. Nys, F. Rousseau, and L. Serrano. 2005. 'The FoldX web server: an online force field', *Nucleic Acids Res*, 33: W382-8.

Selak, M. A., S. M. Armour, E. D. MacKenzie, H. Boulahbel, D. G. Watson, K. D. Mansfield, Y. Pan, M. C. Simon, C. B. Thompson, and E. Gottlieb. 2005. 'Succinate links TCA cycle dysfunction to oncogenesis by inhibiting HIF-alpha prolyl hydroxylase', *Cancer Cell*, 7: 77-85.

Shi, E., J. Chmielecki, C. M. Tang, K. Wang, M. C. Heinrich, G. Kang, C. L. Corless, D. Hong, K. E. Fero, J. D. Murphy, P. T. Fanta, S. M. Ali, M. De Siena, A. M. Burgoyne, S. Movva, L. Madlensky, G. M. Heestand, J. C. Trent, R. Kurzrock, D. Morosini, J. S. Ross, O. Harismendy, and J. K. Sicklick. 2016. 'FGFR1 and NTRK3 actionable alterations in "Wild-Type" gastrointestinal stromal tumors', *J Transl Med*, 14: 339.

Sikorski, R. S., and P. Hieter. 1989. 'A system of shuttle vectors and yeast host strains designed for efficient manipulation of DNA in Saccharomyces cerevisiae', *Genetics*, 122: 19-27.

Siravegna, G., B. Mussolin, M. Buscarino, G. Corti, A. Cassingena, G. Crisafulli, A. Ponzetti, C. Cremolini, A. Amatu, C. Lauricella, S. Lamba, S. Hobor, A. Avallone, E. Valtorta, G. Rospo, E. Medico, V. Motta, C. Antoniotti, F. Tatangelo, B. Bellosillo, S. Veronese, A. Budillon, C. Montagut, P. Racca, S. Marsoni, A. Falcone, R. B. Corcoran, F. Di Nicolantonio, F. Loupakis, S. Siena, A. Sartore-Bianchi, and A. Bardelli. 2015. 'Clonal evolution and resistance to EGFR blockade in the blood of colorectal cancer patients', *Nat Med*, 21: 795-801.

Smith, E. H., R. Janknecht, and L. J. Maher, 3rd. 2007. 'Succinate inhibition of alpha-ketoglutarate-dependent enzymes in a yeast model of paraganglioma', *Hum Mol Genet*, 16: 3136-48.

Sommer, G., V. Agosti, I. Ehlers, F. Rossi, S. Corbacioglu, J. Farkas, M. Moore, K. Manova, C. R. Antonescu, and P. Besmer. 2003. 'Gastrointestinal stromal tumors in a mouse model by targeted mutation of the Kit receptor tyrosine kinase', *Proc Natl Acad Sci U S A*, 100: 6706-11.

Spencer, K. R., and J. M. Mehnert. 2016. 'Mucosal Melanoma: Epidemiology, Biology and Treatment', *Cancer Treat Res*, 167: 295-320.

Stebbing, J., A. Filipovic, L. C. Lit, K. Blighe, A. Grothey, Y. Xu, Y. Miki, L. W. Chow, R. C. Coombes, H. Sasano, J. A. Shaw, and G. Giamas. 2013. 'LMTK3 is implicated in endocrine resistance via multiple signaling pathways', *Oncogene*, 32: 3371-80.

Subramanian, S., R. B. West, C. L. Corless, W. Ou, B. P. Rubin, K. M. Chu, S. Y. Leung, S. T. Yuen, S. Zhu, T. Hernandez-Boussard, K. Montgomery, T. O. Nielsen, R. M. Patel, J. R. Goldblum, M. C. Heinrich, J. A. Fletcher, and M. van de Rijn. 2004. 'Gastrointestinal stromal tumors (GISTs) with KIT and PDGFRA mutations have distinct gene expression profiles', *Oncogene*, 23: 7780-90.

Sun, F., X. Huo, Y. Zhai, A. Wang, J. Xu, D. Su, M. Bartlam, and Z. Rao. 2005. 'Crystal structure of mitochondrial respiratory membrane protein complex II', *Cell*, 121: 1043-57.

Szeto, S. S., S. N. Reinke, B. D. Sykes, and B. D. Lemire. 2007. 'Ubiquinone-binding site mutations in the Saccharomyces cerevisiae succinate dehydrogenase generate superoxide and lead to the accumulation of succinate', *J Biol Chem*, 282: 27518-26.

Taguchi, T., H. Sonobe, S. Toyonaga, I. Yamasaki, T. Shuin, A. Takano, K. Araki, K. Akimaru, and K. Yuri. 2002. 'Conventional and molecular cytogenetic characterization of a new human cell line, GIST-T1, established from gastrointestinal stromal tumor', *Lab Invest*, 82: 663-5.

Taylor, R. W., M. A. Birch-Machin, J. Schaefer, L. Taylor, R. Shakir, B. A. Ackrell, B. Cochran, L. A. Bindoff, M. J. Jackson, P. Griffiths, and D. M. Turnbull. 1996. 'Deficiency of complex II of the mitochondrial respiratory chain in late-onset optic atrophy and ataxia', *Ann Neurol*, 39: 224-32.

Tian, Q., H. F. Frierson, Jr., G. W. Krystal, and C. A. Moskaluk. 1999. 'Activating c-kit gene mutations in human germ cell tumors', *Am J Pathol*, 154: 1643-7.

Tomasiak, T. M., G. Cecchini, and T. M. Iverson. 2007. 'Succinate as Donor; Fumarate as Acceptor', *EcoSal Plus*, 2.

Tomitsuka, E., K. Kita, and H. Esumi. 2009. 'Regulation of succinate-ubiquinone reductase and fumarate reductase activities in human complex II by phosphorylation of its flavoprotein subunit', *Proc Jpn Acad Ser B Phys Biol Sci*, 85: 258-65.

Tomomura, M., N. Morita, F. Yoshikawa, A. Konishi, H. Akiyama, T. Furuichi, and H. Kamiguchi. 2007. 'Structural and functional analysis of the apoptosis-associated tyrosine kinase (AATYK) family', *Neuroscience*, 148: 510-21.

Tufton, N., L. Shapiro, U. Srirangalingam, P. Richards, A. Sahdev, V. K. Kumar, L. McAndrew, L. Martin, D. Berney, J. Monson, S. L. Chew, M. Waterhouse, M. Druce, M. Korbonits, K. Metcalfe, W. M. Drake, H. L. Storr, and S. A. Akker. 2016. 'Outcomes of annual surveillance imaging in an adult and paediatric cohort of Succinate Dehydrogenase B mutation carriers (SDHB)', *Clin Endocrinol (Oxf)*.

Tuveson, D. A., N. A. Willis, T. Jacks, J. D. Griffin, S. Singer, C. D. Fletcher, J. A. Fletcher, and G. D. Demetri. 2001. 'STI571 inactivation of the gastrointestinal stromal tumor c-KIT oncoprotein: biological and clinical implications', *Oncogene*, 20: 5054-8.

Tyner, J. W. 2011. 'Rapid Identification of Therapeutic Targets in Hematologic Malignancies via Functional Genomics', *Ther Adv Hematol*, 2: 83-93.

Tyner, J. W., M. W. Deininger, M. M. Loriaux, B. H. Chang, J. R. Gotlib, S. G. Willis, H. Erickson, T. Kovacsovics, T. O'Hare, M. C. Heinrich, and B. J. Druker. 2009. 'RNAi screen for rapid therapeutic target identification in leukemia patients', *Proc Natl Acad Sci U S A*, 106: 8695-700.

van Baars, F., C. Cremers, P. van den Broek, S. Geerts, and J. Veldman. 1982. 'Genetic aspects of nonchromaffin paraganglioma', *Hum Genet*, 60: 305-9.

Van Coster, R., S. Seneca, J. Smet, R. Van Hecke, E. Gerlo, B. Devreese, J. Van Beeumen, J. G. Leroy, L. De Meirleir, and W. Lissens. 2003. 'Homozygous Gly555Glu mutation in the nuclear-encoded 70 kDa flavoprotein gene causes instability of the respiratory chain complex II', *Am J Med Genet A*, 120a: 13-8.

van Nederveen, F. H., J. Gaal, J. Favier, E. Korpershoek, R. A. Oldenburg, E. M. de Bruyn, H. F. Sleddens, P. Derkx, J. Riviere, H. Dannenberg, B. J. Petri, P. Komminoth, K. Pacak, W. C. Hop, P. J. Pollard, M. Mannelli, J. P. Bayley, A. Perren, S. Niemann, A. A. Verhofstad, A. P. de Bruine, E. R. Maher, F. Tissier, T. Meatchi, C. Badoual, J. Bertherat, L. Amar, D. Alataki, E. Van Marck, F. Ferrau, J. Francois, W. W. de Herder, M. P. Peeters, A. van Linge, J. W. Lenders, A. P. Gimenez-Roqueplo, R. R. de Krijger, and W. N. Dinjens. 2009. 'An immunohistochemical procedure to detect patients with paraganglioma and phaeochromocytoma with germline SDHB, SDHC, or SDHD gene mutations: a retrospective and prospective analysis', *Lancet Oncol*, 10: 764-71.

Van Vranken, J. G., D. K. Bricker, N. Dephoure, S. P. Gygi, J. E. Cox, C. S. Thummel, and J. Rutter. 2014. 'SDHAF4 promotes mitochondrial succinate dehydrogenase activity and prevents neurodegeneration', *Cell Metab*, 20: 241-52.

Van Vranken, Jonathan G., Un Na, Dennis R. Winge, and Jared Rutter. 2015. 'Protein-mediated assembly of succinate dehydrogenase and its cofactors', *Critical reviews in biochemistry and molecular biology*, 50: 168-80.

Vanharanta, S., M. Buchta, S. R. McWhinney, S. K. Virta, M. Peczkowska, C. D. Morrison, R. Lehtonen, A. Januszewicz, H. Jarvinen, M. Juhola, J. P. Mecklin, E. Pukkala, R. Herva, M. Kiuru, N. N. Nupponen, L. A. Aaltonen, H. P. Neumann, and C. Eng. 2004. 'Early-onset renal cell carcinoma as a novel extraparaganglial component of SDHB-associated heritable paraganglioma', *Am J Hum Genet*, 74: 153-9.

Vaser, R., S. Adusumalli, S. N. Leng, M. Sikic, and P. C. Ng. 2016. 'SIFT missense predictions for genomes', *Nat Protoc*, 11: 1-9.
Verweij, J., P. G. Casali, J. Zalcberg, A. LeCesne, P. Reichardt, J. Y. Blay, R. Issels, A. van Oosterom, P. C. Hogendoorn, M. Van Glabbeke, R. Bertulli, and I. Judson. 2004. 'Progression-free survival in gastrointestinal stromal tumours with high-dose imatinib: randomised trial', *Lancet*, 364: 1127-34.
Vladutiu, G. D., and R. R. Heffner. 2000. 'Succinate dehydrogenase deficiency', *Arch Pathol Lab Med*, 124: 1755-8.
Wada, N., Y. Kurokawa, T. Takahashi, T. Hamakawa, S. Hirota, T. Naka, Y. Miyazaki, T. Makino, M. Yamasaki, K. Nakajima, S. Takiguchi, M. Mori, and Y. Doki. 2016. 'Detecting Secondary C-KIT Mutations in the Peripheral Blood of Patients with Imatinib-Resistant Gastrointestinal Stromal Tumor', *Oncology*, 90: 112-7.
Wada, R., H. Arai, S. Kure, W. X. Peng, and Z. Naito. 2016. '"Wild type" GIST: Clinicopathological features and clinical practice', *Pathol Int*, 66: 431-7.
Wagner, A. J., S. P. Remillard, Y. X. Zhang, L. A. Doyle, S. George, and J. L. Hornick. 2013. 'Loss of expression of SDHA predicts SDHA mutations in gastrointestinal stromal tumors', *Mod Pathol*, 26: 289-94.
Wang, H., and D. L. Brautigan. 2002. 'A novel transmembrane Ser/Thr kinase complexes with protein phosphatase-1 and inhibitor-2', *J Biol Chem*, 277: 49605-12.
Wang, J. H., J. Lasota, and M. Miettinen. 2011. 'Succinate Dehydrogenase Subunit B (SDHB) Is Expressed in Neurofibromatosis 1-Associated Gastrointestinal Stromal Tumors (Gists): Implications for the SDHB Expression Based Classification of Gists', *J Cancer*, 2: 90-3.
Weinhold, Nils, Anders Jacobsen, Nikolaus Schultz, Chris Sander, and William Lee. 2014. 'Genome-wide analysis of non-coding regulatory mutations in cancer', *Nat Genet*, 46: 1160-65.
Weisberg, E., and J. D. Griffin. 2003. 'Resistance to imatinib (Glivec): update on clinical mechanisms', *Drug Resist Updat*, 6: 231-8.
West, R. B., C. L. Corless, X. Chen, B. P. Rubin, S. Subramanian, K. Montgomery, S. Zhu, C. A. Ball, T. O. Nielsen, R. Patel, J. R. Goldblum, P. O. Brown, M. C. Heinrich, and M. van de Rijn. 2004. 'The novel marker, DOG1, is expressed ubiquitously in gastrointestinal stromal tumors irrespective of KIT or PDGFRA mutation status', *Am J Pathol*, 165: 107-13.
Williamson, S. R., J. N. Eble, M. B. Amin, N. S. Gupta, S. C. Smith, L. M. Sholl, R. Montironi, M. S. Hirsch, and J. L. Hornick. 2015. 'Succinate dehydrogenase-deficient renal cell carcinoma: detailed characterization of 11 tumors defining a unique subtype of renal cell carcinoma', *Mod Pathol*, 28: 80-94.
Winzeler, E. A., D. D. Shoemaker, A. Astromoff, H. Liang, K. Anderson, B. Andre, R. Bangham, R. Benito, J. D. Boeke, H. Bussey, A. M. Chu, C. Connelly, K. Davis, F. Dietrich, S. W. Dow, M. El Bakkoury, F. Foury, S. H. Friend, E. Gentalen, G. Giaever, J. H. Hegemann, T. Jones, M. Laub, H. Liao, N. Liebundguth, D. J. Lockhart, A. Lucau-Danila, M. Lussier, N. M'Rabet, P. Menard, M. Mittmann, C. Pai, C. Rebischung, J. L. Revuelta, L. Riles, C. J. Roberts, P. Ross-MacDonald, B. Scherens, M. Snyder, S. Sookhai-Mahadeo, R. K. Storms, S. Veronneau, M. Voet, G. Volckaert, T. R. Ward, R. Wysocki, G. S. Yen, K. Yu, K. Zimmermann, P. Philippsen, M. Johnston, and R. W. Davis. 1999. 'Functional characterization of the S. cerevisiae genome by gene deletion and parallel analysis', *Science*, 285: 901-6.
Witte, O. N. 1990. 'Steel locus defines new multipotent growth factor', *Cell*, 63: 5-6.
Xiao, M., H. Yang, W. Xu, S. Ma, H. Lin, H. Zhu, L. Liu, Y. Liu, C. Yang, Y. Xu, S. Zhao, D. Ye, Y. Xiong, and K. L. Guan. 2012. 'Inhibition of alpha-KG-dependent histone and DNA demethylases by fumarate and succinate that are accumulated in mutations of FH and SDH tumor suppressors', *Genes Dev*, 26: 1326-38.
Xu, Y., H. Zhang, L. C. Lit, A. Grothey, M. Athanasiadou, M. Kiritsi, Y. Lombardo, A. E. Frampton, A. R. Green, I. O. Ellis, S. Ali, H. J. Lenz, M. Thanou, J. Stebbing, and G. Giamas. 2014. 'The kinase LMTK3 promotes invasion in breast cancer through GRB2-mediated induction of integrin beta(1)', *Sci Signal*, 7: ra58.

Xu, Y., H. Zhang, V. T. Nguyen, N. Angelopoulos, J. Nunes, A. Reid, L. Buluwela, L. Magnani, J. Stebbing, and G. Giamas. 2015. 'LMTK3 Represses Tumor Suppressor-like Genes through Chromatin Remodeling in Breast Cancer', *Cell Rep*, 12: 837-49.
Yang, M., and P. J. Pollard. 2013. 'Succinate: a new epigenetic hacker', *Cancer Cell*, 23: 709-11.
Yankovskaya, V., R. Horsefield, S. Tornroth, C. Luna-Chavez, H. Miyoshi, C. Leger, B. Byrne, G. Cecchini, and S. Iwata. 2003. 'Architecture of succinate dehydrogenase and reactive oxygen species generation', *Science*, 299: 700-4.
Yantiss, R. K., A. E. Rosenberg, L. Sarran, P. Besmer, and C. R. Antonescu. 2005. 'Multiple gastrointestinal stromal tumors in type I neurofibromatosis: a pathologic and molecular study', *Mod Pathol*, 18: 475-84.
Yuzawa, S., Y. Opatowsky, Z. Zhang, V. Mandiyan, I. Lax, and J. Schlessinger. 2007. 'Structural basis for activation of the receptor tyrosine kinase KIT by stem cell factor', *Cell*, 130: 323-34.
Zhang, C. Q., D. G. Lu, Q. F. Liu, and W. Xiao. 2016. 'Primary extragastrointestinal stromal tumor of the pleura: A case report', *Oncol Lett*, 11: 3135-38.